FATIGUE BEHAVIOR OF GRAPHITE/GLASS/EPOXY COMPOSITES

Final Report

(February 9, 1972 to February 9, 1973)

April, 1973

by

Nagaraja Rao
K. E. Hofer, Jr.

IIT Research Institute

for

Department of the Navy
Naval Air Systems Command
Washington, D. C. 20360
Code Air-52032D

APPROVED FOR PUBLIC RELEASE;
DISTRIBUTION UNLIMITED

IIT RESEARCH INSTITUTE

DISCLAIMER NOTICE

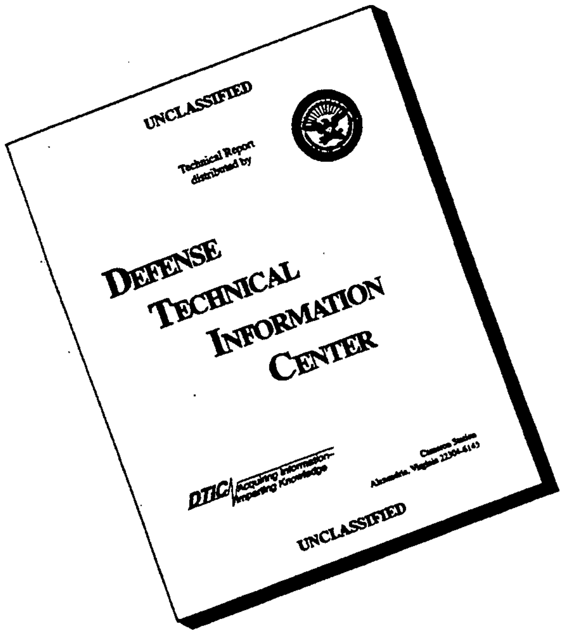

THIS DOCUMENT IS BEST QUALITY AVAILABLE. THE COPY FURNISHED TO DTIC CONTAINED A SIGNIFICANT NUMBER OF PAGES WHICH DO NOT REPRODUCE LEGIBLY.

IIT Research Institute
Technology Center
Chicago, Illinois 60616

Final Report

FATIGUE BEHAVIOR OF GRAPHITE/GLASS/EPOXY COMPOSITES

Contract No. N00019-72-C-0294

by

Nagaraja Rao
K. E. Hofer, Jr.

IIT Research Institute

for

Department of the Navy
Naval Air Systems Command
Washington, D. C. 20360

April, 1973

FOREWORD

This is the final report of IIT Research Institute Project No. D6070 titled, "Fatigue Behavior of Graphite/Glass/Epoxy Composites" conducted during the period from February 9, 1972 through February 8, 1973 for the Naval Air Systems Command, United States Department of the Navy under contract No. N-00019-72-C-0294. Mr. Max Stander (AIR 52032D) was the program monitor on behalf of the Naval Air Systems Command.

The program was conducted in the Mechanics of Materials Division of IIT Research Institute, Chicago, Illinois. Mr. N. Rao and Mr. K. E. Hofer, Jr. were Project Engineer and Project Manager respectively. The personnel who substantially contributed to the work reported herein are: Messrs. L. C. Bennett, K. E. Hofer, Jr., R. LaBedz, H. Lane, and N. Rao.

Respectfully submitted,
IIT RESEARCH INSTITUTE

Nagaraja Rao

Nagaraja Rao
Research Engineer

K. E. Hofer Jr

K. E. Hofer, Jr., Manager
Materials Engineering and
Building Technology

Approved:

All Daniel, for

R. H. Cornish
Director of Research
Mechanics of Materials
Research Division

TABLE OF CONTENTS

LIST OF ILLUSTRATIONS

LIST OF ILLUSTRATIONS - (Cont'd)

LIST OF ILLUSTRATIONS - (Cont'd)

LIST OF TABLES

LIST OF TABLES - Cont'd)

SECTION I

1.0 INTRODUCTION

The advanced composite materials possess characteristics of stiffness and strength which are most desirable for advanced naval aircraft. Glass composite materials, on the other hand, possess the equally desirable characteristic of low cost. The appropriate combination of these many features can be obtained by a suitable blending of the two or more composite materials.

Technically, the blending of two or more fiber types in a laminate, can be achieved by (1) mixing the fibers in the tow or roving, (2) intra-ply mixing of glass rovings with graphite tows or, (3) interleaving or interply mixing of two separate fibrous prepreg systems or any combination of the above. There are additional economic advantages to the third approach where prepreg tapes with a common resin system are prepared for two separate fibers: glass and graphite. For this reason the third approach was selected for some further study particularly with regard to the fatigue performance and its relative behavior to prior studies of the separate composites.

The specific objective of the program was to utilize a commercially available glass and a commerically available high strength and high modulus graphite with a common epoxy matrix to maximize the technical performance of the hybrid composite in fatigue applications.

The low costs of the glass/epoxy prepreg system compared to the graphite/epoxy prepreg system make this combination attractive. The graphite/glass/epoxy system, if successful, could be applied to a variety of Naval Aircraft primary structural components, skins, fuselage, etc. The material will provide both

low cost coupled with high fatigue performance.* Future hybrid composites could be prepared from one of the three approaches. One of the results of this program has been the determination that hybrids perform better both statically and in fatigue, when the separate fiber components are blended throughout the laminate. The current study also showed that the range of glass: graphite ratios where hybrids perform well may be restricted to a zone of approximately 0.5 to 2.0.

An open literature and company product availability search resulted in the selection of TR 286 epoxy resin, Modmor II Graphite and S-Glass as the ternary system constituents for major part of the program. An additional study of modulus degradation due to stress cycling was performed using HMS graphite instead of the HTS variety. Three fiber volume percent ratios were chosen in studying tensile properties, fatigue lives, crack propagation and modulus degradation of graphite/glass/epoxy hybrid composites.

---

* It has been well established in previous programs for NASC that graphite/epoxy and boron/epoxy composites possess exceptional fatigue performances (Ref. 3)

SECTION II

2.0 TEST PROGRAM

The program consisted of the following task work areas:

2.1 Task Area I: Review of State of Art of Mixed Fiber and Mixed Ply (laminate) advanced Composites

The literature of mixed fiber composite systems is not extensive. The most comprehensive work is that of Evensen[2]. The rule of mixtures and ternary diagrams utilized by Evensen were reviewed and were utilized in the development of this program. The review of the above work along with others of which a summary is presented as the Appendix B to this report.

2.2 Task Area II: Static Testing Program

The static testing program is delineated briefly in Table I. The principal properties of the mixed fiber composites were determined in the 0° and 90° tension modes. In plane shear tests were also conducted. Finally an off-axis laminate 0° $\pm$ 45° with graphite and glass fibers were tested to check the validity of the analytical prediction methods for the mixed fiber composite materials.

2.3 Task Area III: Tensile Fatigue Program

A tension fatigue program were conducted as shown in Table II. The materials and specimens were prepared similar to those prepared for the static test program.

2.4 Task Area IV: Shear Fatigue Program

A cantilever shear fatigue program were performed as shown in Table III. The stress ratio of -1 (fully reversed loading) was used and the specimens were removed prior to failure and inspected microscopically for cracking and crack propagation.

Table I

STATIC TEST PROGRAM

Ratio of Graphite* To Glass by Volume (v/v)	NUMBER OF SPECIMENS REQUIRED 0° Tension Tests	90° Tension Tests	$\pm$ 45° Shear Tests	0° $\pm$ 45° Tension Tests
1:1	3	3	3	3
2:1	3	3	3	3
3:1	3	3	3	3

*Modmor II Graphite and S-Glass with PR-286 resin system

Table II

TENSION FATIGUE PROGRAM

Ratio of Graphite To Glass by Volume (v/v)*	NUMBER OF SPECIMENS REQUIRED 0° Fatigue Tests	0° ± 45° Fatigue Tests
1:1	5	5
2:1	5	5
3:1	5	5

*Modmor II Graphite and S-Glass with PR286 resin system

Table III

SHEAR FATIGUE PROGRAM

Ratio of Graphite* To Glass by Volume (v/v)	NUMBER OF SPECIMENS REQUIRED ± 45° Fatigue Tests	0° ± 45° Fatigue Tests
1:1	5	5
2:1	5	5
3:1	5	5

*Modmor II Graphite and S-Glass with PR 286 resin system

2.5 Task Area V: Modulus Degradation due to Fatigue

Table IV presents the program that was conducted to study the effect of fatigue stress cycling on tensile modulus of unidirectional composite specimens. In these tests, HMS graphite, S-Glass with PR 286 resin in prepreg form were used for the test specimens. As shown in Table IV, a set of specimens of PR 286/ Modmor II/S-Glass (0° $\pm$ 45° fiber orientation) were also tested after subjecting them to about 2×10^6 fatigue stress cycles each (R = 0.1) to observe modulus degradation.

Table 1V

MODULUS DEGRADATION STUDY

Material System	Ratio of Graphite to Glass by Volume (v/v)	No. of Specimens: No Fatigue Stress Cycles Prior to Static Test	No. of Specimens: 2×10^6 Fatigue Stress Cycles (R=0.1) Prior to Test
PR286/HMS Graphite S-Glass (0° Fiber Orientation	1:0	3	3
	1:1	3	3
PR286/Modmor II Graphite/S-Glass (0° ± 45° Fiber Orientation	1:1	3*	1**
	2:1	6*	2**
	3:1	6*	1**

* From the Static Test program

** From the Fatigue Test program

SECTION III

3.0 MATERIAL PROCUREMENT AND SPECIMEN FABRICATION

The materials selected for the hybrid composite were a high tensile strength graphite fiber, a high strength glass fiber and an epoxy resin. The graphite fiber selected after reviewing the literature and an examination of prior experience and data from previous NASC contracts was the Morganite Modmor II HTS fiber. The glass fiber selected on a similar basis was S-Glass roving with the 901 finish. The epoxy resin system was PR 286, a product of the 3M Company. For the modulus degradation study, Modmor II graphite was replaced by HMS graphite.

The materials were utilized in the form of three inch wide prepreg tapes which were stacked appropriately in interply fashion to form the hybrid composites. The panels were subsequently partitioned into sub-panels, blanked and tabbed where necessary as required and cut into individual specimens.

Fig. 1 shows the ternary representation of the PR 286/ Modmor II graphite/S-Glass composite systems with three different volume fractions. The volumetric content of resin was held close to 40 percent with graphite/glass ratios of 1:1, 2:1 and 3:1.

3.1 Specimen Fabrication

The laminates were prepared using conventional low-pressure autoclave processes. The lay-up, cure cycle and specimen fabrication are briefly described below.

3.1.1 Layup Procedure

The green (uncured) prepreg layup was prepared with the desired number and orientation of plies. It was placed on a caul plate coated with a release agent. A TX-1040 release ply was placed over the prepreg. The bleeder plies were then added in the ratio of one ply per two plies of prepreg tapes. The entire

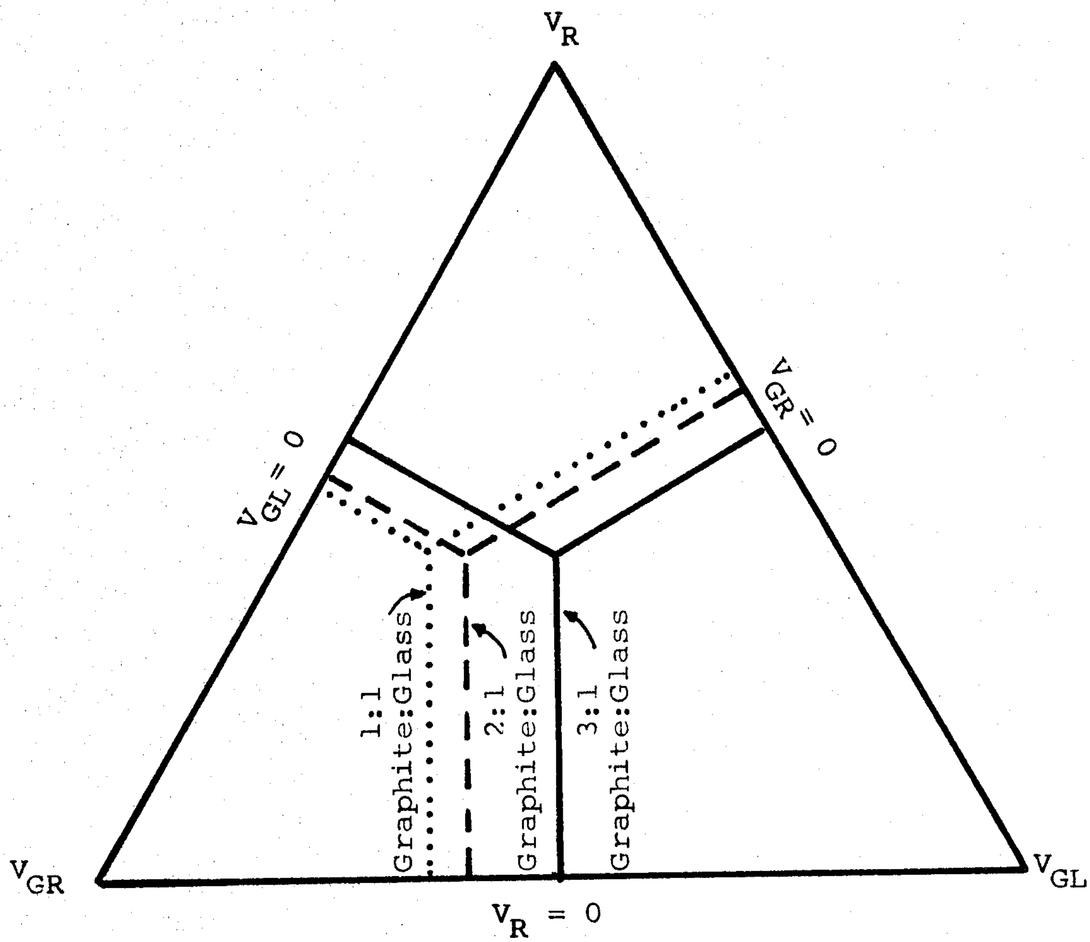

	TOTAL	RESIN	GRAPHITE	GLASS
1:1	100	40	30	30
2:1	100	40	40	20
3:1	100	40	45	15

Fig. 1 TERNARY DIAGRAM REPRESENTING THREE DIFFERENT VOLUME FRACTIONS FOR PR286/MODMOR II GRAPHITE/S GLASS COMPOSITE

layup was covered with plastic film (Mylar) and pinholes were made in the corners to permit gases to escape. The entire assembly was then taped into position to prevent movement.

An upper caul plate was then added to the stack. The entire layup was further covered with one layer of Style 181 glass fabric and finally with a capran vacuum bag. Vacuum was applied and maintained until the autoclave reached 250°F., after which the vacuum line was bled to the atmosphere.

After insertion of the stack into the cold autoclave, 85 to 90 psi pressure was applied. Then the temperature was applied at a rate of rise of approximately 6°F/minute to the cure temperature of 350°F. This temperature was maintained for two hours, after which the system was cooled to 150°F. Cured laminates were then blanked, tabbed (where necessary) and cut into individual specimens.

Table V presents the details of each type of laminate fabricated and includes test specimen types, fiber orientations, volumetric ratios of graphite to glass, number of plies and ply arrangements.

3.1.2 <u>Test Specimens</u>

For the static tensile tests and tension fatigue programs, 9 in. long IITRI type tab ended specimens were used. The stress strain curves were obtained from electrical resistance foil strain gages mounted at the center of the specimen gage section.

For the shear fatigue tests, thick 2 in. x 3/4" cantilever beam specimens (See Fig. 2) made of the required number of plies were used with an effective span of 1/2 in. The tests were conducted in the fully reversed mode (R = -1).

Table V

SPECIMEN CONFIGURATIONS

Type of Test and Specimen	Fiber Orientation	Ratio of Graphite to Glass by Volume v/v and number of plies	Ply Arrangement *
Static Tension and Tension Fatigue (IITRI Coupon)	0°	1:1 (2 + 2 = 4)	RLLR
		2:1 (4 + 2 = 6)	RRLLRR
		3:1 (6 + 2 = 8)	RRRLLRRR
	90°	1:1 (4 + 4 = 8)	RRRLLRRR
		2:1 (4 + 2 = 6)	RRLLLLRR
		3:1 (6 + 2 = 8)	RRRLLRRR
	±-45°	1:1 (4 + 4 = 8)	+-+--+-+ RLLRRLLR
		2:1 (8 + 4 = 12)	+-+-+--+-+-+ RRLLRRRRLLRR
		3:1 (12 + 4 = 16)	+-+-+-+--+-+-+-+ RRRRLLRRRRLLRRRR

* R = 0° or 90° Graphite ply
L = 0° or 90° Glass ply

$\overset{+-}{RR}$ = ± 45° Graphite ply
$\overset{+-}{LL}$ = ± 45° Glass ply

Table V (continued)

SPECIMEN CONFIGURATIONS

Type of Test and Specimen	Fiber Orientation	Ratio of Graphite to Glass by Volume v/v and number of plies	Ply Arrangement *
Static Tension and Fatigue (IITRI Coupon)	0° ± 45°	1:1 (4 + 4 = 8) 2:1 (8 + 4 = 12) 3:1 (12 + 4 = 16)	-+ +- RLLRRLLR +- -+ RRLLRRRRLLRR +- -+ RRRRLLRRRRLLRRRR
Shear Fatigue (Cantilever Beam) (Uniformly distributed Interply hybrid concept)	± 45°	1:1 (16 + 16 = 32) 2:1 (24 + 12 = 36) 3:1 (24 + 8 = 32)	+-+-+-+-+-+-+-+- [RRLLRRLLRRLLRRLL]$_s$ +-+-+-+-+-+-+-+-+- [RRRRLLRRRRLLRRRRLL]$_s$ +-+-+-+-+-+-+-+- [RRRRLLRRRRLLRRRR]$_s$
	0° ± 45°	1:1 (16 + 16 = 32) 2:1 (24 + 12 = 36) 3:1 (24 + 8 = 32)	+- +- +- +- [RRLLRRLLRRLLRRLL]$_s$ +- +- +- [RRRRLLRRRRLLRRRRLL]$_s$ +- +- [RRRRLLRRRRLLRRRR]$_s$

<u>NOTE:</u> In the 0° ± 45° composite specimens, all glass plies are ± 45° and all graphite plies are 0°

Table V (continued)

SPECIMEN CONFIGURATIONS

Type of Test and Specimen	Fiber Orientation	Ratio of Graphite to Glass by Volume v/v and number of plies	Ply Arrangement *
Shear Fatigue Cantilever Beam (Core-Shell Concept)	$\pm 45°$	1:1 (16 + 16 = 32)	+-+-+-+-+-+-+ [RRRRRRRRLLLLL]

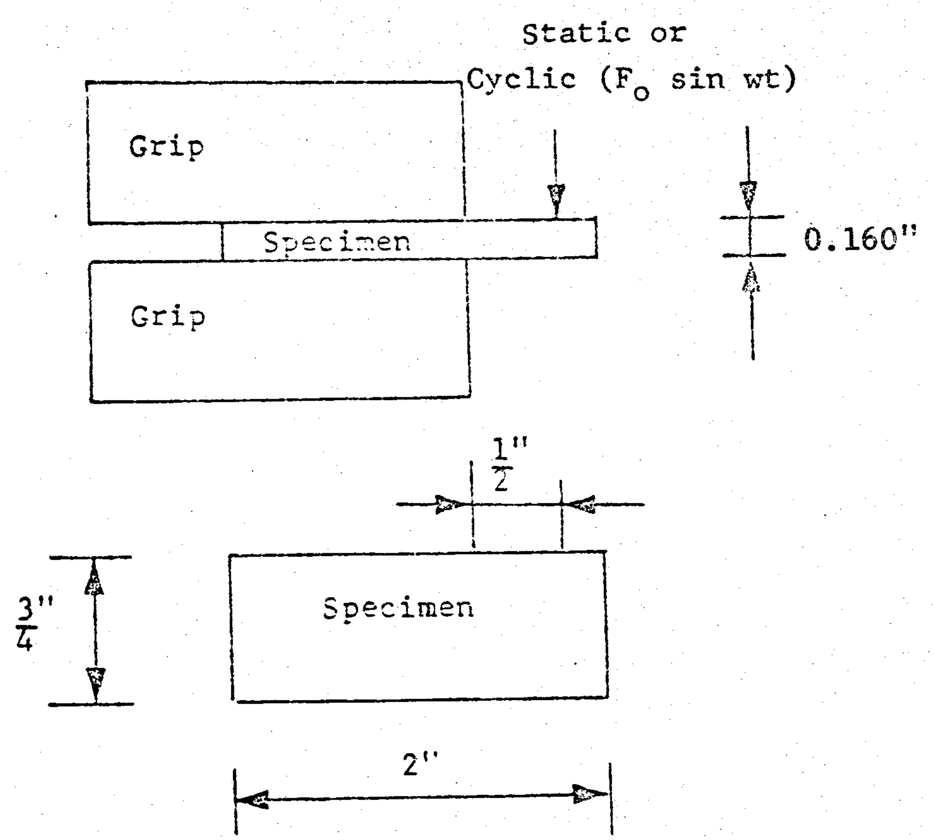

FIG. 2 CANTILEVER BEAM SPECIMENS AND METHOD OF LOADING

Two concepts of mixed ply ternary composite systems were examined by fabricating them and conducting preliminary tests. Fig. 3 presents photomicrographs of the two systems which were (1) Uniformly distributed Interply Hybrid Concept and (2) a Core-Shell interply concept. After some preliminary work the former system was selected for further study. The reasons for the choice are described in the next section.

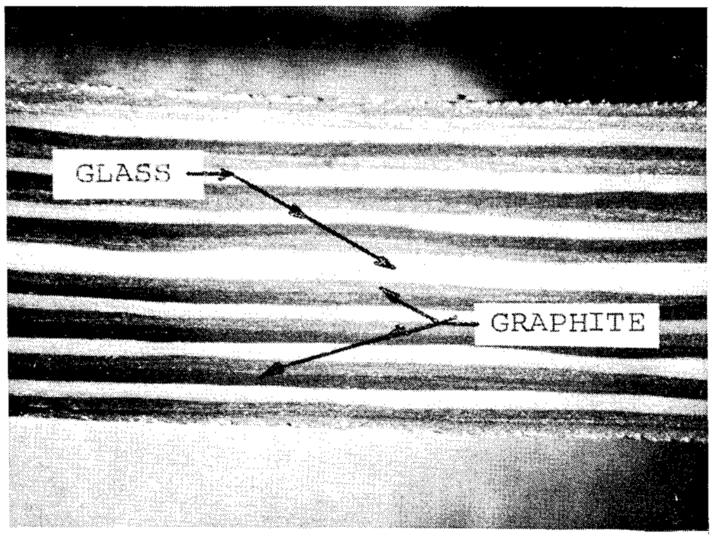

(a)
Interply Hybrid Concept

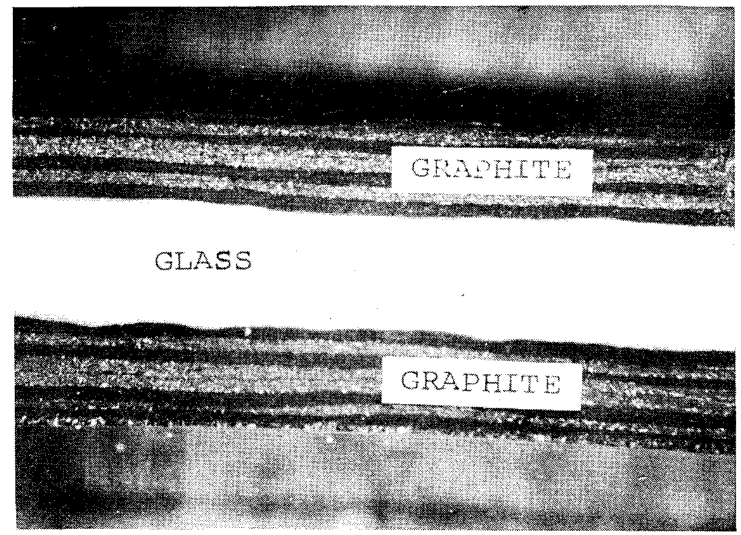

(b)
Core-Shell Concept

Fig. 3 PHOTOMICROGRAPHS (10x) OF PR286/MODMOR II GRAPHITE/ S GLASS (1 : 1 GRAPHITE: GLASS VOLUME) TERNARY COMPOSITE 32 PLY $\pm$ 45° LAMINATES

SECTION IV

4.0 TEST RESULTS

4.1 Static Test Program

Table VI presents a summary of the static tension test data of PR-286/Modmor II Graphite/S-Glass materials for three different graphite to glass fiber volumetric ratios (1:1, 2:1 and 3:1) in 0° fiber orientation. The individual stress strain (longitudinal and transverse) curves for each specimen are presented in the Appendix A (Figs. A-1 through A-9). Fig. 4 shows a summary of stress-strain (longitudinal) behavior in the 0° orientation for the three volumetric ratios along with similar data for S-Glass and Modmor II Graphite composites with epoxy resin.

Hybrid composites demonstrate a distinct improvement in stiffness achieved by replacement of glass fiber volume with graphite (about 75 percent at 1:1 ratio). However, it is also obvious that the strain capability of the hybrid composite is significantly lower than the glass fiber composite. Even with 1:1 graphite/glass ratio, the ultimate strain of the mixed fiber composite stays close to that of pure graphite composite (about 7×10^3 μ-in/in).

Tables VII and VIII and Figs. 5 and 6 show a summary of the static tension test data of PR 286/Modmor II Graphite/S-Glass Materials for three different graphite to glass fiber volumetric ratios (1:1, 2:1 and 3:1) in 90° and 0° ± 45° fiber orientations respectively. Additional 0° Graphite plies are necessary to increase the stiffness of glass/graphite 0° ± 45° hybrids where the 45° plies are all glass (See Table VIII). On the other hand additional graphite plies appear to decrease the transverse modulus of unidirectional hybrid composites. Table IX shows the summary of static test data for ± 45° PR 286/Modmor II Graphite/

TABLE VI

SUMMARY OF STATIC TENSILE PROPERTIES OF

0° PR-286/MODMOR II GRAPHITE/S-GLASS COMPOSITES

Volumetric Ratio of Graphite/ Glass	No. of Plies Graphite + Glass	Specimen Number	Specimen Thickness (in.)	σ_{ult} ksi	ε_{ult} (μ-in/in)	E (psi x 10^6)	ν (in/in)
1:1	2 + 2 = 4	0-T-1-1	0.023	124	7,884	15.7	0.232
		0-T-1-2	0.023	109	7,320	14.7	0.218
		0-T-1-3	0.024	112	7,323	15.1	-
		AVERAGE:		115	7,509	15.2	0.225
2:1	4 + 2 = 6	0-T-2-1	0.033	149	6,166	19.6	0.287
		0-T-2-2	0.035	139	7,515	18.1	0.259
		0-T-2-3	0.033	126	7,056	16.5	0.265
		AVERAGE:		138	6,912	18.1	0.270
3:1	6 + 2 = 8	0-T-3-1	0.047	134	6,719	19.8	0.296
		0-T-3-2	0.048	150	7,342	18.6	0.248
		0-T-3-3	0.049	140	7,313	18.2	0.227
		AVERAGE:		141	7,125	18.9	0.257

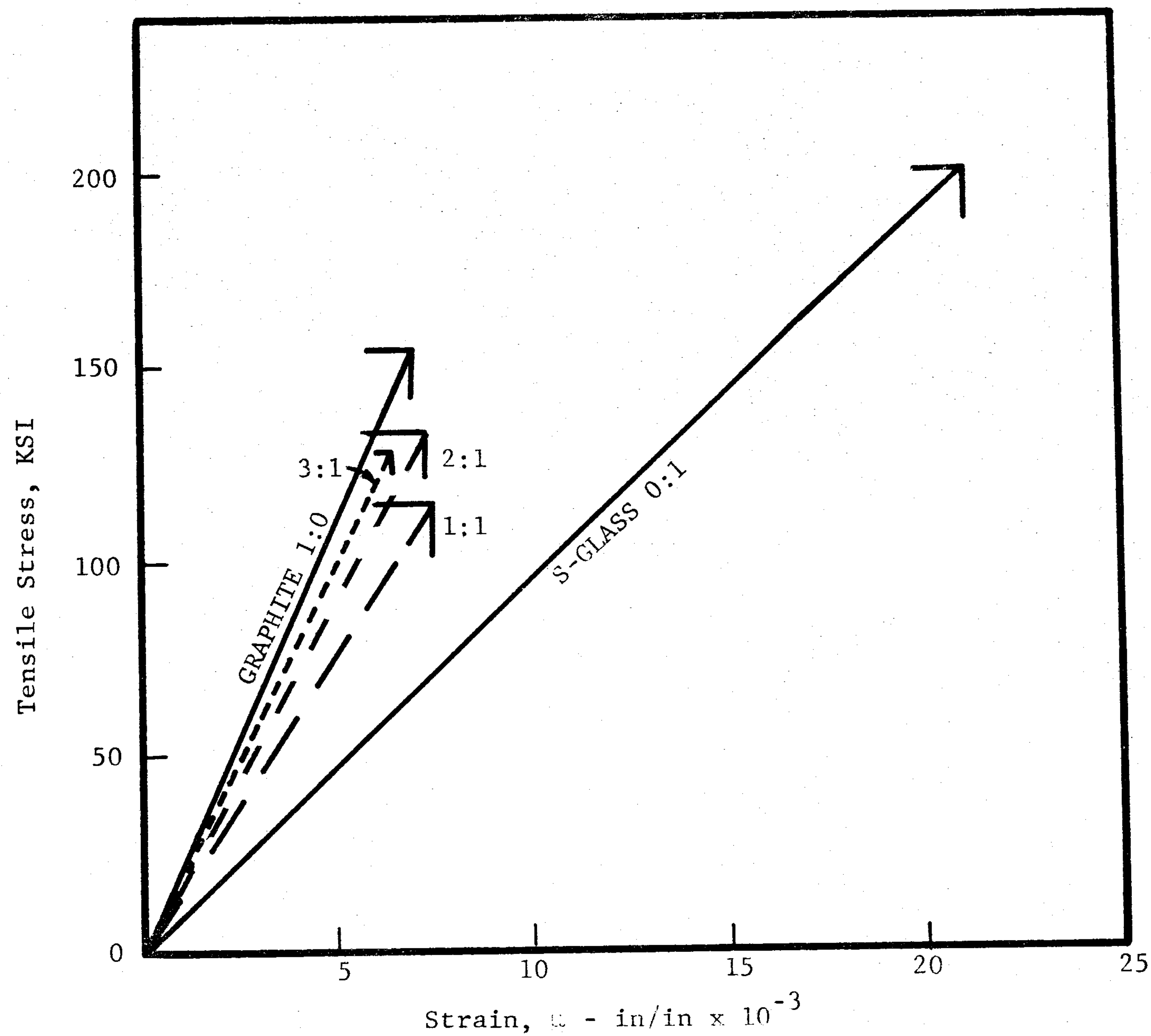

Fig. 4 SUMMARY TENSILE 0° STRESS STRAIN DIAGRAMS FOR PR-286/MODMOR II GRAPHITE/S-GLASS COMPOSITES OF VARIOUS FIBER VOLUME RATIOS AS COMPARED TO CONVENTIONAL GLASS, GRAPHITE COMPOSITES WITH EPOXY RESIN.

TABLE VII

SUMMARY OF STATIC TENSILE PROPERTIES OF

90° PR-286/MODMOR II GRAPHITE/S-GLASS COMPOSITES

Volumetric Ratio of Graphite/ Glass	No. of Plies Graphite + Glass	Specimen Number	Specimen Thickness (in.)	σ_{ult} ksi	ε_{ult} (μ-in/in)	E (psi x 10^6)	ν (in/in)
1:1	4 + 4 = 8	90-T-1-1	0.044	6.34	2,961	2.09	.085
		90-T-1-2	0.043	7.09	2,151	2.35	-
		90-T-1-3	0.044	6.80	2,953	2.33	0.042
		AVERAGE		6.75	3,021	2.26	0.064
2:1	4 + 2 = 6	90-T-2-1	0.033	7.95	4,318	1.93	-
		90-T-2-2	0.033	7.55	3,866	1.97	-
		90-T-2-3	0.034	8.35	4,664	1.85	-
		AVERAGE		7.95	4,283	1.92	-
3:1	6 + 2 = 8	90-T-3-1	.048	-	-	1.54	-
		90-T-3-2	.048	7.26	4,858	1.65	-
		90-T-3-3	.047	7.76	4,829	1.55	-
		AVERAGE		7.51	4,844	1.58	-

Table VIII

SUMMARY OF STATIC TENSILE PROPERTIES OF

(0° $\pm$ 45°) PR-286/MODMOR II GRAPHITE/S-GLASS COMPOSITES

Volumetric Ratio of Graphite/ Glass	No. of Plies Graphite + Glass	Specimen Number	Specimen Thickness (in.)	σ_{ult} ksi	ε_{ult} (μ-in/in)	E (psi x 10^6)	ν (in/in)
1:1	4 + 4 = 8	045-T-1-1	0.043	114	7552	14.8	-
		045-T-1-2	0.044	90.7	6331	14.4	-
		045-T-1-3	0.044	107	7127	14.6	-
		AVERAGE		104	7000	14.6	-
2:1	8 + 4 = 12	045-T-2-1	0.070	123	6970	17.2	-
		045-T-2-2	0.072	129	7044	18.1	-
		045-T-2-3	0.070	115	6469	17.7	-
		045-T-2-6	0.070	124	7427	16.7	0.49
		045-T-2-7	0.067	105	6375	16.3	0.48
		045-T-2-8	0.068	114	6637	15.6	-
		AVERAGE		118	6820	17.0	0.48
3:1	12 + 4 = 16	045-T-3-1	0.097	143	7762	17.8	-
		045-T-3-2	0.096	144	7514	18.6	-
		045-T-3-3	0.097	156	7497	20.4	-
		045-T-3-6	0.094	133	7278	18.1	0.49
		045-T-3-7	0.095	125	6807	18.3	0.46
		045-T-3-8	0.094	139	7574	18.7	0.36
		AVERAGE		140	7405	18.7	0.44

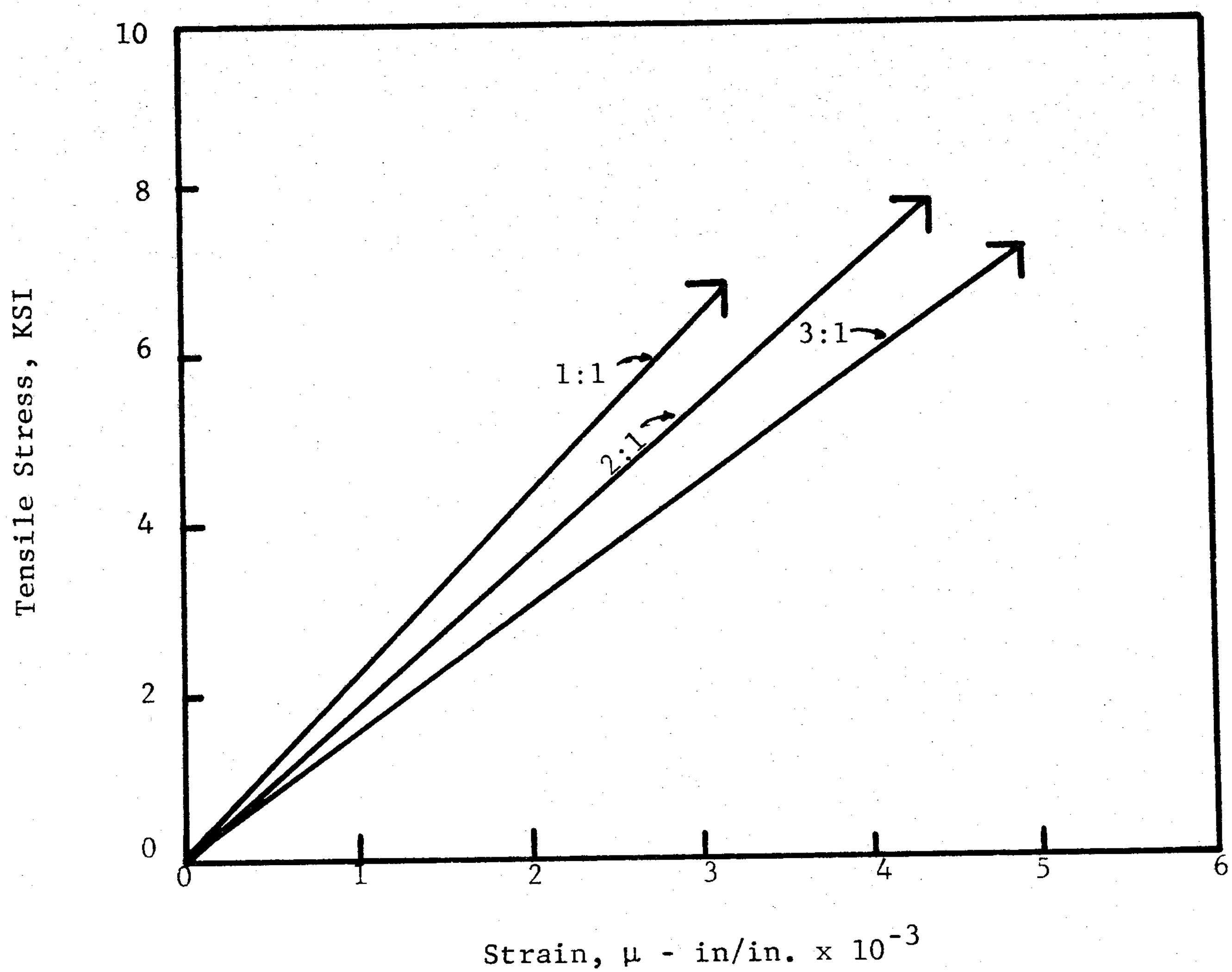

Fig. 5 SUMMARY TENSILE 90° STRESS STRAIN DIAGRAM FOR PR-286/MODMOR II GRAPHITE/S-GLASS COMPOSITES OF VARIOUS FIBER VOLUME RATIOS

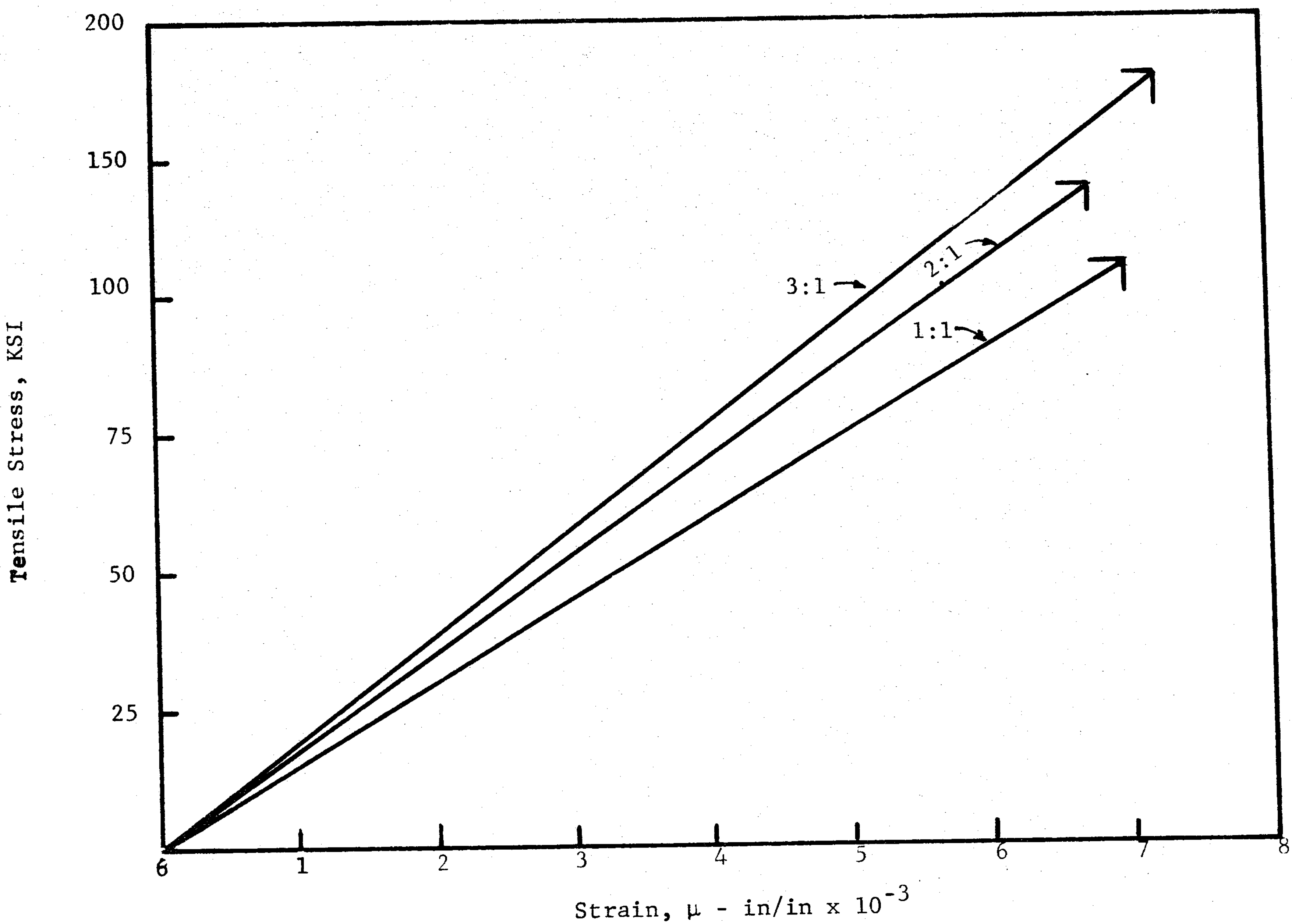

FIG. 6 SUMMARY 0° ± 45° STRESS STRAIN DIAGRAM FOR PR-286/MODMOR II GRAPHITE/S-GLASS COMPOSITES OF VARIOUS FIBER VOLUME RATIOS

Table IX

SUMMARY OF STATIC TENSILE PROPERTIES OF

$\pm$ 45° PR-286/MODMOR II GRAPHITE/S-GLASS COMPOSITES

Volumetric Ratio of Graphite/Glass	No. of Plies Graphite + Glass	Specimen Number	Specimen Thickness (in.)	σ_{ult} ksi	ε_{ult} (μ-in/in)
1:1	4 + 4 = 8	45-T-1-1	0.045	18.3	> 9485
		45-T-1-2	0.043	19.3	> 9815
		45-T-1-3	0.043	18.6	>11661
		AVERAGE		18.7	
2:1	8 + 4 = 12	45-T-2-1	0.071	19.2	> 9669
		45-T-2-2	0.072	19.3	> 9793
		45-T-2-3	0.072	18.6	> 8558
		AVERAGE		19.0	
3:1	12 + 4 = 16	45-T-3-1	0.097	20.6	>10456
		45-T-3-2	0.097	20.0	> 9774
		45-T-3-3	0.098	19.8	> 8767
		AVERAGE		20.1	

S-Glass hybrids for three different graphite to glass fiber volumetric ratios (1:1, 2:1 and 3:1).

4.2 Tensile Fatigue Program

Fig. 7 shows a comparison of the fatigue performance of 0° PR 286/Modmor II Graphite/S-Glass composites at three graphite to glass fiber volumetric ratios (1:1, 2:1 and 3:1). Also shown in the figure are the general typical graphite/epoxy S-N curve for 0° fiber orientation and the range of 0° glass/epoxy fatigue life curves (shaded area representing the range with the average curve drawn in the middle). A substantial improvement in the fatigue lives of hybrid composites over the glass-epoxy life range is evident. The improvement is less significant beyond the graphite to glass fiber volumetric ratio of 1:1 which can be seen from graphite (1:0) curve and the apparent higher position of 2:1 curve as compared to 3:1. Fig. 8 presents a comparison of fatigue performance of 0° ± 45° PR 286/Modmor II graphite/S-glass composite laminates of the three graphite to glass fiber volumetric ratios (1:1, 2:1 and 3:1). Substantial improvement in fatigue life can be seen as the graphite fiber volume ratio increases from 1:1 to 2:1. The improvement from 2:1 to 3:1 appears to be marginal.

4.3 Shear Fatigue

Shear fatigue of hybrid composites was also performed. The testing was oriented towards a qualitative assessment of the hybrid composite in its resistance to microscopic crack development and propagation. In earlier NASC sponsored work, extensive crack propagation studies of binary advanced composite systems were carried out. These studies on the mode of fatigue failure and its progress for the separate composites were utilized in the analysis of the progress of fatigue failure in the current hybrid

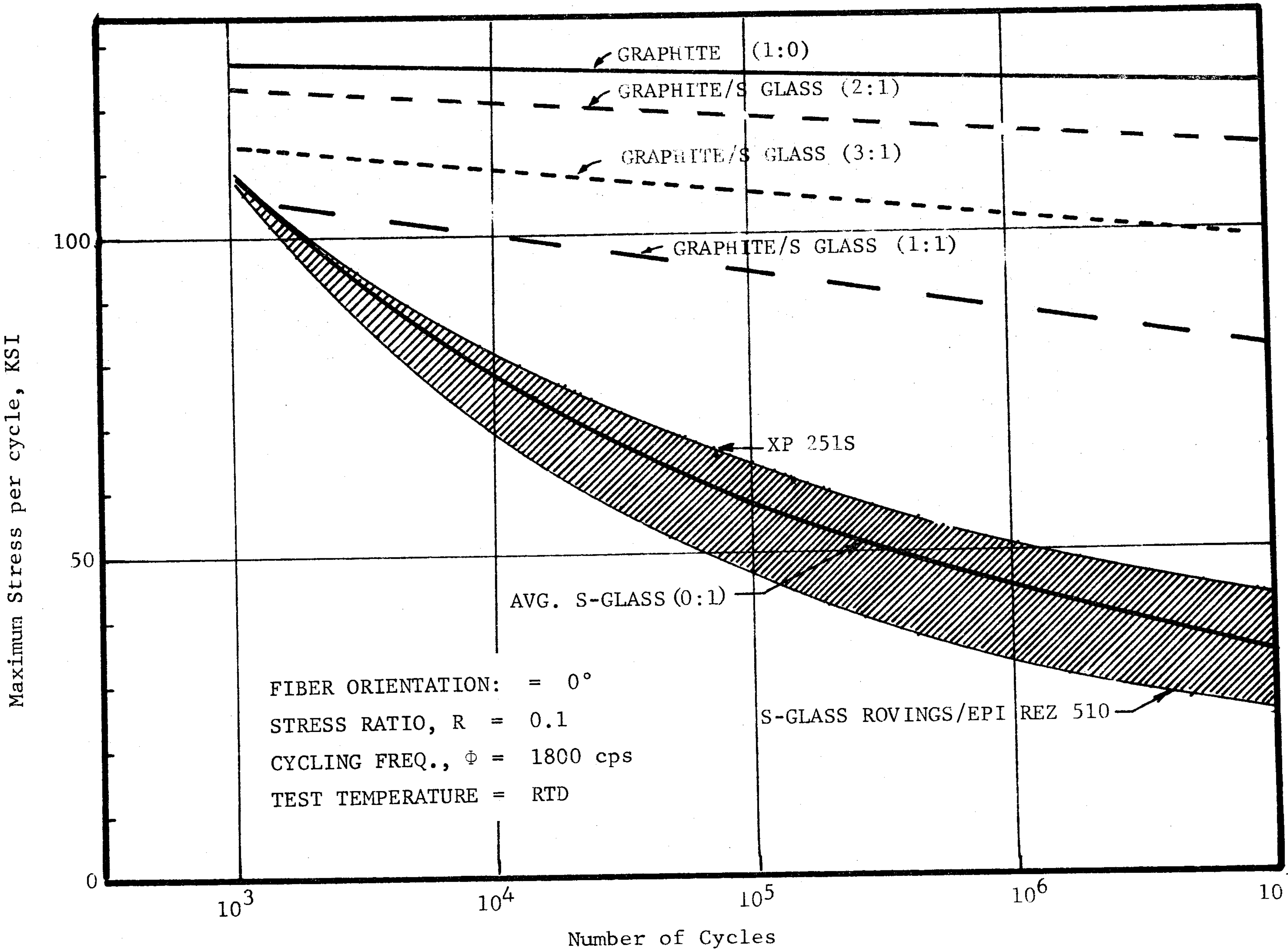

Fig. 7 FATIGUE LIFE S-N DIAGRAM FOR S-GLASS AND PR 286/MODMOR II GRAPHITE/S-GLASS COMPOSITES

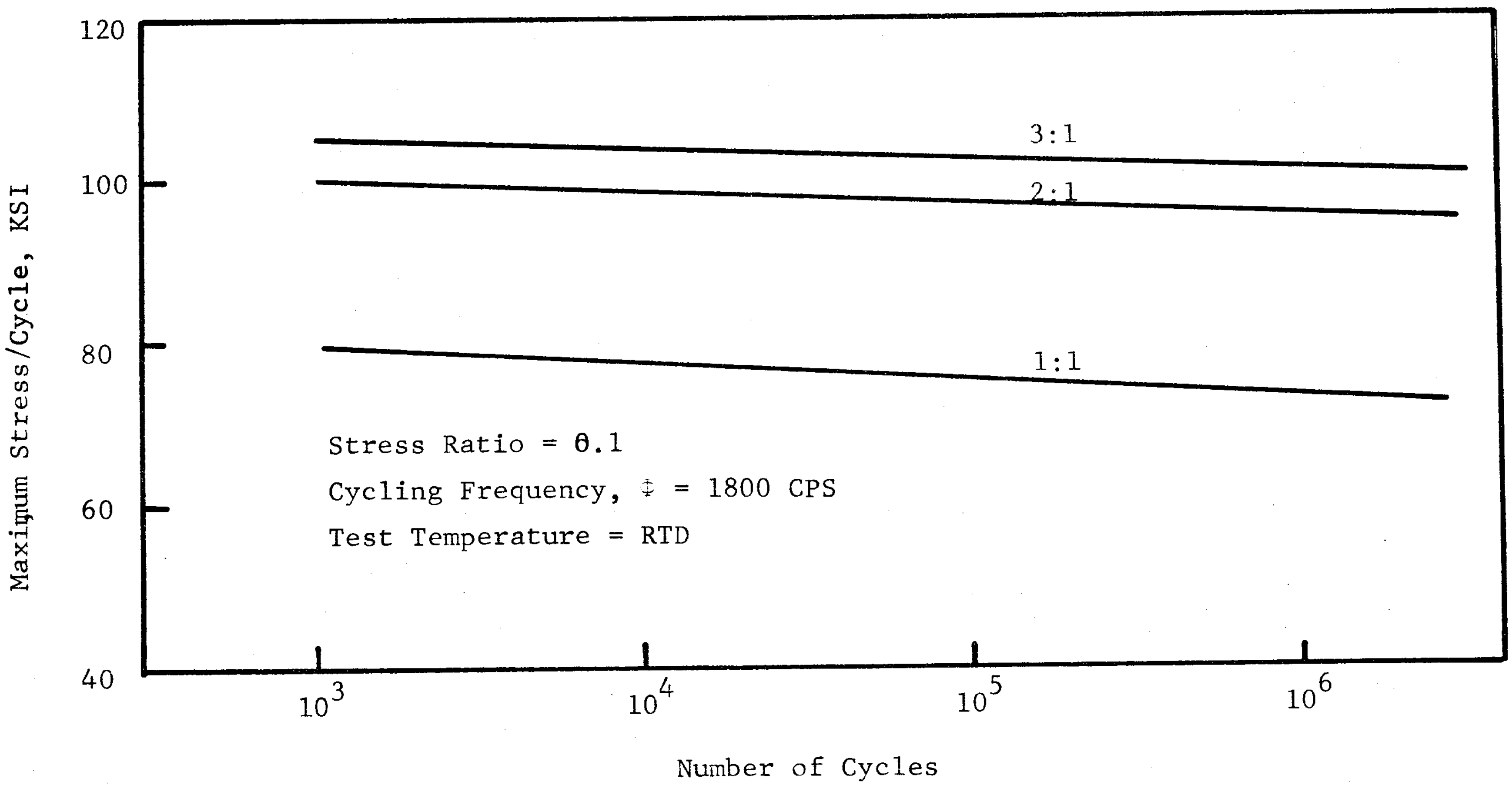

FIG. 8 SUMMARY TENSION FATIGUE LIFE S-N DIAGRAMS FOR 0° ± 45 PR-286/MODMOR II GRAPHITE/S-GLASS COMPOSITES OF VARIOUS GRAPHITE TO GLASS FIBER RATIOS

composite study. It was originally hoped that the high strain capability of the glass phase of the hybrid would attenuate the rapid progress of hybrid fatigue crack propagation.

In a preliminary effort, a 32 ply ternary composite (graphite/glass = 1:1) was prepared in two different ways. (See Fig. 3 in Section 3). The first way utilized the core-shell concept in which 16 plies of glass prepregs were covered on either side with 8 plies of Modmor II graphite prepreg. The second hybrid was prepared using uniformly distributed plies of graphite and glass prepreg. The hybrid stack contained graphite prepreg on the top and the bottom. Under static loading both hybrids showed an interlaminar shear strength of about 5 ksi. But the mode of failure and cracking appeared to be different. In the core-shell type hybrid with the glass plies in the middle, severe interlaminar separation between the glass and graphite strata were the dominant feature with some graphite cracking and some interlaminar separation in the glass core. (See Figs 9a and 10). The uniformly distributed hybrid material consistently showed the cracking to be more evenly distributed throughout the composite although the glass plies did show less cracking due to their high strain capability. (See Figs 9b and 11). On the basis of these tests, further work was performed on the uniformly distributed graphite/glass hybrids only.

Tables X and XI show a detailed listing of ± 45° and 0° ± 45° PR 286/Modmor II graphite/S-glass uniformly distributed hybrid composites which were studied microscopically after various shear fatigue stress cycles. Table XII presents a similar listing for ± 45° core-shell hybrids. Figs. 12 through 18 represent typical photomicrographs showing the extent of damage and cracking due to fatigue stress cyclic loadings.

(a) MAGNIFICATION 8X

16 S-GLASS PLIES PLACED IN THE MIDDLE WITH
8 PLIES OF GRAPHITE COVERING

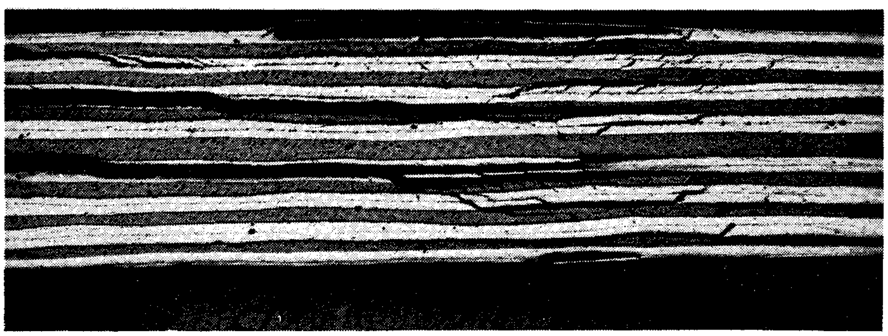

(b) MAGNIFICATION 8X

S-GLASS AND GRAPHITE PLIES ALTERNATELY PLACED

Fig. 9 PHOTOMICROGRAPHS OF 32 PLY $\pm$ 45° PR 286/MODMOR II GRAPHITE/S GLASS COMPOSITE (1:1) FAILED UNDER STATIC LOADING

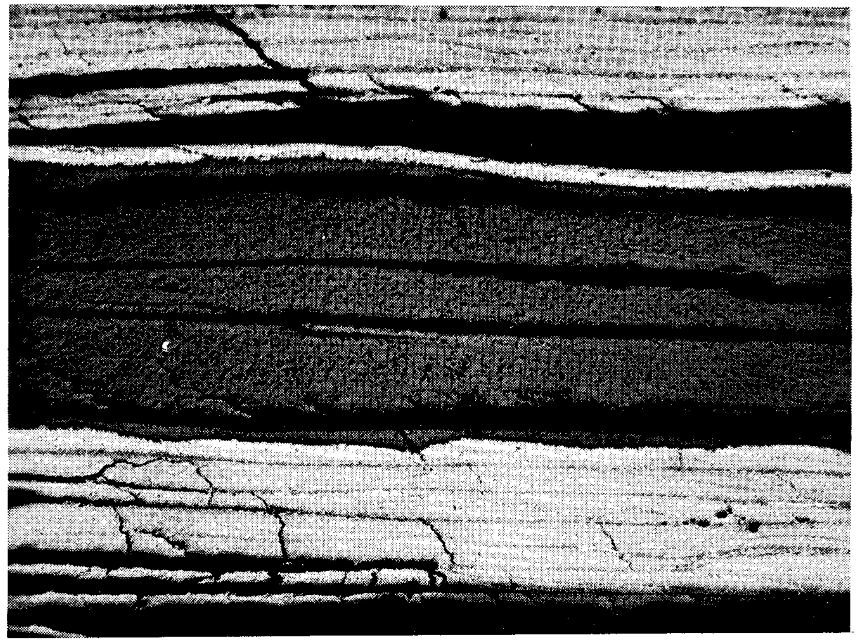

MAGNIFICATION 20X

Fig. 10 PHOTOMICROGRAPH OF 32 PLY $\pm$ 45° PR 286/MODMOR II GRAPHITE/S-GLASS COMPOSITE (1:1) FAILED UNDER STATIC LOADING (16 S-GLASS PLIES PLACED IN THE MIDDLE WITH 8 PLIES OF GRAPHITE COVERING)

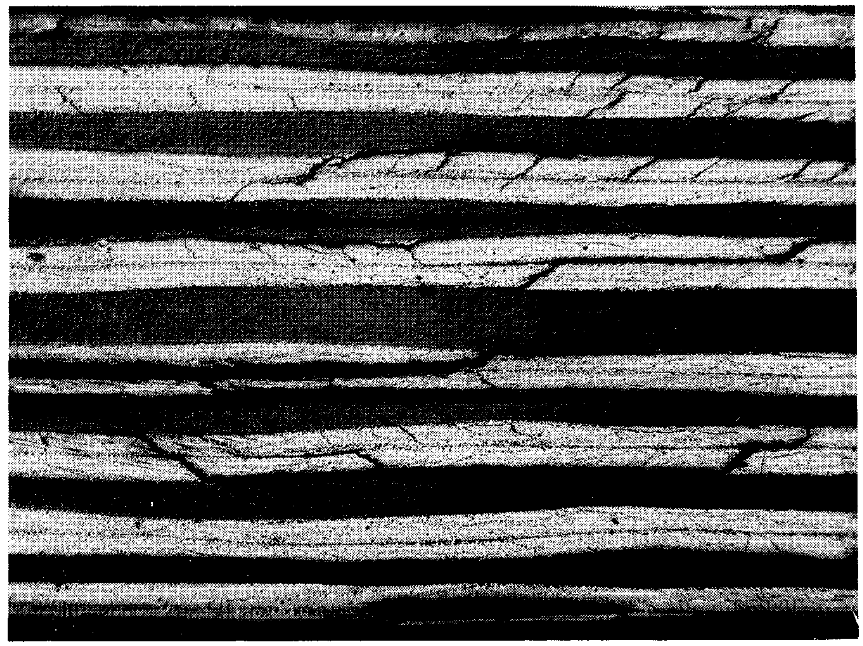

MAGNIFICATION 20X

Fig. 11 PHOTOMICROGRAPH OF 32 PLY $\pm$ 45° PR 286/MODMOR II GRAPHITE/S-GLASS COMPOSITE (1:1) FAILED UNDER STATIC LOADING (S-GLASS AND GRAPHITE PLIES ALTERNATELY PLACED)

Table X

LIST OF $\pm$ 45° PR-286/MODMOR II GRAPHITE/S-GLASS CANTILEVER BEAM SPECIMENS TESTED TO VARIOUS NUMBER OF SHEAR FATIGUE STRESS CYCLES FOR SUBSEQUENT MICROSCOPIC STUDY

(Uniformly Distributed Hybrid Concept)

Specimen No.	Thickness (in.)	Width (in.)	Graphite/Glass Ratio No. of Plies	Max. Shear Stress/Cycle (ksi)	No. of Stress Cycles (R = -1)
45-5-1-2	0.169	0.755	1:1	$\pm$ 2.5	8×10^3 *
45-5-1-3	0.167	0.753	(32 plies)	$\pm$ 2.0	1.43×10^5 *
45-4-1-4	0.173	0.756		$\pm$ 2.0	10^4
45-5-1-5	0.171	0.753		$\pm$ 2.0	10^4
45-5-1-6	0.167	0.751		$\pm$ 2.0	10^5
45-5-1-7	0.168	0.755		$\pm$ 2.0	10^5
45-5-2-1	0.200	0.498	2:1	$\pm$ 2.0	10^4
45-5-2-2	0.198	0.500	(36 plies)	$\pm$ 2.0	10^5
45-5-2-3	0.195	0.499		$\pm$ 2.0	9×10^3 *
45-5-2-4	0.198	0.500		$\pm$ 2.0	22×10^3 *
45-5-2-5	0.195	0.500		$\pm$ 2.0	10^5
45-5-3-1	0.190	0.504	3:1	$\pm$ 2.0	10^4
45-5-3-2	0.185	0.503	(32 plies)	$\pm$ 2.0	10^4
45-5-3-3	0.180	0.504		$\pm$ 2.0	10^5
45-5-3-4	0.187	0.504		$\pm$ 2.0	11×10^3 *
45-5-3-5	0.186	0.504		$\pm$ 2.0	10^5

* Specimen failure at these number of cycles.

Table XI

LIST OF 0° $\pm$ 45° PR-286/MODMOR II GRAPHITE/S-GLASS CANTILEVER BEAM SPECIMENS TESTED TO VARIOUS NUMBER OF SHEAR FATIGUE STRESS CYCLES FOR SUBSEQUENT MICROSCOPIC STUDY

(Uniformly Distributed Hybrid Concept)

Specimen No.	Thickness (in.)	Width (in.)	Graphite/Glass Ratio No. of Plies	Max. Shear Stress/Cycle (ksi)	No. of Stress Cycles (R = -1)
045-5-1-1		0.503	1:1	$\pm$ 2.0	5×10^5
045-5-1-2	0.163	0.504	(32 plies)	$\pm$ 2.0	10^4
045-5-1-3	0.171	0.503		$\pm$ 2.0	10^4
045-5-1-4	0.175	0.504		$\pm$ 2.0	10^5
045-5-1-5	0.174	0.504		$\pm$ 2.0	10^5
045-5-2-1	0.190	0.503	2:1	$\pm$ 2.0	10^4
045-5-2-2	0.210	0.500	(36 plies)	$\pm$ 2.0	10^4
045-5-2-3	0.210	0.500		$\pm$ 2.0	10^5
045-5-2-4	0.210	0.501		$\pm$ 2.0	10^5
045-5-2-5	0.201	0.501		$\pm$ 2.0	5×10^5
045-5-3-1	0.185	0.505	3:1	$\pm$ 2.0	10^4
045-5-3-2	0.192	0.502	(32 plies)	$\pm$ 2.0	10^4
045-5-3-3	0.181	0.503		$\pm$ 2.0	10^5
045-5-3-4	0.197	0.502		$\pm$ 2.0	10^5

Table XII

LIST OF $\pm$ 45° PR-286/MODMOR II GRAPHITE/S-GLASS CANTILEVER BEAM SPECIMENS TESTED TO VARIOUS NUMBER OF SHEAR FATIGUE STRESS CYCLES FOR SUBSEQUENT MICROSCOPIC STUDY (CORE SHELL CONCEPT SPECIMENS)

Specimen No.	Thickness (in.)	Width (in.)	Graphite/Glass Ratio No. of Plies	Max. Shear Stress/Cycle (ksi)	No. of Stress Cycles (R = -1)
G45-5-1-2	0.161	0.746	1:1 (32 plies)	$\pm$ 4.0	Immediate Failure
G45-5-1-3	0.160	0.750		$\pm$ 3.0	Immediate Failure
G45-5-1-4	0.162	0.751		$\pm$ 1.0	2.5×10^6 *
G45-5-1-5	0.162	0.751		$\pm$ 2.0	10^4 *
G45-5-1-6	0.156	0.749		$\pm$ 2.0	34×10^3*

* Specimen failure at these cycles.

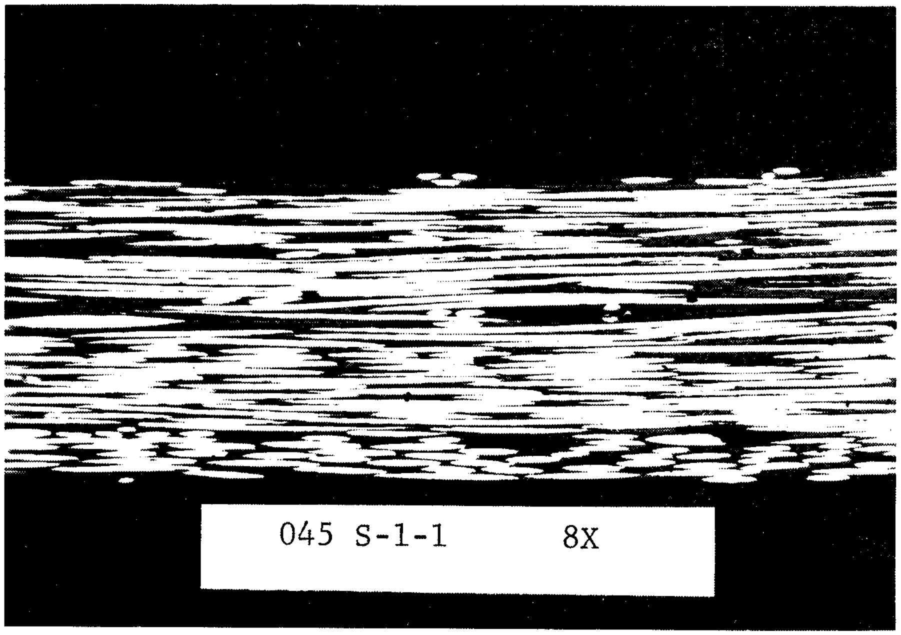

Fig. 12 PHOTOMICROGRAPH OF LONGITUDINAL SECTION OF 0 ± 45° PR-286/ MODMOR II GRAPHITE/S-GLASS (1:1) COMPOSITE CONTILEVER BEAM SPECIMEN AFTER BEING SUBJECTED TO 5 x 10^5 SHEAR FATIGUE STRESS CYCLES (MAX. ± 2 KSI, R= -1)

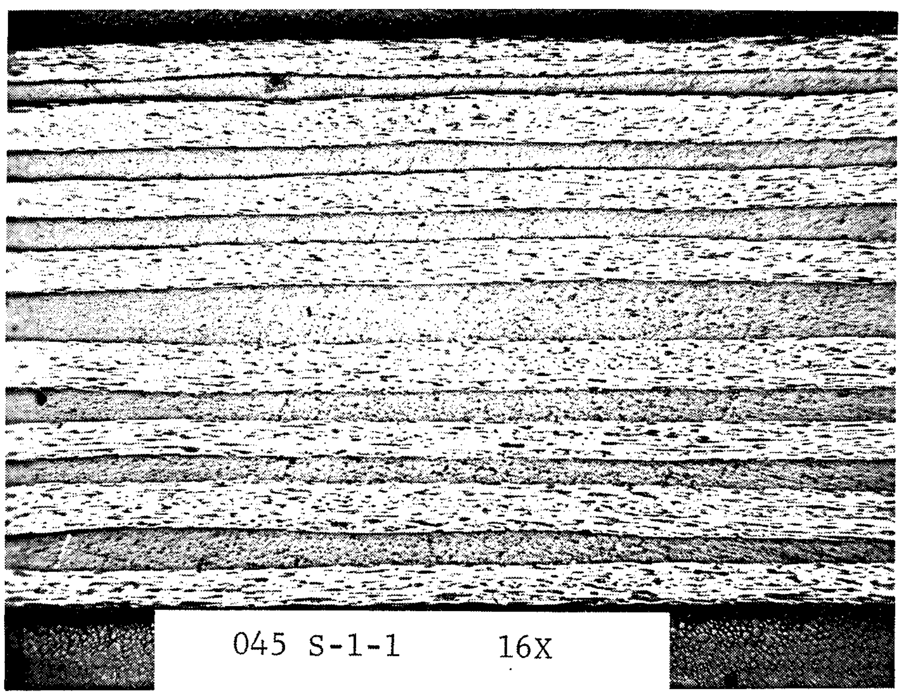

Fig. 13 PHOTOMICROGRAPH OF LONGITUDINAL SECTION OF 0 ± 45° PR-286/ MODMOR II GRAPHITE/S-GLASS (1:1) COMPOSITE CONTILEVER BEAM SPECIMEN AFTER BEING SUBJECTED TO 5 x 10^5 SHEAR FATIGUE STRESS CYCLES (MAX. ± 2 KSI, R = -1)

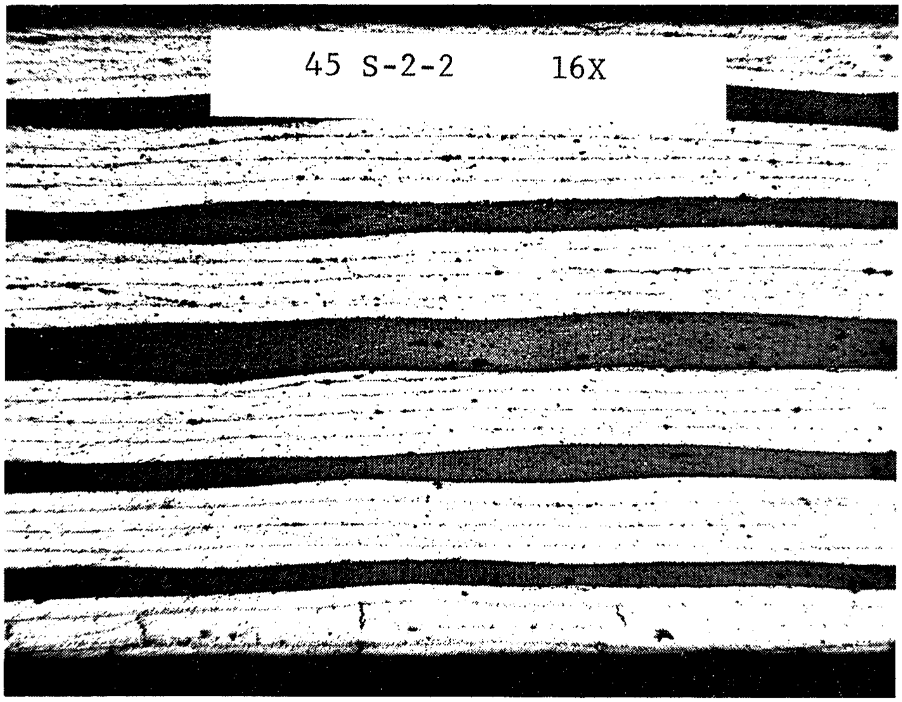

Fig. 14 PHOTOMICROGRAPH OF LONGITUDINAL SECTION OF $\pm$ 45° PR-286/ MODMOR II GRAPHITE/S-GLASS (2:1) COMPOSITE CANTILEVER BEAM SPECIMEN AFTER BEING SUBJECTED TO 10^5 SHEAR FATIGUE STRESS CYCLES (MAX. $\pm$ 2 KSI, R = -1)

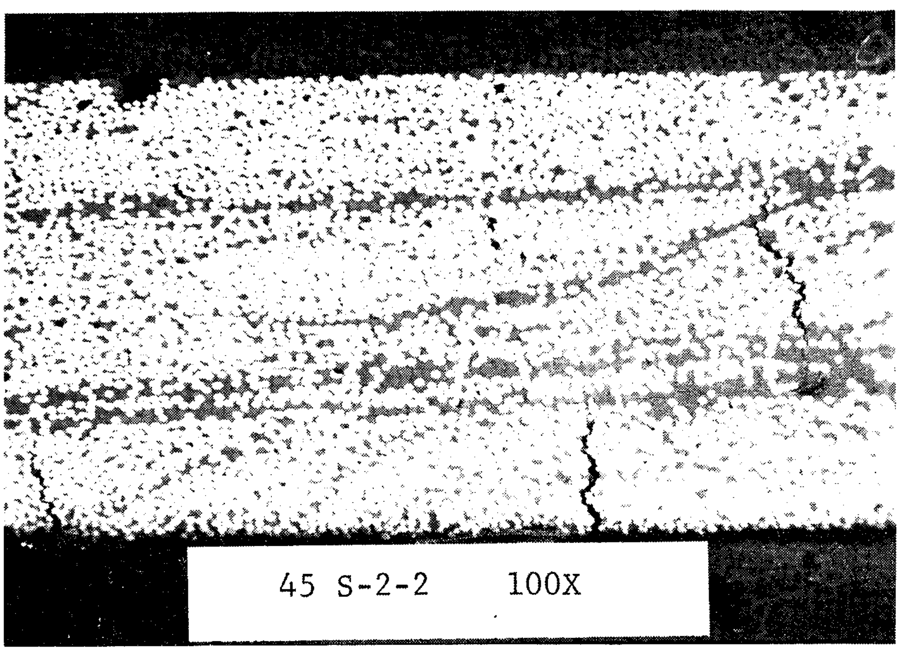

Fig. 15 PHOTOMICROGRAPH OF LONGITUDINAL SECTION OF $\pm$ 45° PR-286/ MODMOR II GRAPHITE/S-GLASS (2:1) COMPOSITE CANTILEVER BEAM SPECIMEN AFTER BEING SUBJECTED TO 10^5 SHEAR FATIGUE STRESS CYCLES (MAX. $\pm$ 2 KSI, R = -1)

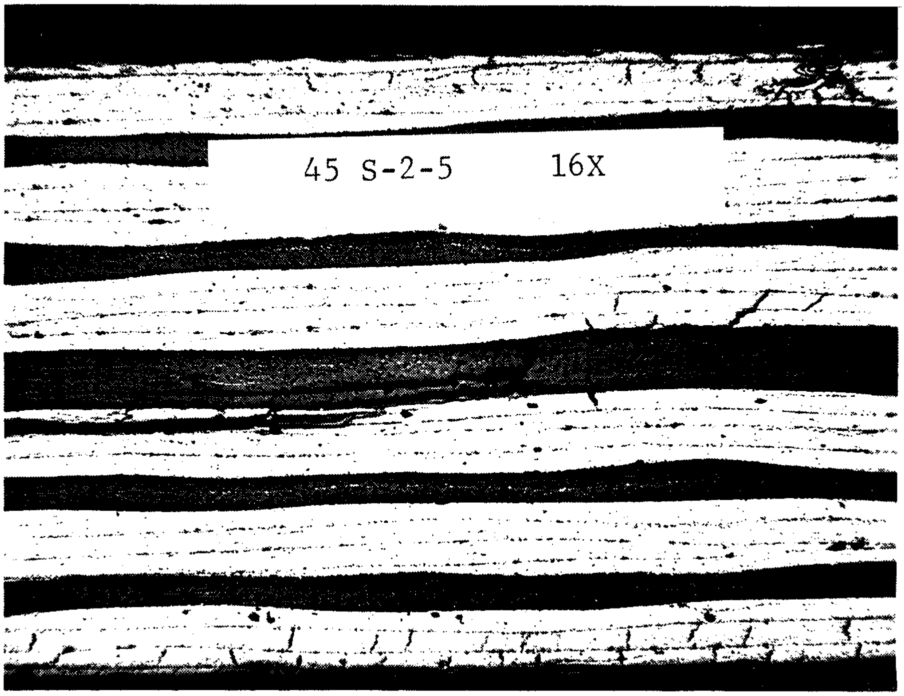

Fig. 16 PHOTOMICROGRAPH OF LONGITUDINAL SECTION OF $\pm$ 45° PR-286/ MODMOR II GRAPHITE/S-GLASS (2:1) COMPOSITE CANTILEVER BEAM SPECIMEN AFTER BEING SUBJECTED TO 10^5 SHEAR FATIGUE STRESS CYCLES (MAX. $\pm$ 2 KSI, R = -1)

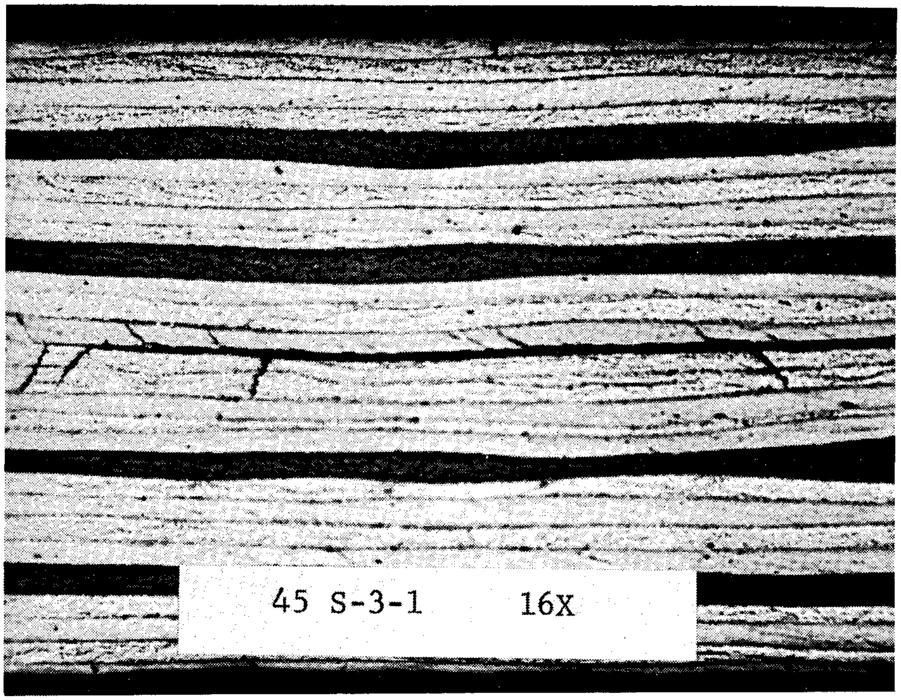

Fig. 17 PHOTOMICROGRAPH OF LONGITUDINAL SECTION OF $\pm$ 45° PR-286/ MODMOR II GRAPHITE/S-GLASS (3:1) COMPOSITE CANTILEVER BEAM SPECIMEN AFTER BEING SUBJECTED TO 10^4 SHEAR FATIGUE STRESS CYCLES (MAX. $\pm$ 2 KSI, R= -1)

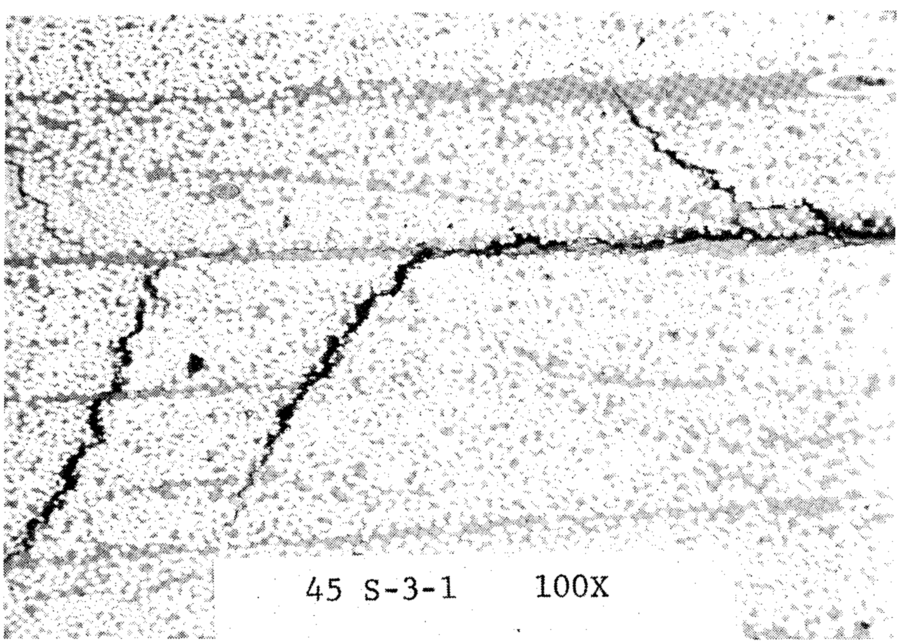

Fig. 18 PHOTOMICROGRAPH OF LONGITUDINAL SECTION OF $\pm$ 45° PR-286/ MODMOR II GRAPHITE/S-GLASS (3:1) COMPOSITE CANTILEVER BEAM SPECIMEN AFTER BEING SUBJECTED TO 10^4 SHEAR FATIGUE STRESS CYCLES (MAX. $\pm$ 2 KSI, R= -1)

All the specimens were subjected to various number of fatigue stress cycles with an alternating maximum stress of 2 ksi with a stress ratio of R = -1 (Tension-Compression - Tension). The specimens were removed from the testing machine, prior to failure, after various numbers of stress cycles (from 10^4 cycles to 5×10^5 cycles), and sectioned longitudinally. They were then mounted and polished for microscopic study.

The $\pm$ 45° core-shell hybrids (shown in Table XII) fabricated with graphite/glass fiber volumetric ratio of 1:1 shows poor fatigue capability compared to the uniformly distributed $\pm$ 45° hybrids. This correlates with the earlier findings (figures 9 through 11) for statically tested hybrids. The glass plies, with high strain capability, appear to provide some resistance to overall crack propagation in the hybrid. Comparison of Tables X and XI shows that there were some unintentional failures of $\pm$ 45° specimens while the 0° $\pm$ 45° hybrids successfully survived the number of cycles. This was obviously due to the presence of 0° plies in the latter specimens. Both these were uniformly distributed hybrid specimens. In addition, there were practically no cracks found in the 0° $\pm$ 45° specimens even though the specimens were subjected to similar cyclic stresses. In fact Figs. 12 and 13 are similar to photomicrographs of specimens taken after 5×10^5 cycles $\pm$ 2.0 ksi.

Study of Figures 14 through 18 show the effectiveness of the presence of S-glass fibers. Hybrids with graphite/glass fiber volumetric ratio of 1:1 show hardly any cracking. When the glass fiber volume was reduced to 33% of the total fiber volume (2:1 graphite/glass hybrids), cracking becomes very evident at 10^5 cycles (figures 14, 15 and 16). When the glass fiber volume is reduced to 25% of the total fiber volume (3:1 graphite/glass

hybrids), the cracking is very extensive even at 10^4 cycles (Figures 17 and 18) almost to failure.

4.4 Modulus Degradation due to Fatigue Stress Cycling

HMS graphite was chosen in place of Modmor II graphite to study degradation of unidirectional hybrid modulus with stress cycling. The same resin system, PR 286, as well as S-glass were retained. Unidirectional (0°) graphite composites were employed as the control or baseline data point for this series of tests. Hybrids were limited to one ratio of graphite/glass fiber volume, i.e, 1 to 1. In addition modulus degradation of 0° $\pm$ 45° Modmor II/S-glass hybrids for all the three fiber volumetric ratios was under taken.

Table XIII and XIV show 0° PR 286/HMS graphite and 0° PR 286/HMS graphite/S-glass hybrids respectively prior to and after 2 x 10^6 stress cycles. The maximum stress ($R = 0.1$) per cycle ranged from 45 to 53 ksi representing 58 to 69 percent of the ultimate tensile strength in the case of HMS Graphite/epoxy and 37 to 43 percent in the case of the graphite/glass/epoxy hybrids.

It can be seen from these tables that the residual ultimate tensile strength dropped by about 7% for the 0° HMS graphite composite after stress cycling whereas the drop is about 27% for the 0° hybrid composite after stress cycling. However, there appears to be no significant degradation in modulus in either case. But the ultimate strain capability of the hybrid appears to be reduced by 28% due to stress cycling whereas there is no such change in the HMS graphite composite.

It is interesting to note that the fatigue life S-N curve for the 1:1 unidirectional PR 286/HMS graphite/S-glass hybrid falls close to that of the unidirectional PR 286/graphite (See Fig. 19). Recall that the 0° (1:1) PR 286/Modmor II graphite/S-glass hybrid fatigue performance was significantly lower than

Table XIII

EFFECT OF FATIGUE STRESS CYCLING ON STATIC TENSILE PROPERTIES OF
0° PR-286/HMS GRAPHITE COMPOSITES

No. of Fatigue Stress Cycles (R=0.1) Prior to Tests	No. of Plies	Specimen Number	Specimen Thickness (in.)	σ_{ult} ksi	ε_{ult} (μ-in/in)	E (psi x 10^6)	ν (in/in)
None	6	0-TM-1	0.030	77.3	2550	30.3	0.29
		0-TM-2	0.031	75.8	2400	31.5	0.20
		C-TM-3	0.031	78.1	2450	31.3	0.33
		Average		77.1	2466	31.0	0.27
2×10^6	6	0-TM-10	0.032	75.0	2700	28.4	0.37
		0-TM-11	0.032	66.8	2200	30.2	0.37
		0-TM-12	0.031	74.2	2400	32.4	0.20
		Average		72,0	2430	30.3	

Table XIV

EFFECT OF FATIGUE STRESS CYCLING ON STATIC TENSILE
PROPERTIES OF 0° PR-286/HMS GRAPHITE/S-GLASS COMPOSITES (1:1)

No. of Fatigue Stress Cycles (R=0.1) Prior to Test	No. of Plies Graphite + Glass	Specimen Number	Specimen Thickness (in.)	σ_{ult} ksi	E (psi x 10^6)	ε_{ult} (μ-in/in)	ν (in/in)
None	1:1 (2 + 2) = 4	0-TM-1-1	0.036	134	21.4	6200	0.27
		0-TM-1-2	0.035	123	21.6	5700	0.25
		0-TM-1-3	0.036	108	21.4	4950	0.25
		Average		122	21.5	5620	0.25
2.0×10^6	1:1 (2 + 2) = 4	0-TM-1-10	0.039	88.5	21.5	4300	0.26
		0-TM-1-11	0.036	82.0	22.8	3500	0.21
		0-TM-1-5	0.037	95.4	21.7	4350	0.24
		Average		88.6	22.0	4050	0.24

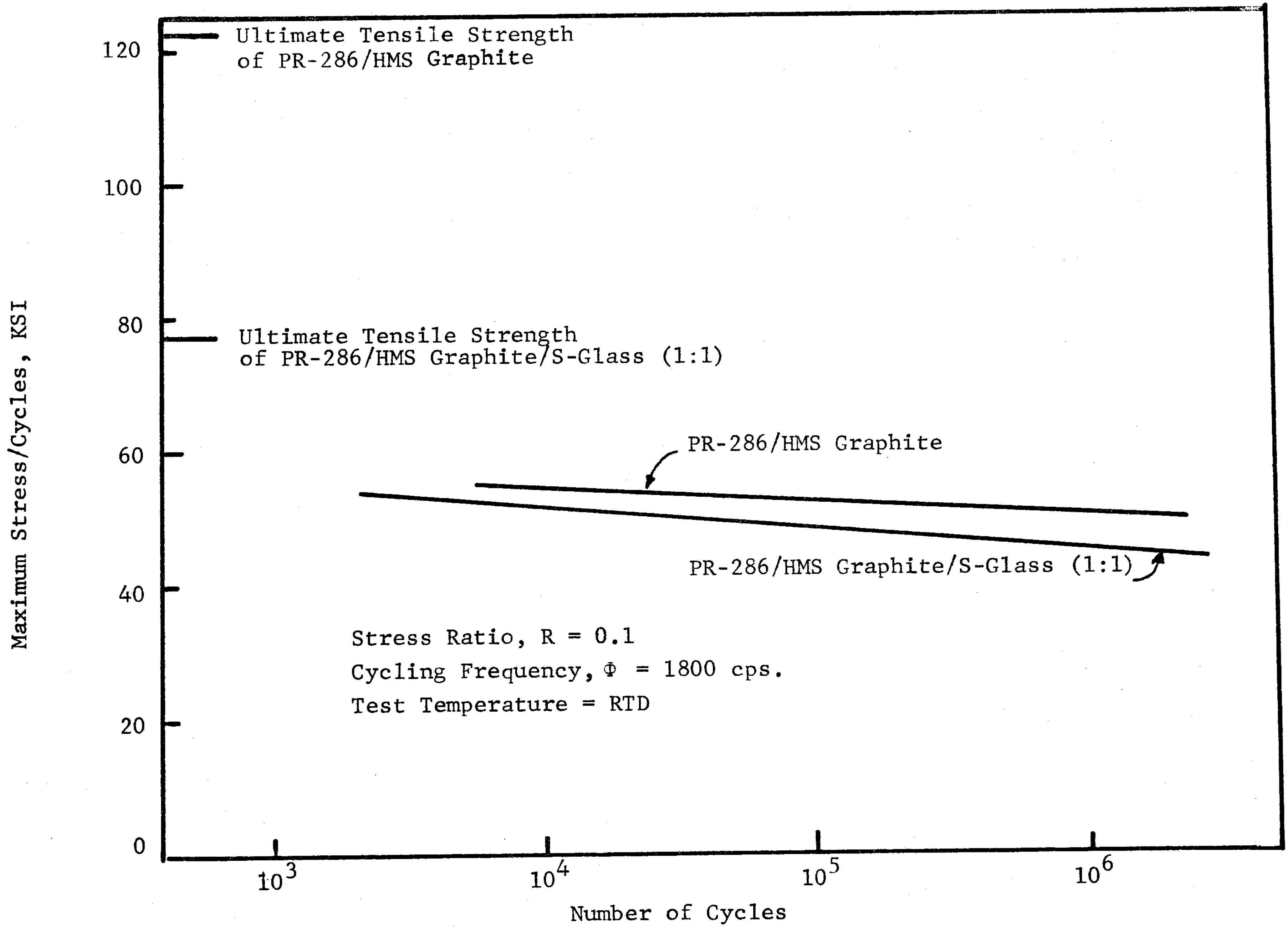

FIG. 19 SUMMARY TENSION FATIGUE LIFE S-N DIAGRAMS FOR 0° PR-286/HMS GRAPHITE AND PR-286/HMS GRAPHITE/S-GLASS COMPOSITES (1:1)

the corresponding graphite/epoxy composite.

Table XV shows the compiled data for the 0° ± 45° PR 286/ Modmor II graphite/S-Glass hybrids prior to and after stress cycling (between 2×10^6 to 2.5×10^6 cycles, R = 0.1). The maximum stresses per cycle were 70 ksi (or 67% σ_{ult}) for graphite/glass fiber volume ratio 1:1, 90 to 93 ksi (or about 78% σ_{ult}) for 2:1 specimens and 142 ksi (or 100% σ_{ult}) for 3:1 specimens.

The data indicate that there is no significant reduction in ultimate tensile strength of 0° ± 45° hybrid (Modmor II) composites due to stress cycling. It also appears that the modulus is unaffected and that there is no significant change in ultimate strain capability due to stress cycling.

Table XV

EFFECT OF FATIGUE STRESS CYCLING ON STATIC TENSILE PROPERTIES

OF (0°$\pm$45°) PR-286/MODMOOR II GRAPHITE/S-GLASS COMPOSITES

No. of Fatigue Stress Cycles (R=0.1) Prior to Test	Volumetric Ratio of Graphite/Glass and No. of Plies	Specimen Number	Specimen Thickness (in.)	σ_{ult} ksi	ε_{ult} (μ-in/in)	E (psi x 10^6)	ν (in/in)
None	1:1 (4 + 4) = 8		Average*	104	7000	14.6	
2.05 x 10^6		045-T-1-5	0.044	98.5			
None	2:1 (8 + 4) = 12		Average*	118	6820	17.0	0.48
2.5 x 10^6		045-T-2-4	0.069	117	6978	16.7	0.43
		045-T-2-6	0.070	127	6800	18.0	0.45
None	3:1 (12 + 4) = 16		Average*	140	7405	18.7	0.44
2.3 x 10^6		045-T-3-4	0.097	142	7100	18.7	0.39

* From Static Test Data

SECTION V

5.0 CONCLUSIONS AND RECOMMENDATIONS

The following conclusions are drawn as a result of this study:

1. From the study of static and fatigue tests conducted on selected graphite/glass/epoxy hybrid composites and from the review of existing literature, it is concluded that hybrid composites perform generally satisfactorally in fatigue and will survive rigorous stress cycling.

2. Of the two systems examined, namely uniformly distributed interply hybrids and core shell hybrids, the first appears to provide a better mechanical performance. The alternation of S-glass plies providing high strain capability with the higher stiffness contributed by the graphite fiber achieves a more integral hybrid composite. Under static loads the evenly distributed cracks indicate better load distribution. In the core-shell hybrids, a severe modulus mismatch at the interface between the glass core and the graphite shell creates high interlaminar shear stresses thus promoting early failures. In fatigue the sudden and often early failures indicated a general lack of integrity in core-shell hybrids.

3. Static tensile tests of 0° PR 286/Modmor II graphite/S-glass specimens indicate substantially the effectiveness in the use of the rule of mixtures to predict elastic moduli of the hybrids. The ultimate strain capability of the hybrids is limited by that of the graphite phase.

4. The 0° ± 45° PR 286/Modmor II graphite/S-Glass hybrids behave statically similar to the unidirectional hybrids. The 90° behavior cannot be predicted strictly from a rule of mixtures.

5. The fatigue resistance of 0° PR 286/Modmor II Graphite/S-glass hybrid remains substantial even when 50 percent of the fiber volume consists of glass. The loss of hybrid composite fatigue life due to 50% replacement of graphite fibers by glass is relatively small when the cost savings that can be achieved are considered. This conclusion is also applicable to 0° $\pm$ 45° fiber orientation hybrids.

6. The superiority of uniformly distributed hybrids over core-shell hybrids also became evident in fatigue properties. The $\pm$ 45° (1:1) core-shell hybrids showed very poor fatigue capability.

7. The effectiveness of high strain capability S-Glass in uniformly distributed graphite/glass interply hybrids was demonstrated by microscopic study. Thus the off-axis laminates (0° $\pm$ 45°) clearly perform better in fatigue as the glass fiber volume percent increases. At 50 V% glass no fatigue cracks are evident at 2×10^6 cycles; at 33 V% glass, fatigue cracks first appear at 10^5 cycles and finally at 25 V% glass, fatigue cracks are evident, even at 10^4 cycles.

8. The fatigue life of 0° HMS graphite/S-glass is not substantially reduced with the addition of S-glass whereas in the case of 0° HTS Graphite/S-glass composites, a greater reduction is encountered.

9. Static residual ultimate tensile strength tests on unidirectional high modulus graphite/S-glass hybrids suggest that while there is some reduction in strength and ultimate strain capability of hybrids as compared to graphite glass composites due to fatigue stress cycling, the moduli remain essentially the same.

10. It appears that there is very little reduction in residual ultimate tensile strength and strain or modulus of 0° ± 45° Modmor II graphite/S-glass hybrids due to fatigue stress cycling.

The following recommendations for future study are made on the basis of the above conclusions:

1. With the feasibility of hybrid composites using graphite and glass plies with a common resin system clearly established, further work is required to form a design data base.

2. Further investigation of the mechanisms which account for the differences in fatigue behavior of HMS and HTS graphite hybrid composites with glass is needed.

3. The present study was concerned primarily with the tensile fatigue ($R = 0.1$) behavior of hybrid composites. It is also necessary to investigate their behavior under fully reversed ($R = -1$) cyclic loading.

4. The work in the present investigation was related to interply hybrids. It is important to examine whether the conclusions arrived at from the tests can also be extended to intraply hybrid composites, using a mixture of two fibers in a single ply.

5. Quasi-isotropic hybrid laminates should be investigated because of their importance to general structural components.

References

1. Evensen, H.R., "Boron/Graphite Hybrid Composite Development Study" Whittaker Corporation, Final Report, August, 1970, NASA Contract No. NAS 8-24510.

2. Pinckney, R.L. and Freeman, R.B., "Determination of Physical and Structural Properties of Mixed-modulus Composite materials" The Boeing Company Technical Report No. USA AVL ABS 71-7 June, 1971, U.S. Army Mobility Research and Development Laboratory Contract No. DAA J02-69-C-0059.

3. Rao, N. and Hofer, K. E., "An Investigation of Fatigue Behavior of Reinforced Plastics for Primary Aircraft Structures", IITRI Report D6010 to Naval Air Systems Command, February, 1970.

4. Novak, R. C. and DeCrescente, M.A., "Impact Behavior of Unidirectional Resin Matrix Composites Tested in the Fiber Direction", Composite Materials: Testing and Design, (Second Conference), ASTM STP497, American Society for Testing and Materials, 1972, pp. 311-323.

5. Chamis, C.C., Hanson, M.P. and Serafini, T.T., "Impact Resistance of Unidirectional Fiber Composites", Composite Materials: Testing and Design (Second Conference), ASTM STP497, American Society for Testing and Materials, 1972, pp. 324-349.

APPENDIX A

STATIC AND FATIGUE TEST DATA

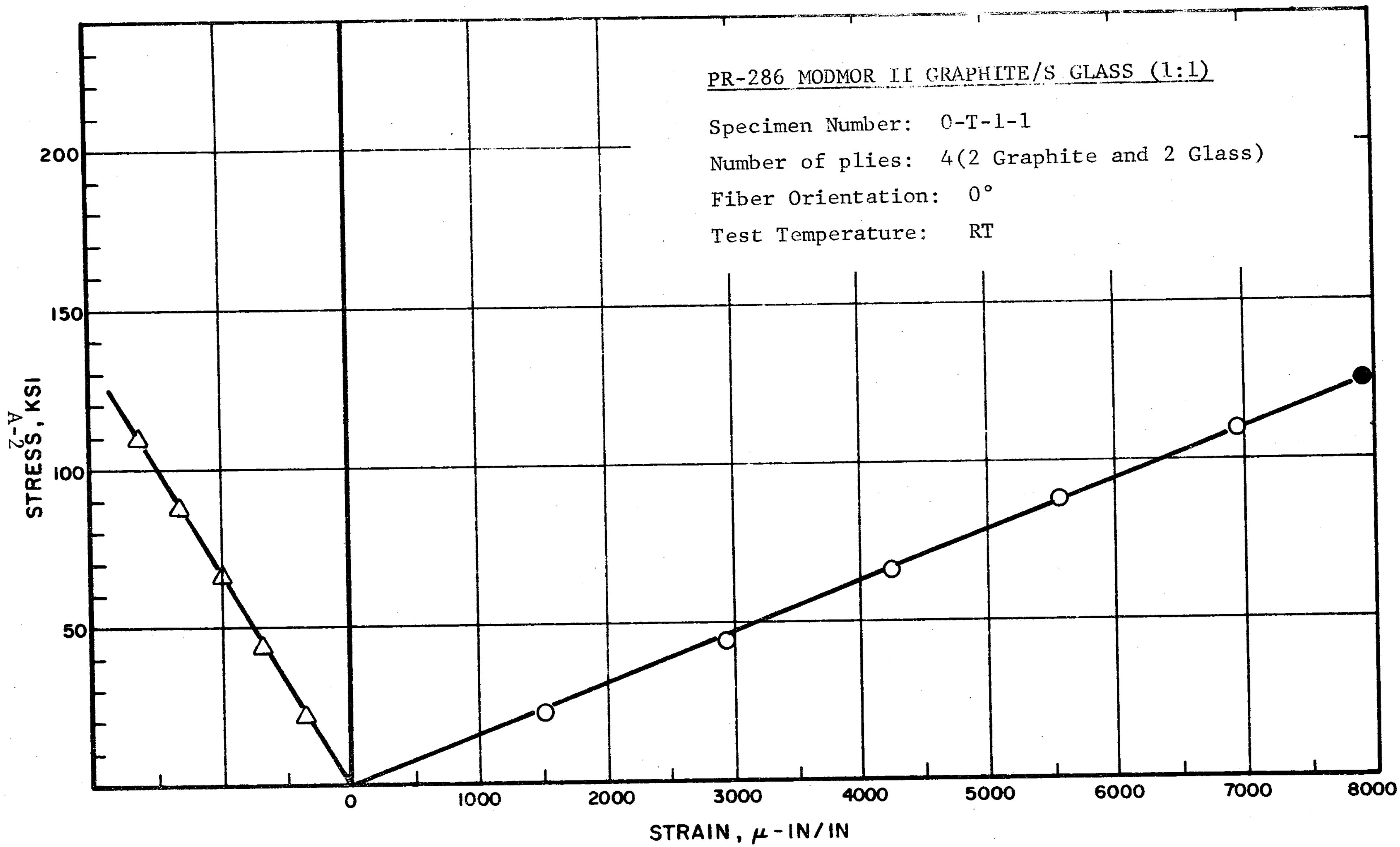

Fig. A-1 TENSION STRESS STRAIN DIAGRAM FOR PR-286/MODMOR II GRAPHITE/S GLASS COMPOSITE (1:1) TESTED AT ROOM TEMPERATURE

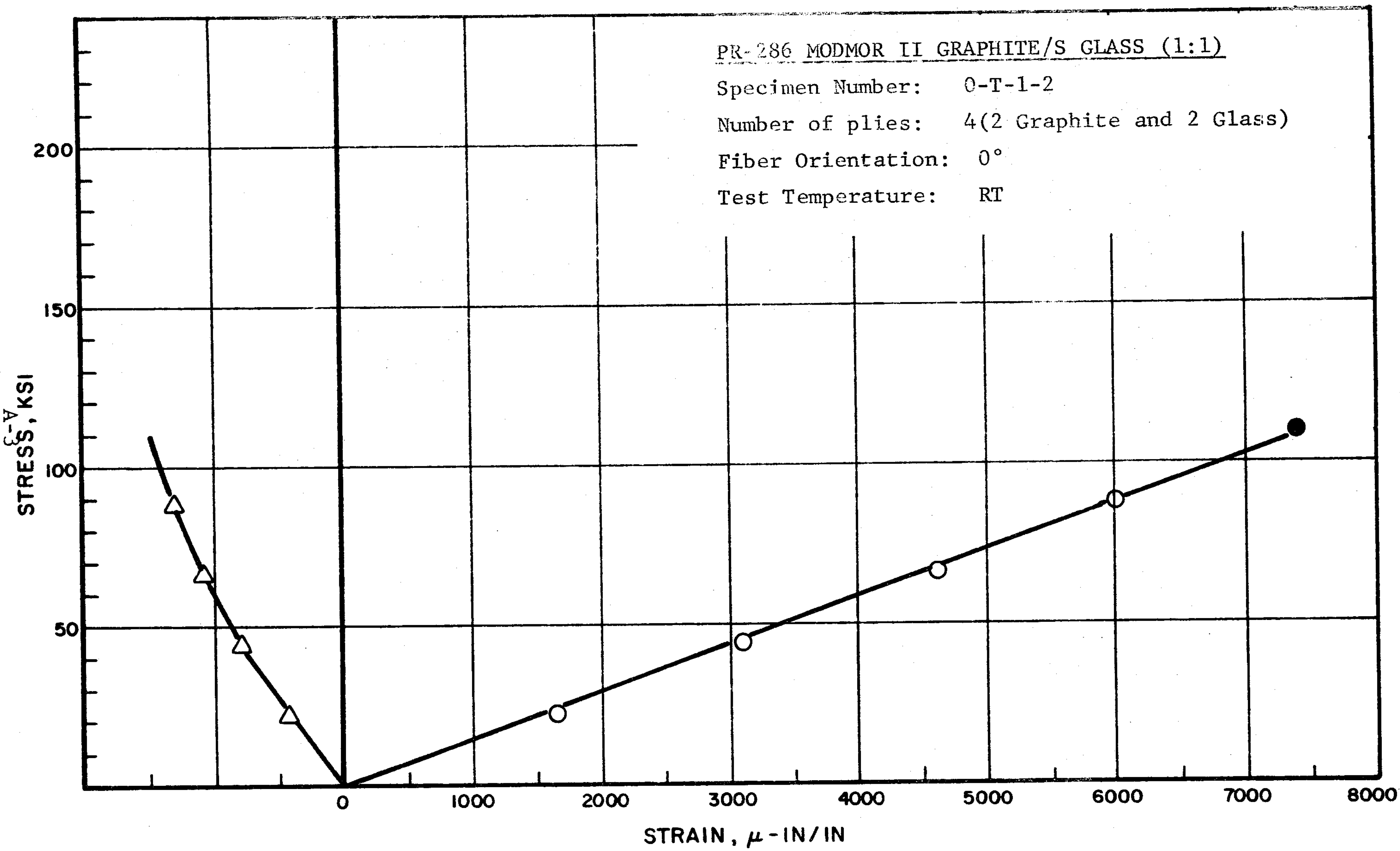

Fig. A-2 TENSION STRESS STRAIN DIAGRAM FOR PR-286/MODMOR II GRAPHITE/S GLASS COMPOSITE (1:1) TESTED AT ROOM TEMPERATURE.

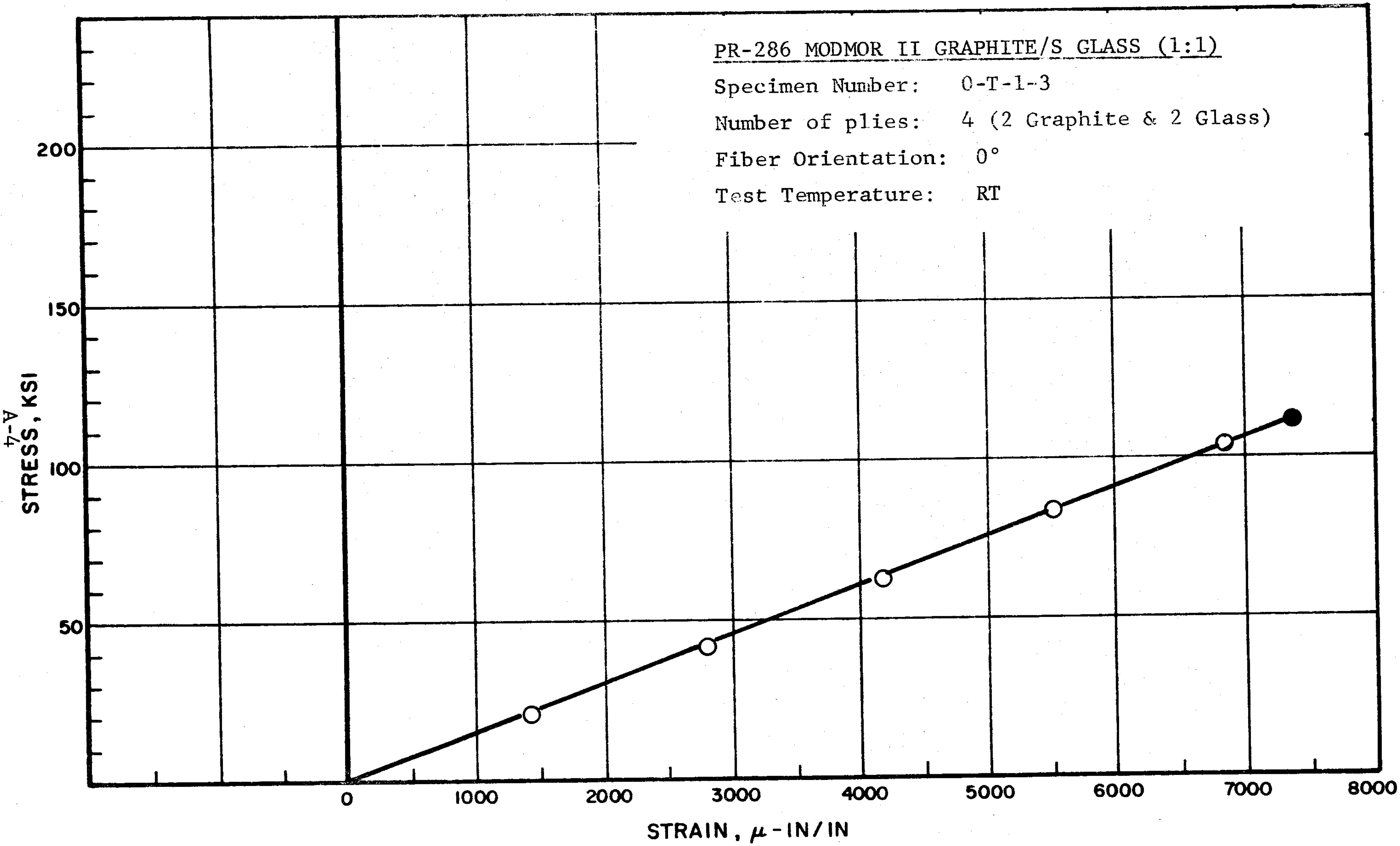

Fig. A-3 TENSION STRESS STRAIN DIAGRAM FOR PR-286/MODMOR II GRAPHITE/S GLASS COMPOSITE (1:1) TESTED AT ROOM TEMPERATURE

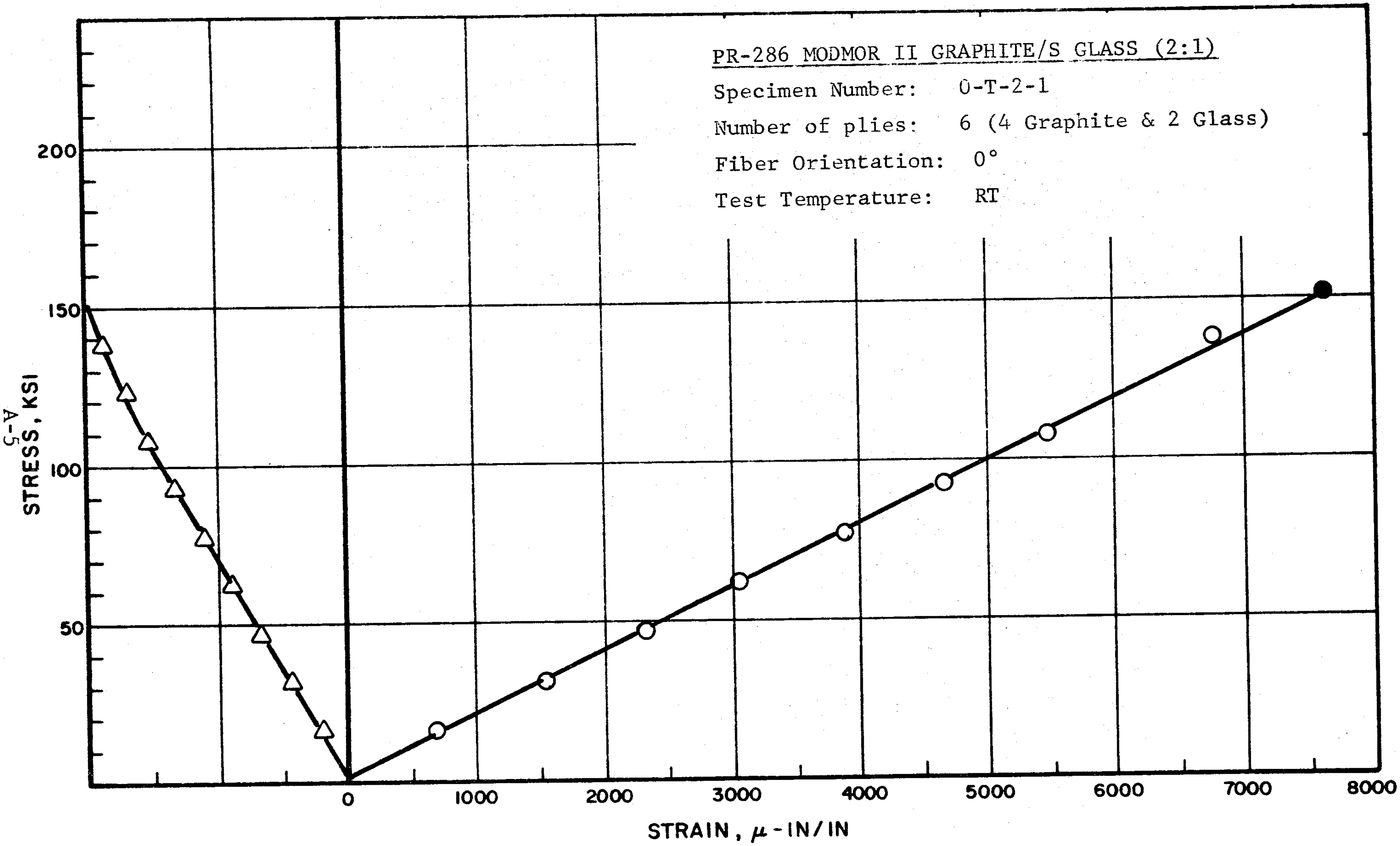

Fig. A-4 TENSION STRESS STRAIN DIAGRAM FOR PR-286/MODMOR II GRAPHITE/S GLASS COMPOSITE (2:1) TESTED AT ROOM TEMPERATURE

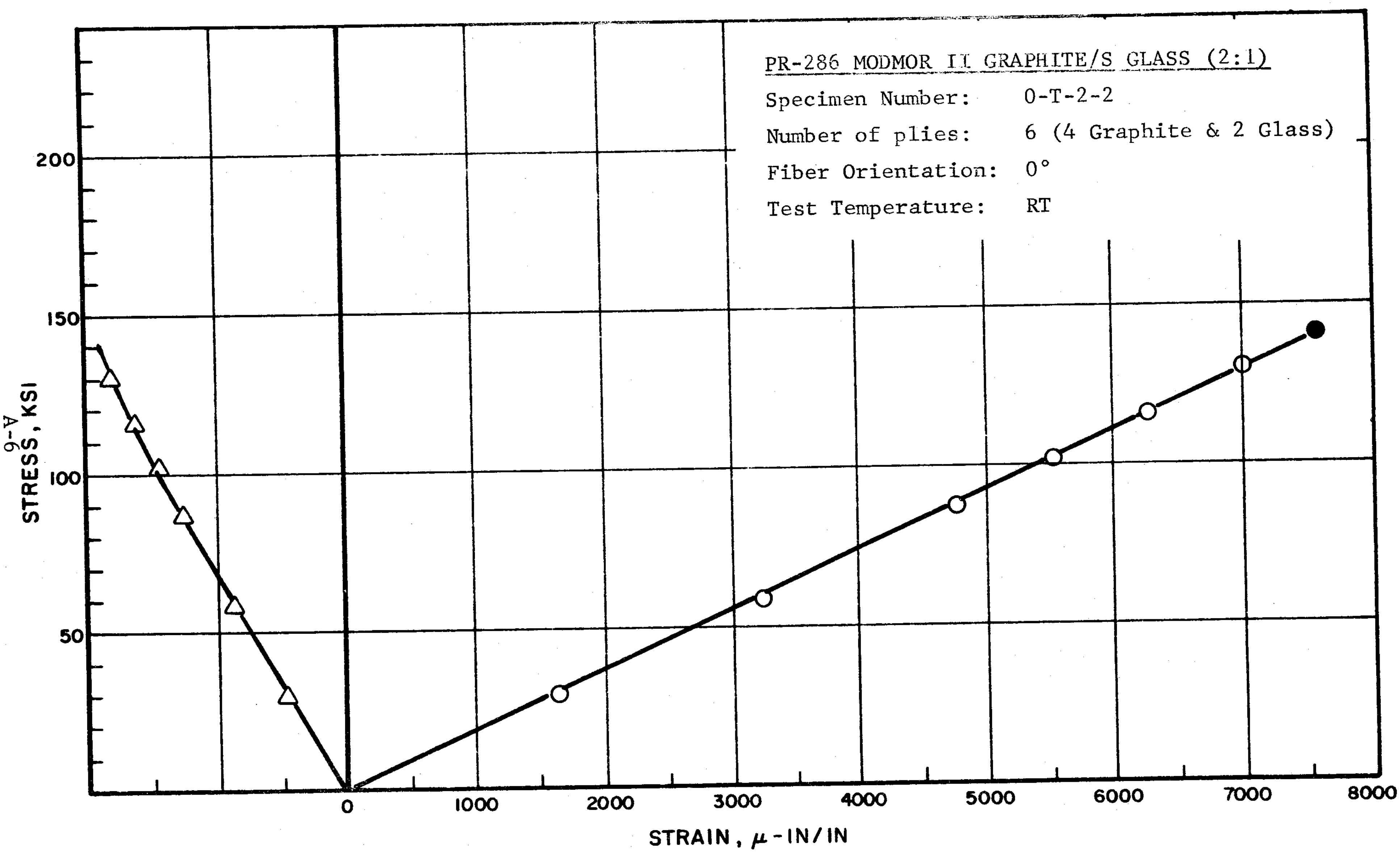

Fig. A-5 TENSION STRESS STRAIN DIAGRAM FOR PR-286/MODMOR II GRAPHITE/S GLASS COMPOSITE (2:1) TESTED AT ROOM TEMPERATURE

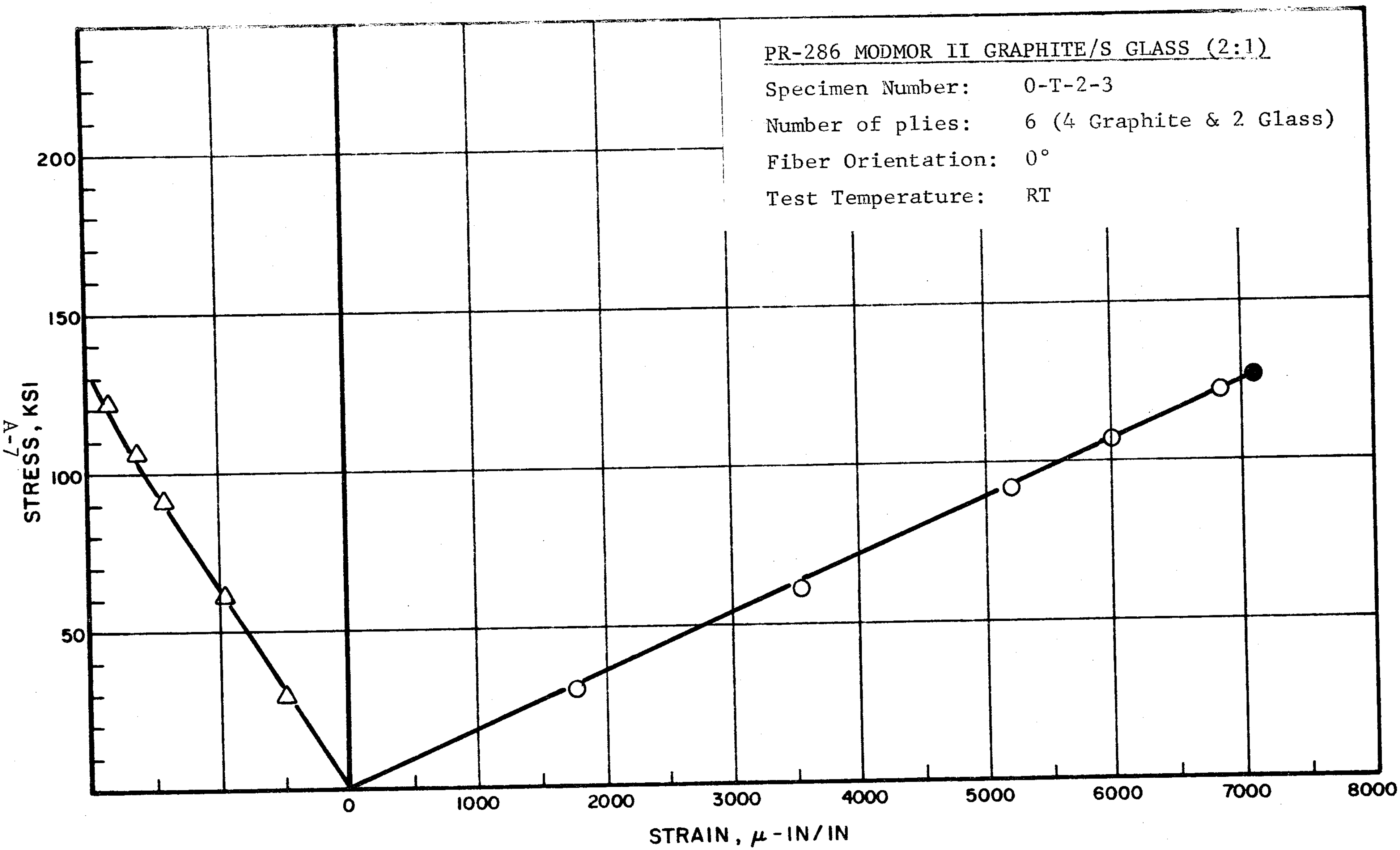

Fig. A-6 TENSION STRESS STRAIN DIAGRAM FOR PR-286/MODMOR II GRAPHITE/S GLASS COMPOSITE (2:1) TESTED AT ROOM TEMPERATURE

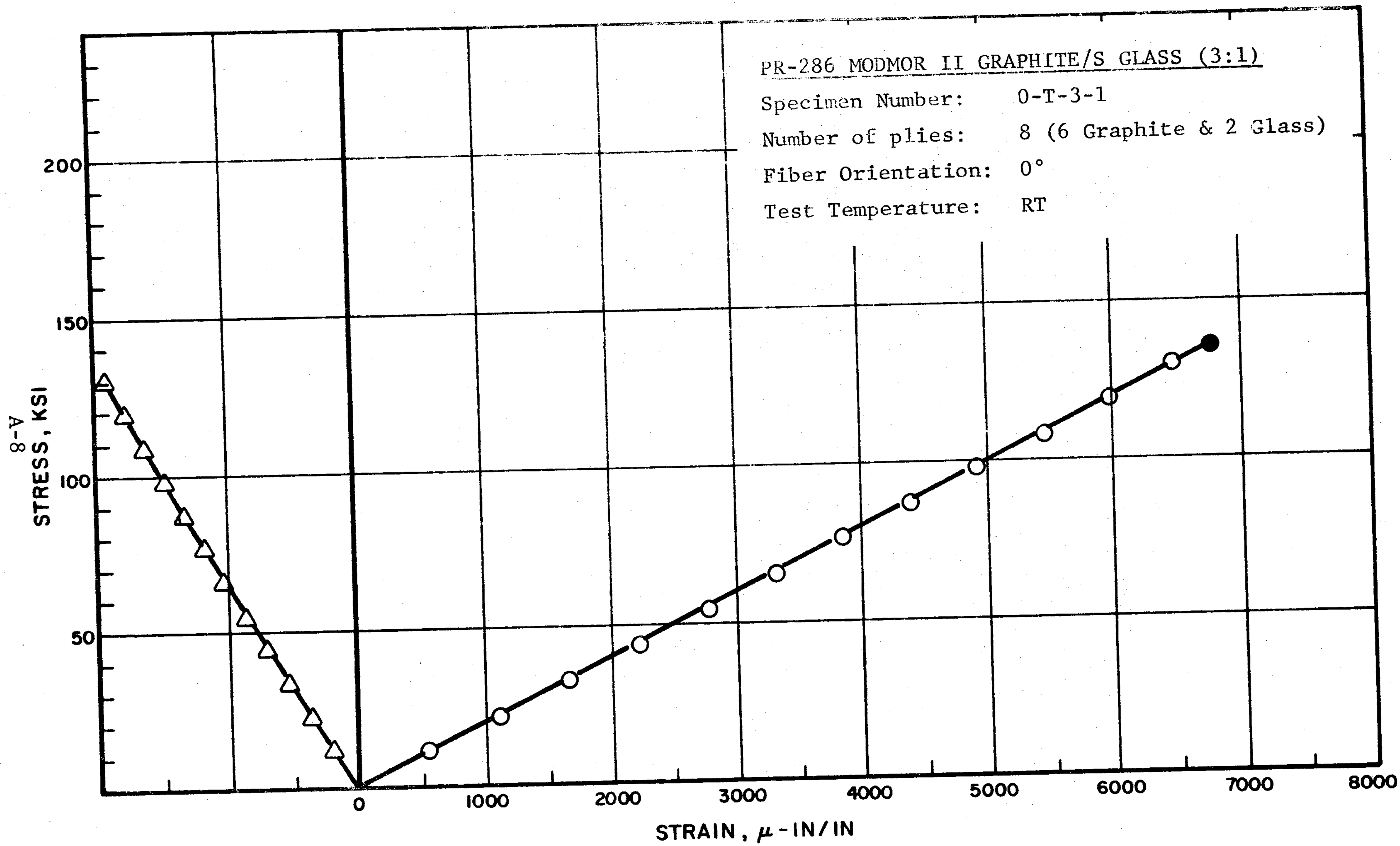

Fig. A-7 TENSION STRESS STRAIN DIAGRAM FOR PR-286/MODMOR II GRAPHITE/S GLASS COMPOSITE (3:1) TESTED AT ROOM TEMPERATURE

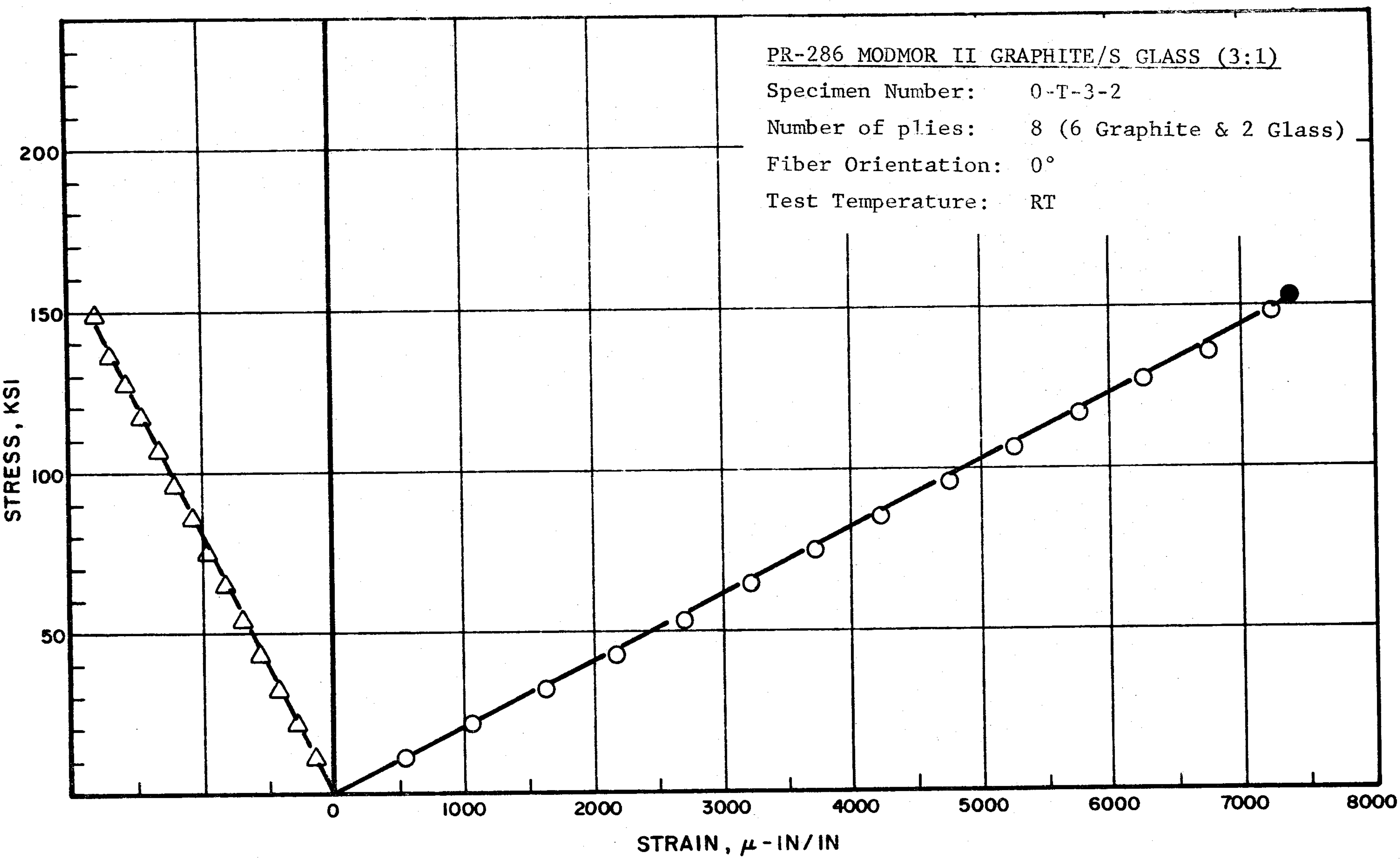

Fig. A-8 TENSION STRESS STRAIN DIAGRAM FOR PR-286/MODMOR II GRAPHITE/S GLASS COMPOSITE (3:1) TESTED AT ROOM TEMPERATURE

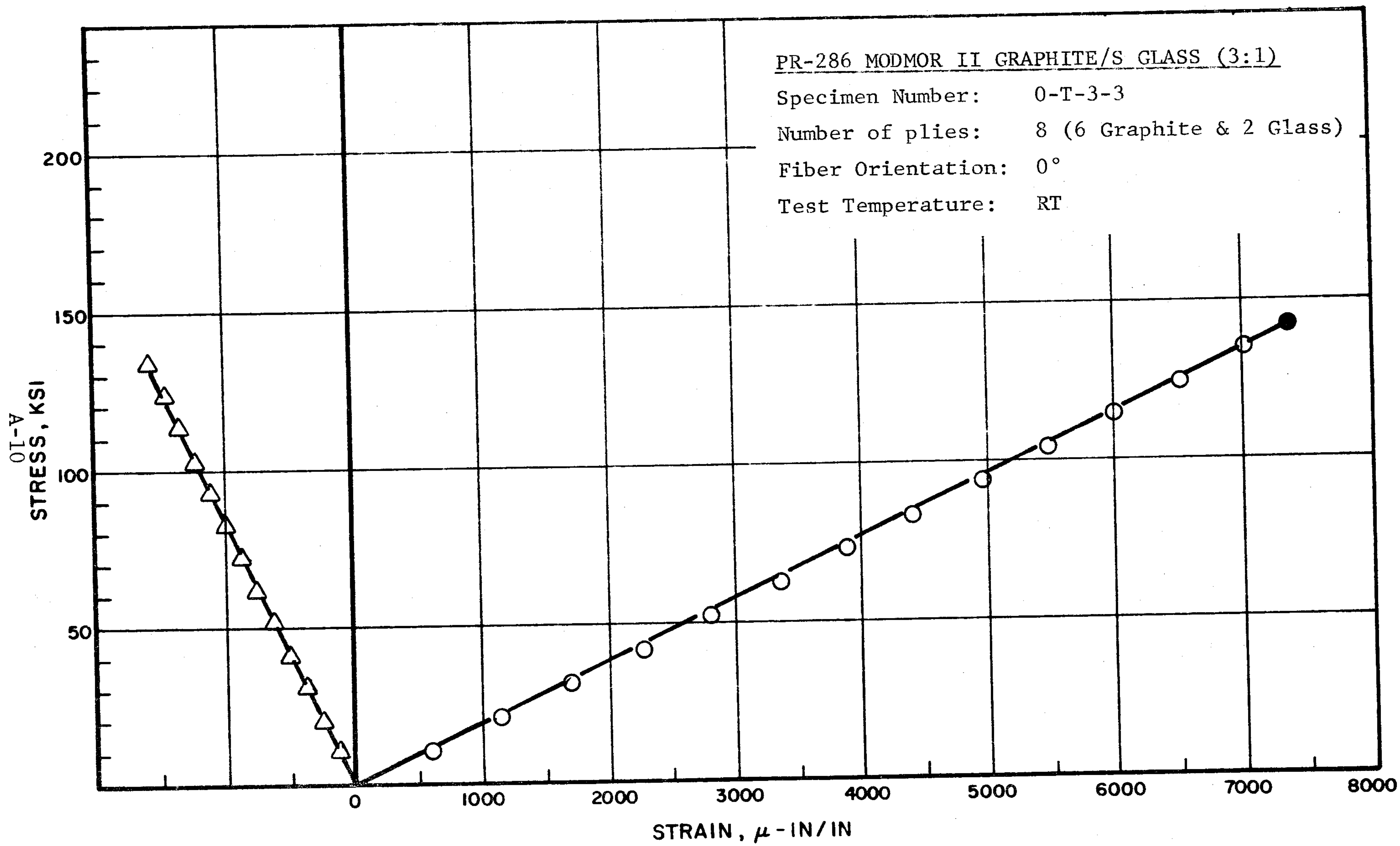

Fig. A-9 TENSION STRESS STRAIN DIAGRAM FOR PR-286/MODMOR II GRAPHITE/S GLASS COMPOSITE (3:1) TESTED AT ROOM TEMPERATURE

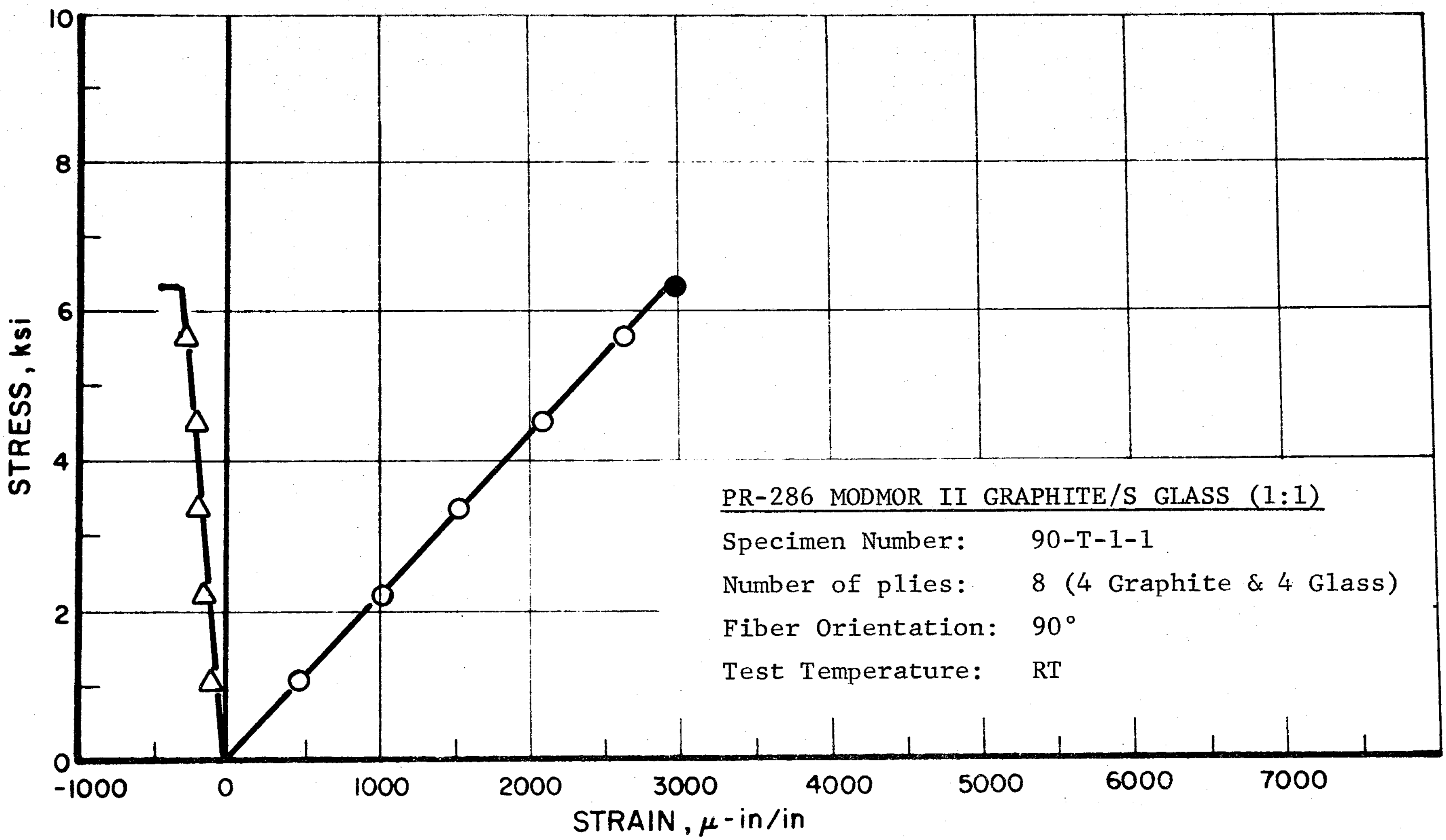

Fig. A-10 TENSION STRESS STRAIN DIAGRAM FOR PR-286/MODMOR II GRAPHITE/S GLASS COMPOSITE (1:1) TESTED AT ROOM TEMPERATURE

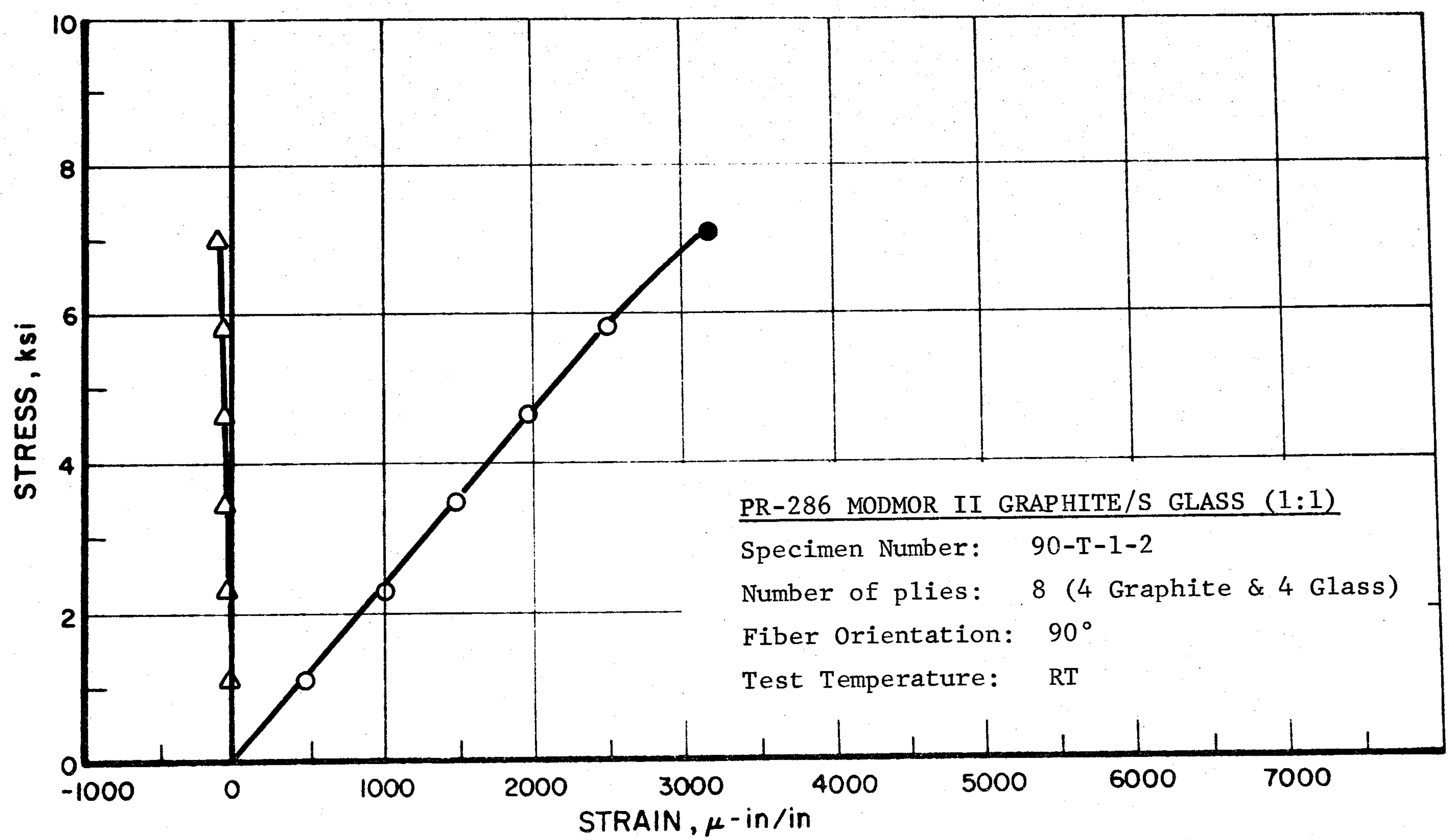

Fig. A-11 TENSION STRESS STRAIN DIAGRAM FOR PR-286/MODMOR II GRAPHITE/S GLASS COMPOSITE (1:1) TESTED AT ROOM TEMPERATURE

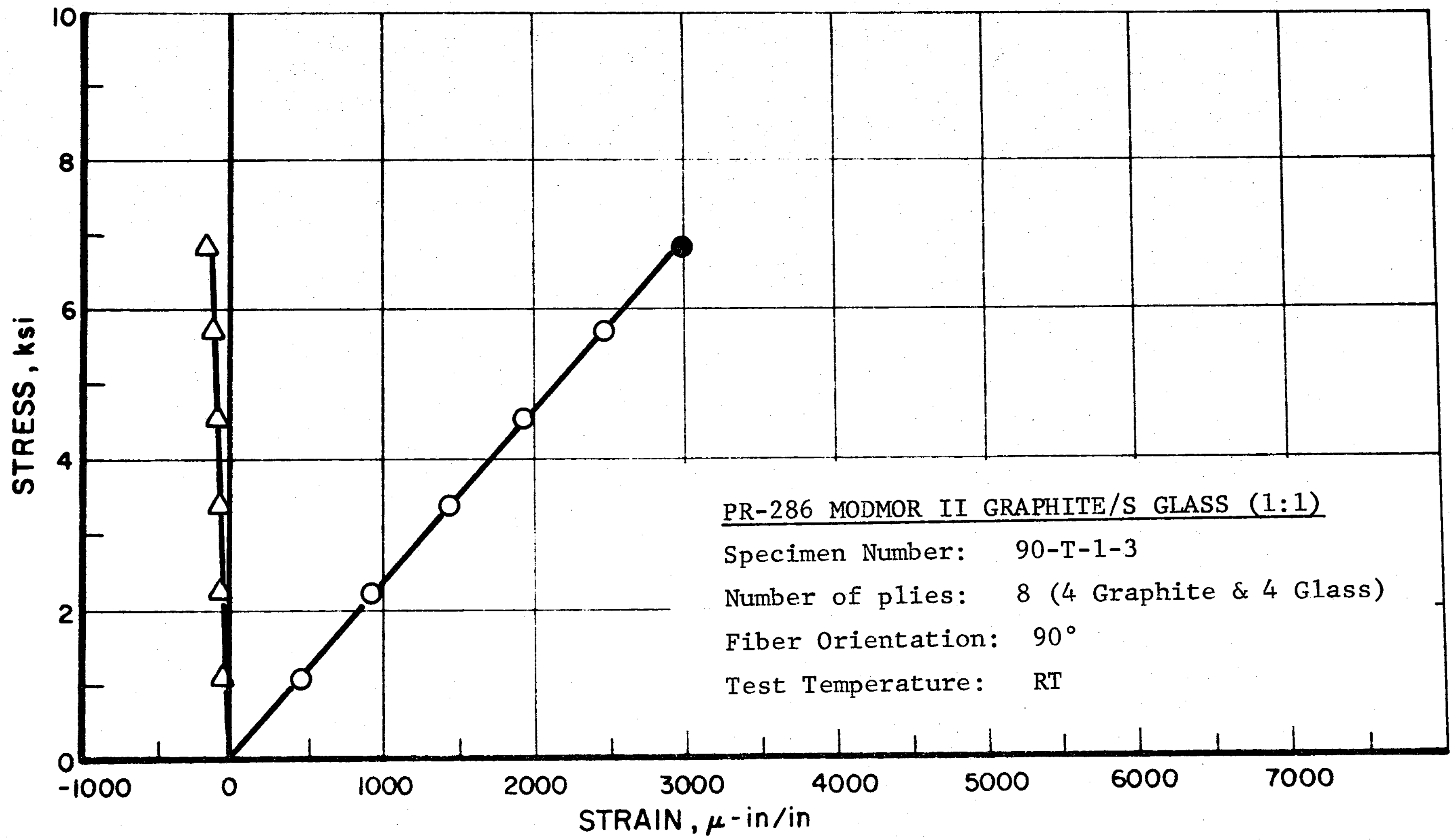

Fig. A-12 TENSION STRESS STRAIN DIAGRAM FOR PR-286/MODMOR II GRAPHITE/S GLASS COMPOSITE (1:1) TESTED AT ROOM TEMPERATURE

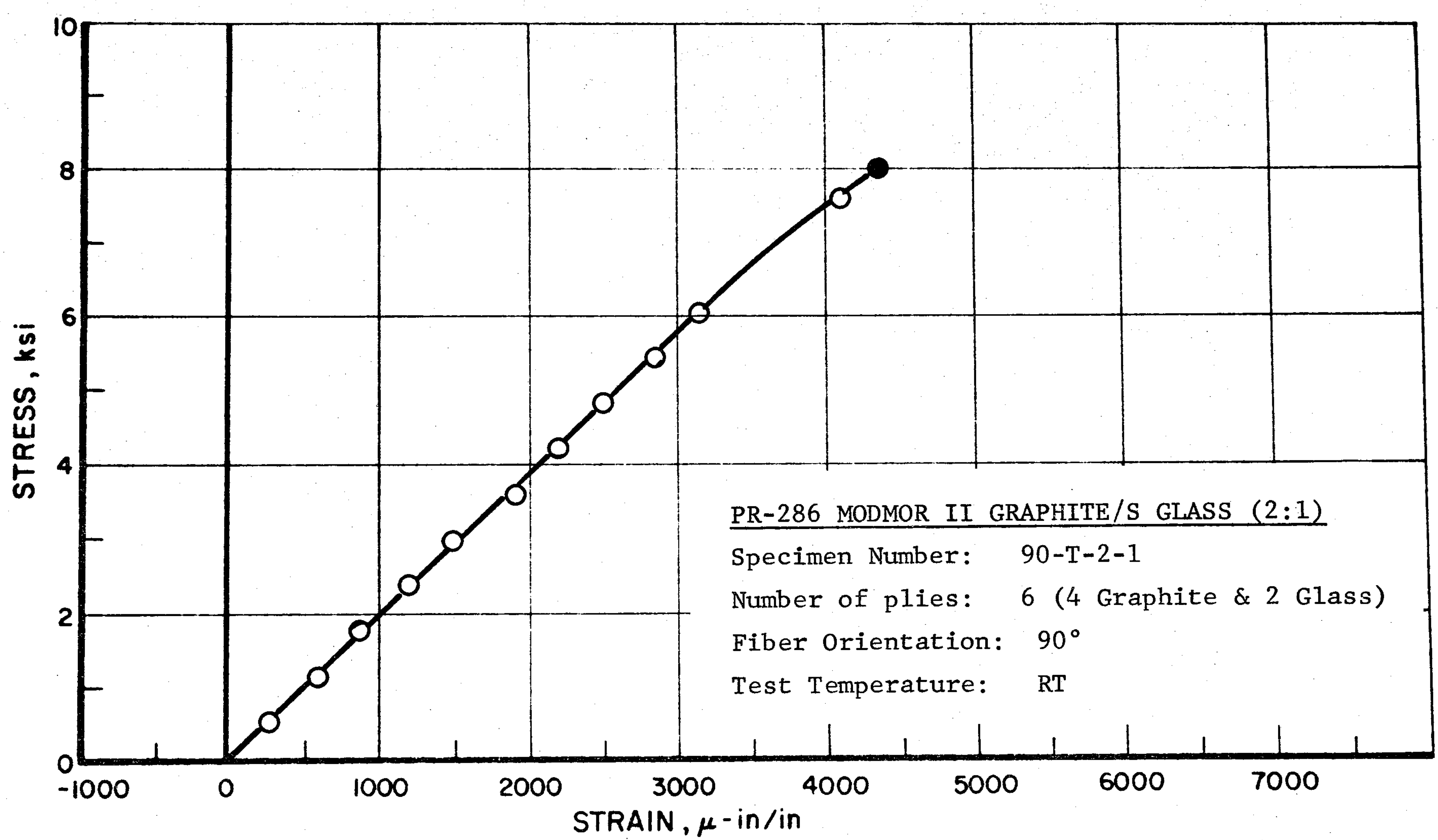

Fig. A-13 TENSION STRESS STRAIN DIAGRAM FOR PR-286/MODMOR II GRAPHITE/S GLASS COMPOSITE (2:1) TESTED AT ROOM TEMPERATURE

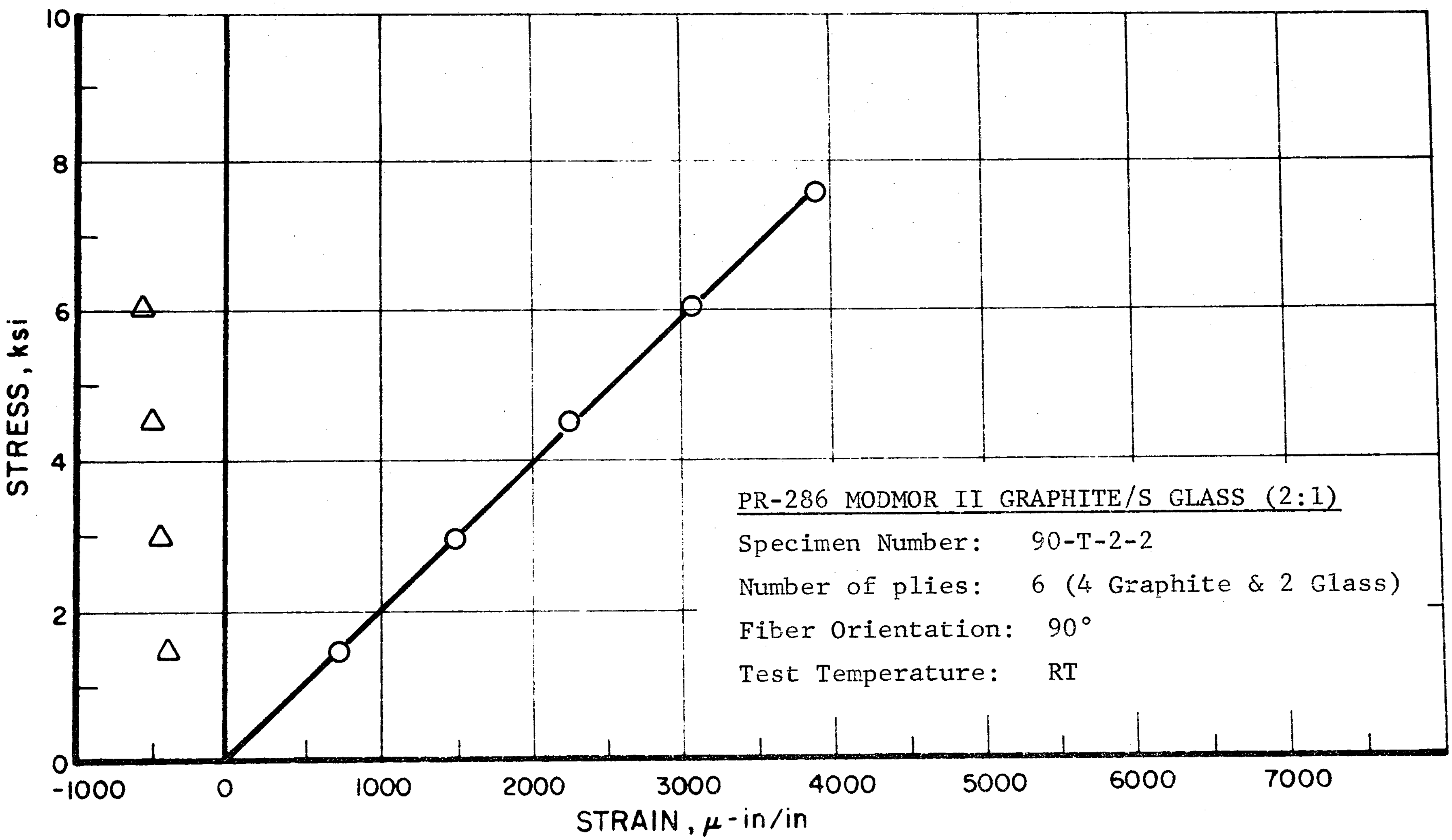

Fig. A-14 TENSION STRESS STRAIN DIAGRAM FOR PR-286/MODMOR II GRAPHITE/S GLASS COMPOSITE (2:1) TESTED AT ROOM TEMPERATURE

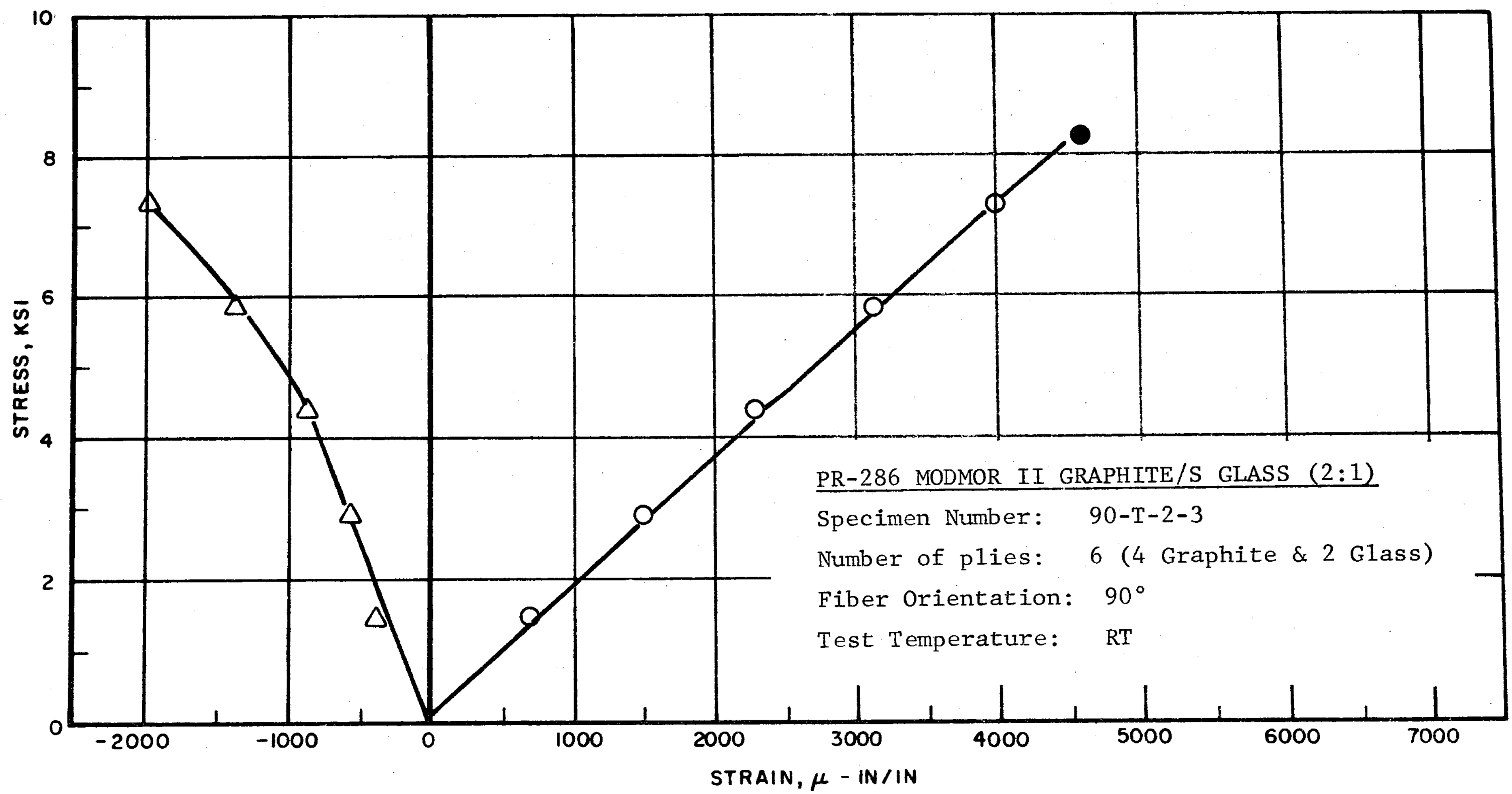

Fig. A-15 TENSION STRESS STRAIN DIAGRAM FOR PR-286/MODMOR II GRAPHITE/S GLASS COMPOSITE (2:1) TESTED AT ROOM TEMPERATURE

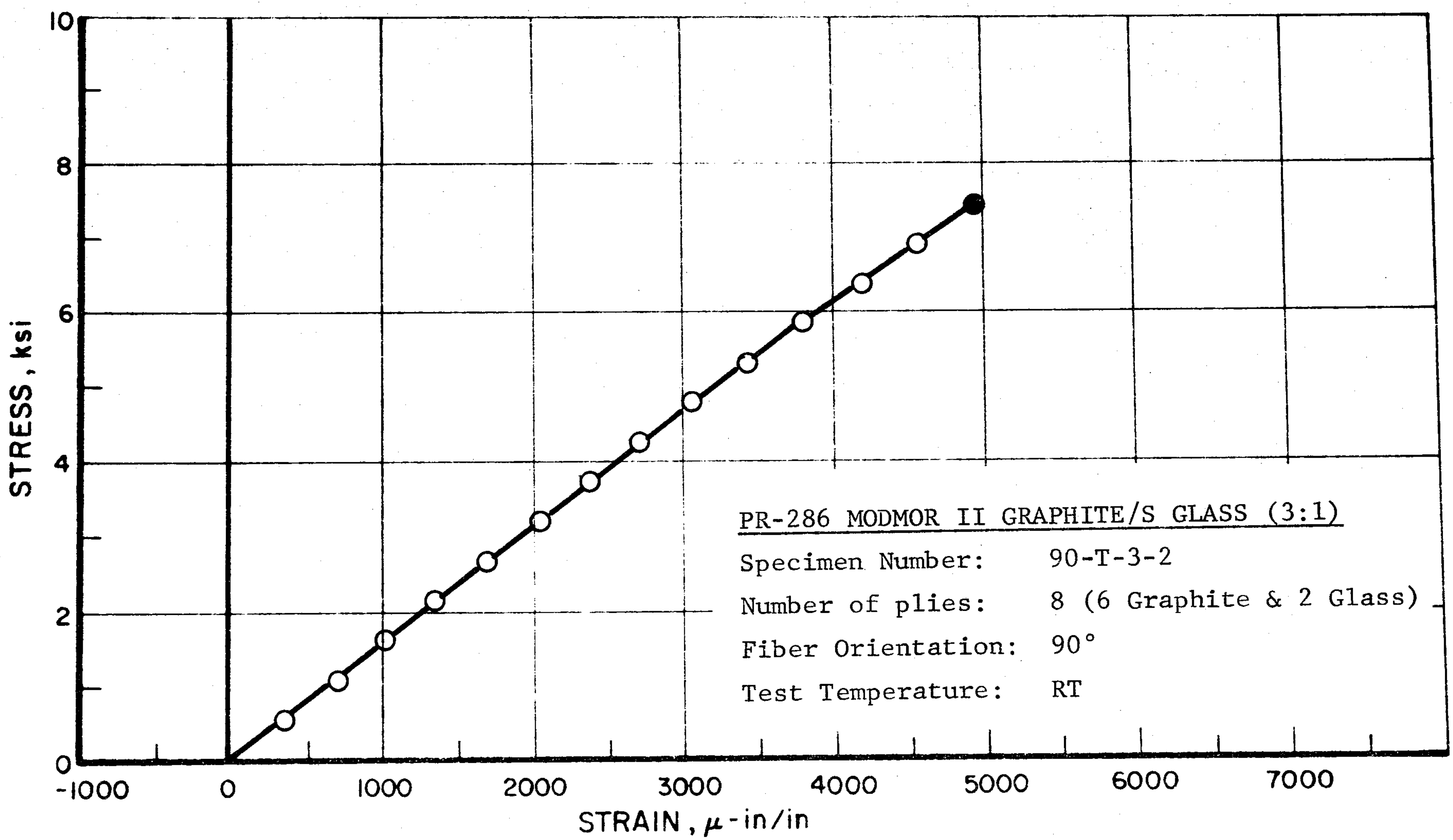

Fig. A-16 TENSION STRESS STRAIN DIAGRAM FOR PR-286/MODMOR II GRAPHITE/S GLASS COMPOSITE (3:1) TESTED AT ROOM TEMPERATURE

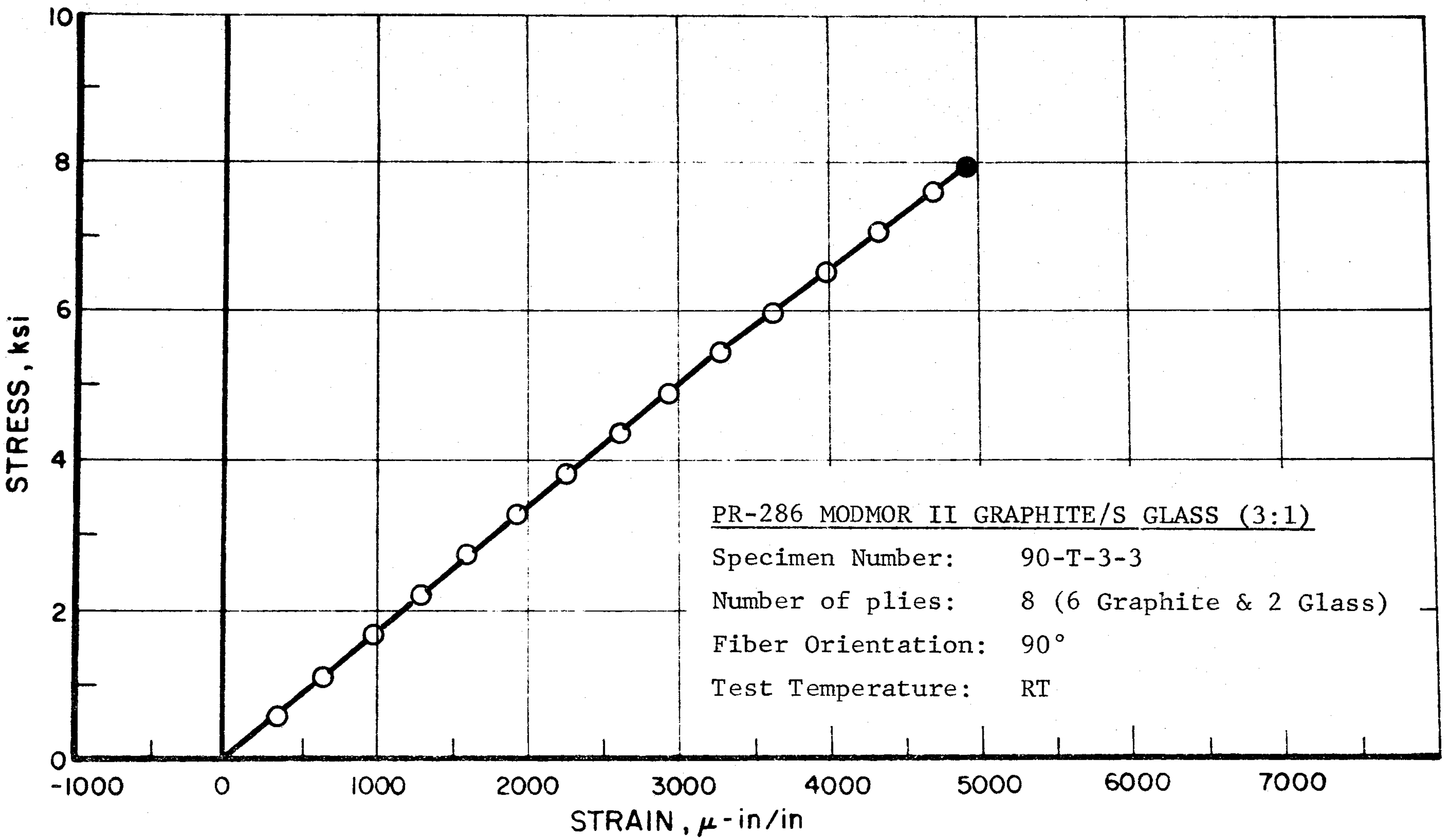

Fig. A-17 TENSION STRESS STRAIN DIAGRAM FOR PR-286/MODMOR II GRAPHITE/S GLASS COMPOSITE (3:1) TESTED AT ROOM TEMPERATURE

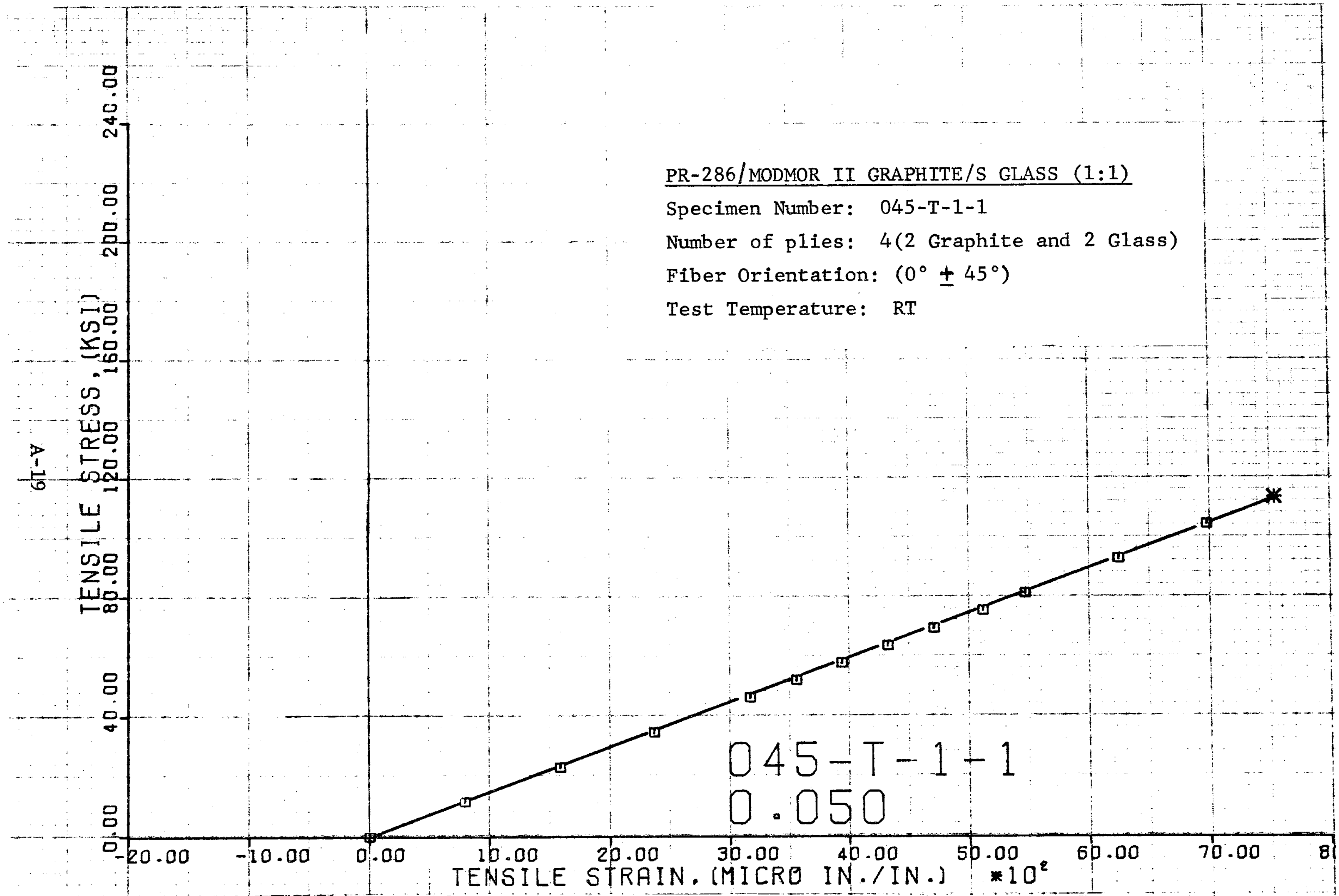

Fig. A-18 TENSION STRESS STRAIN DIAGRAM FOR PR-286/MODMOR II GRAPHITE /S GLASS COMPOSITE (1:1) TESTED AT ROOM TEMPERATURE

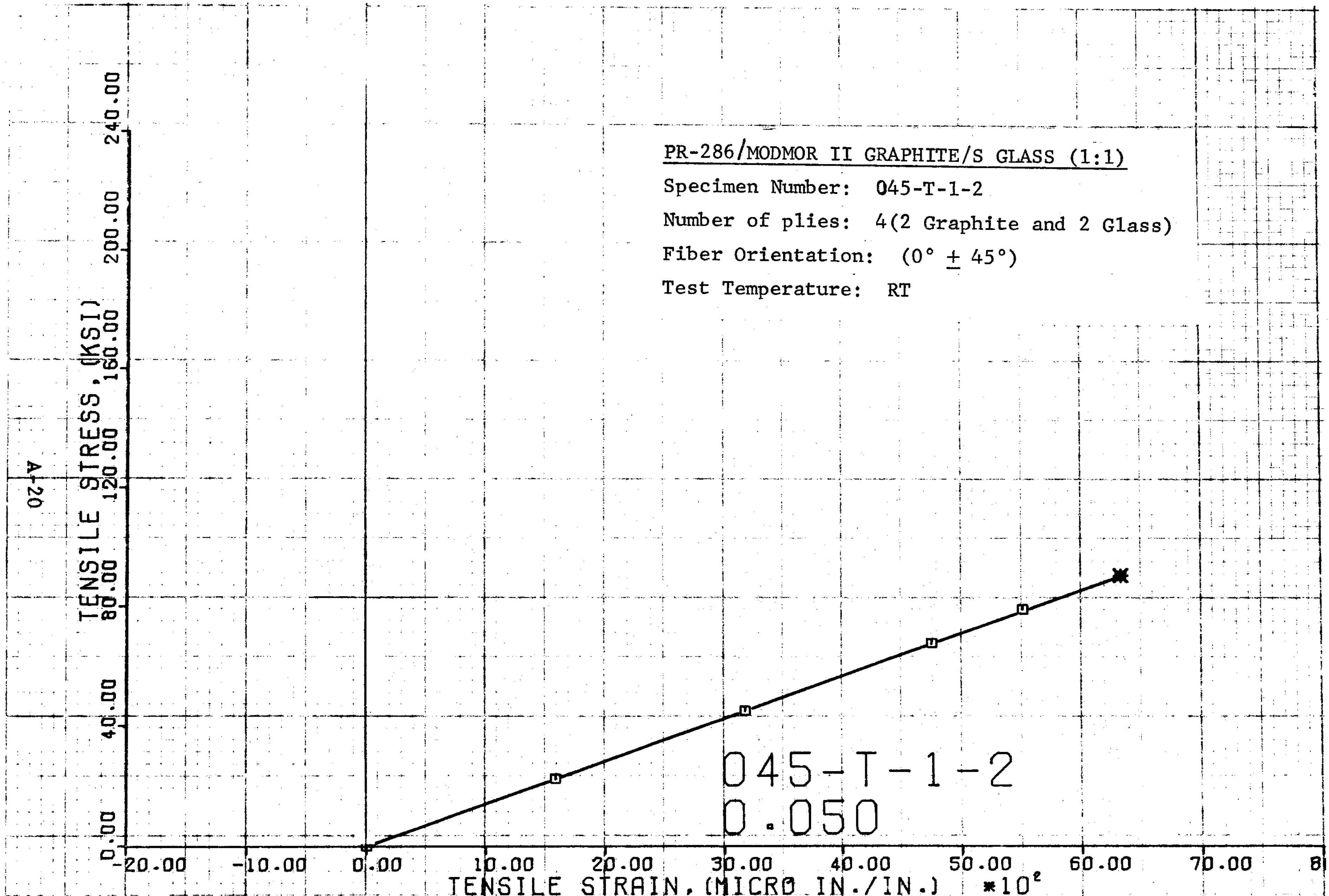

Fig. A-19 TENSION STRESS STRAIN DIAGRAM FOR PR-286/MODMOR II GRAPHITE/S GLASS COMPOSITE (1:1) TESTED AT ROOM TEMPERATURE

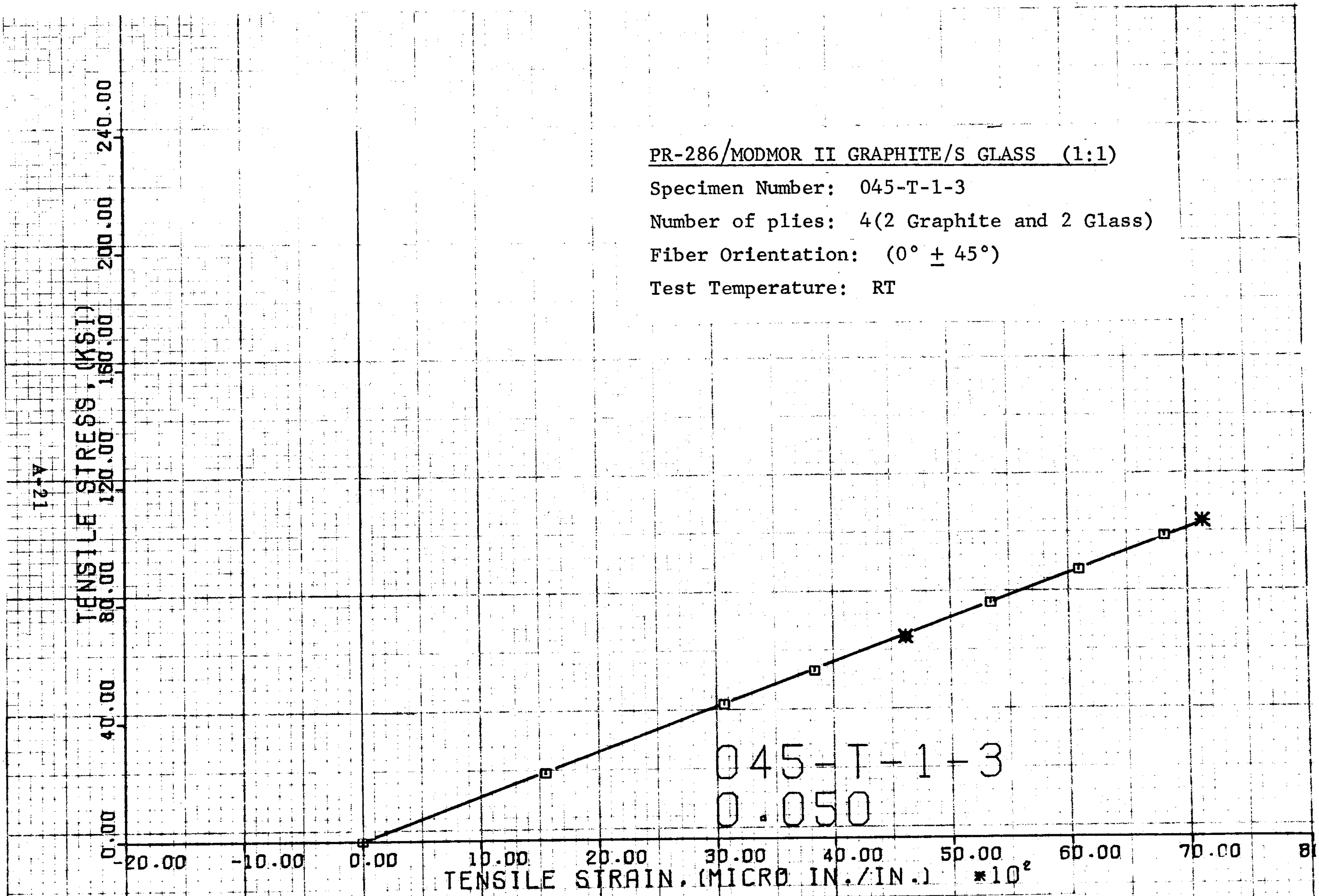

Fig. A-20 TENSION STRESS STRAIN DIAGRAM FOR PR-286/MODMOR II GRAPHITE/S GLASS COMPOSITE (1:1) TESTED AT ROOM TEMPERATURE

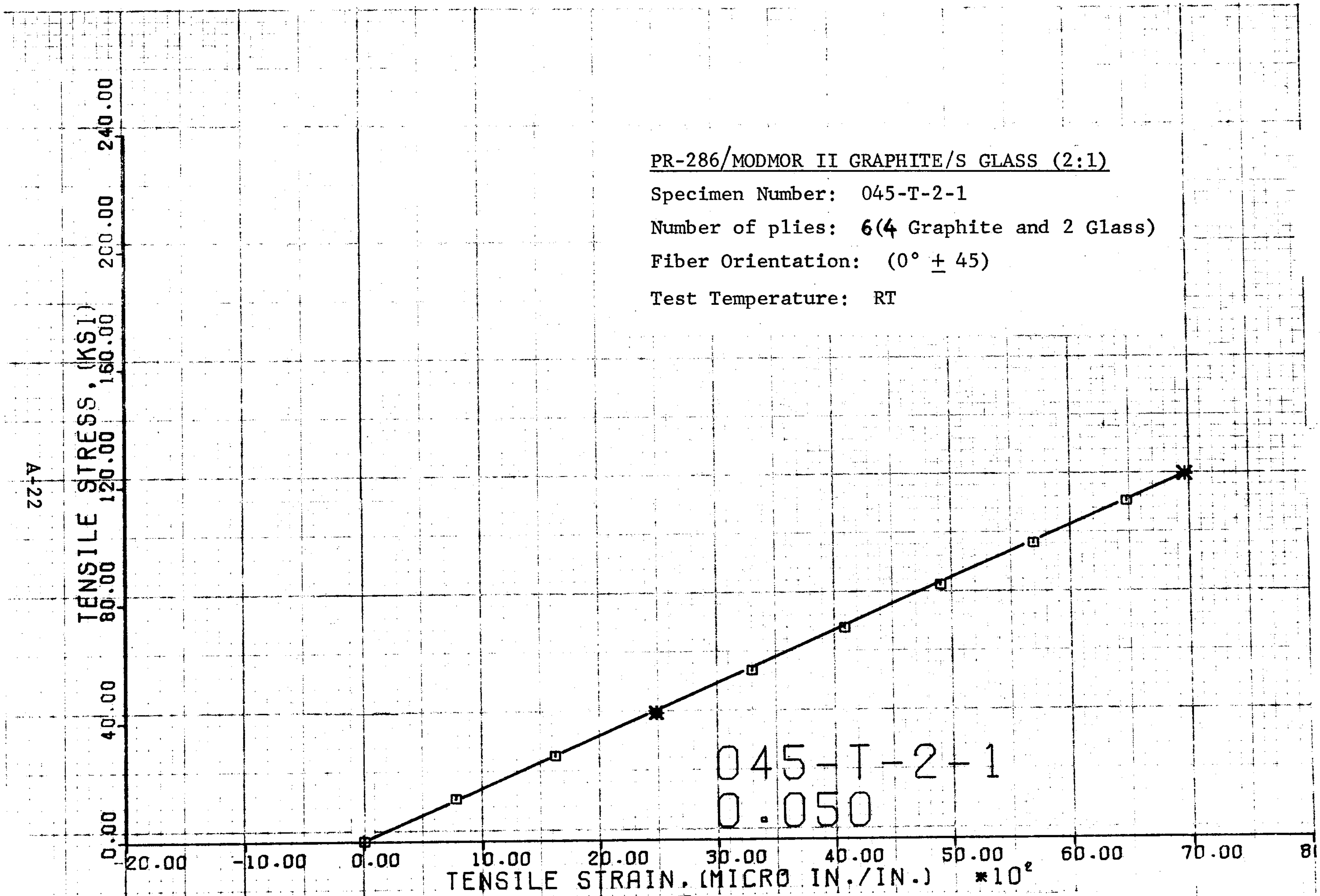

Fig. A-21 TENSION STRESS STRAIN DIAGRAM FOR PR-286/MODMOR II GRAPHITE/S GLASS COMPOSITE (2:1) TESTED AT ROOM TEMPERATURE

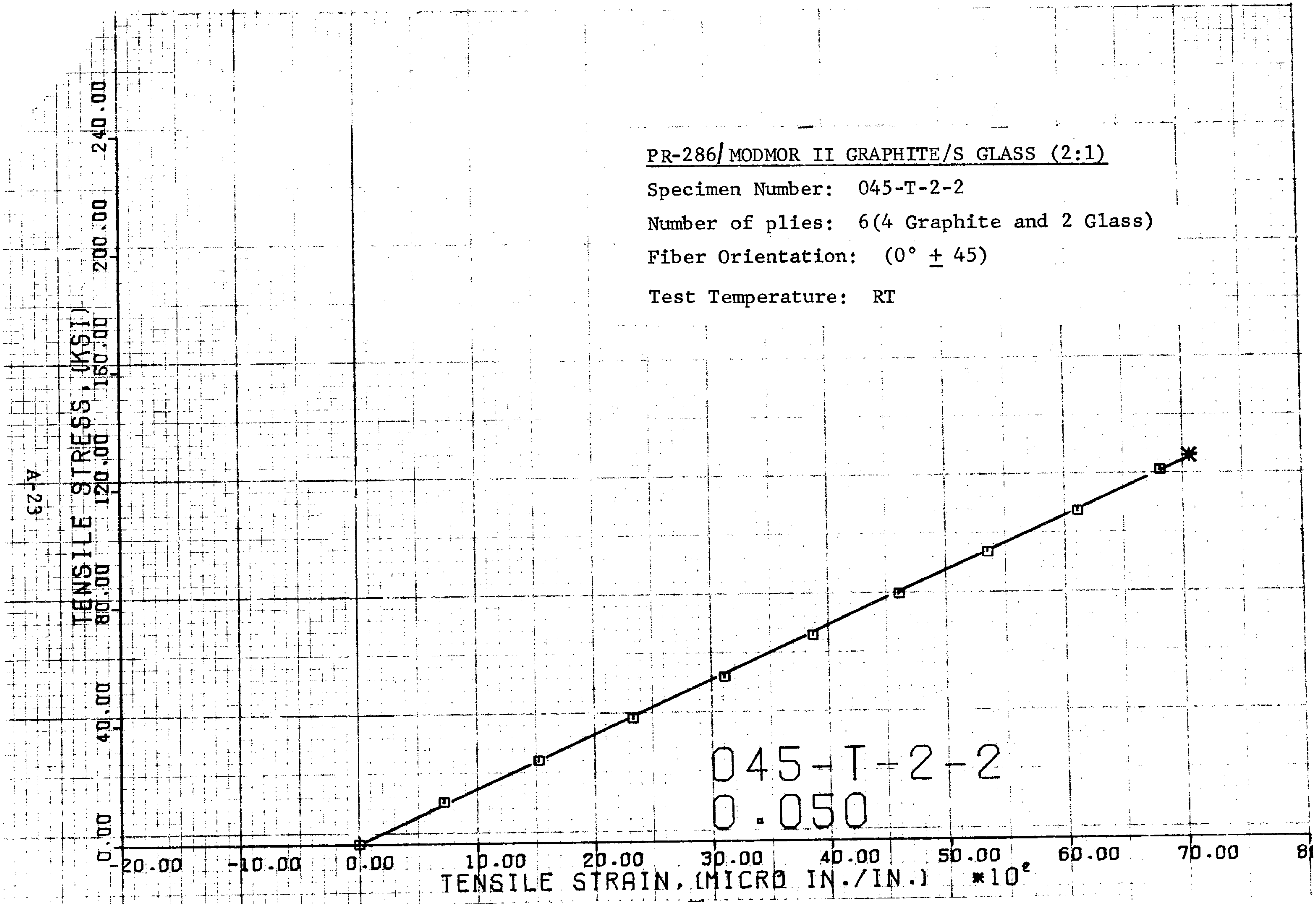

Fig. A-22 TENSION STRESS STRAIN DIAGRAM FOR PR-286/MODMOR II GRAPHITE/S GLASS COMPOSITE (2:1) TESTED AT ROOM TEMPERATURE

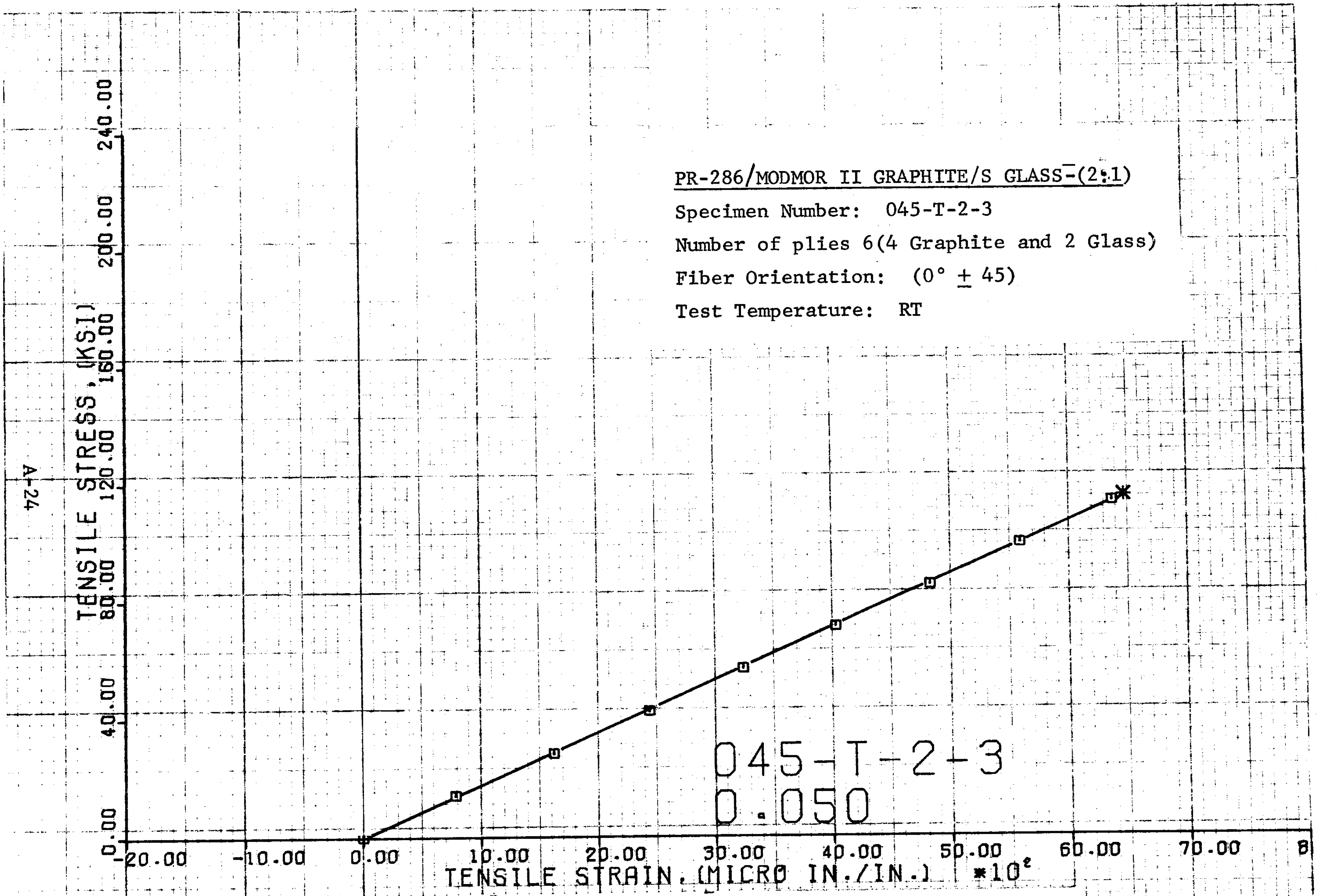

Fig. A-23 TENSION STRESS STRAIN DIAGRAM FOR PR-286/MODMOR II GRAPHITE/S GLASS COMPOSITE (2:1) TESTED AT ROOM TEMPERATURE

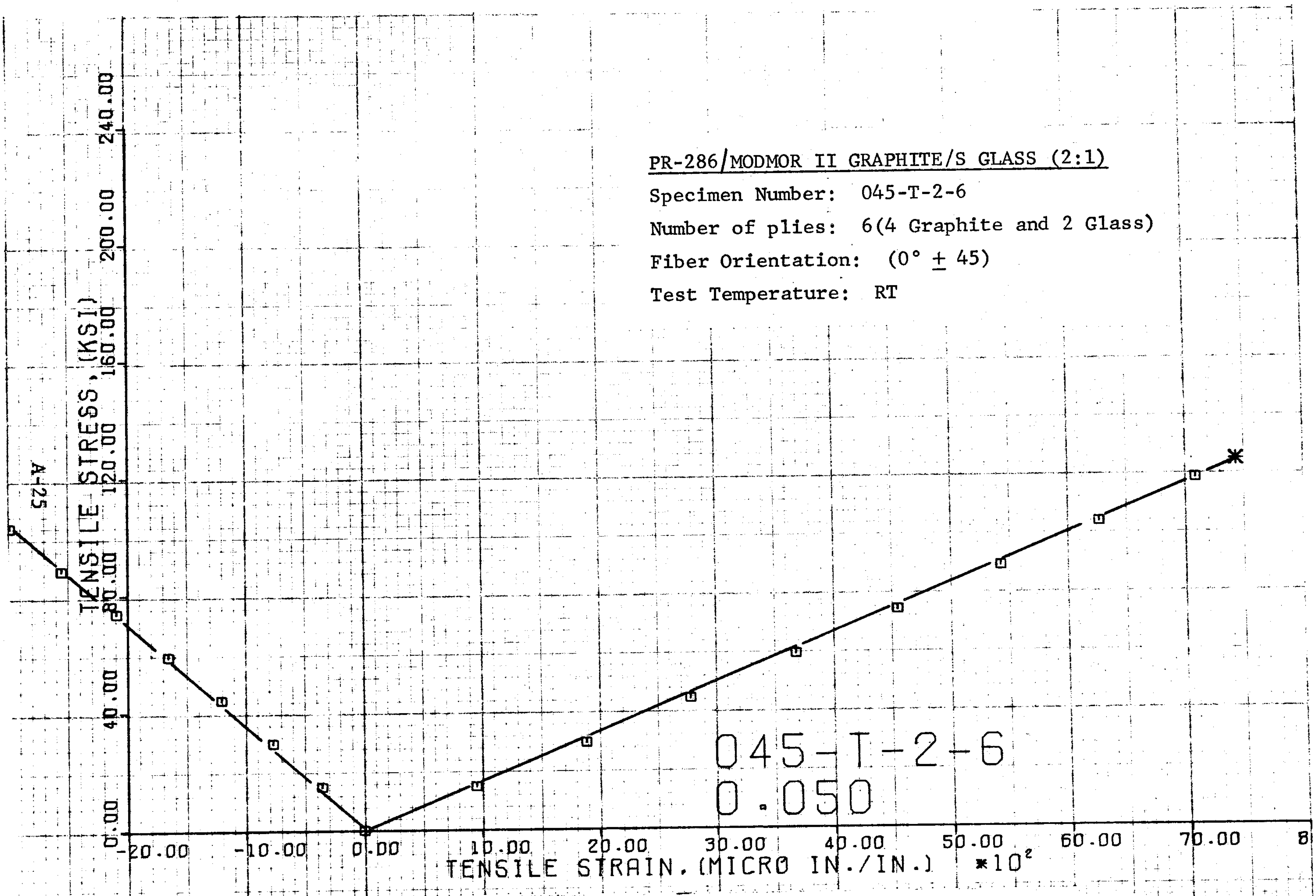

Fig. A-24 TENSION STRESS STRAIN DIAGRAM FOR PR-286/MODMOR II GRAPHITE/S GLASS COMPOSITE (2:1) TESTED AT ROOM TEMPERATURE

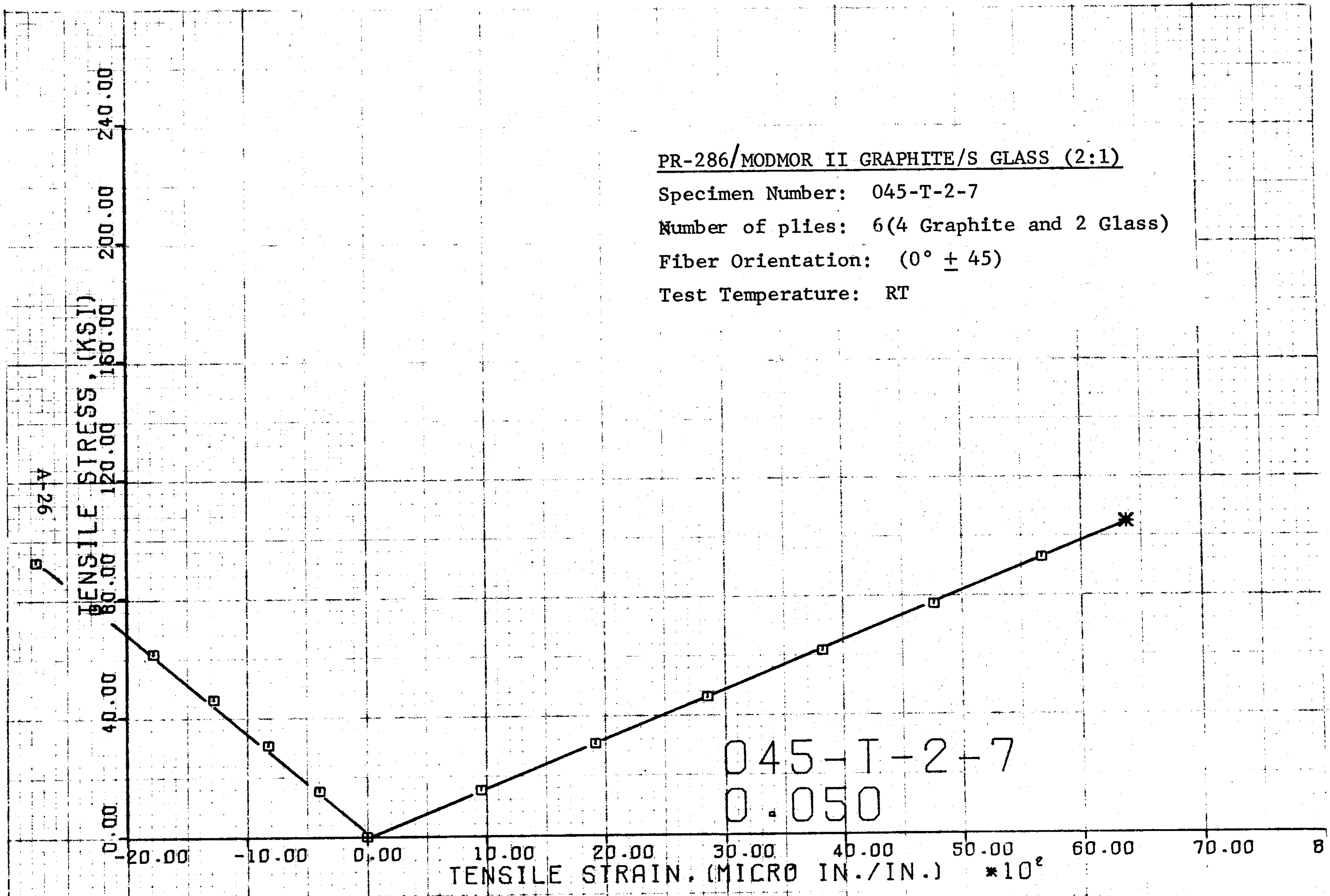

Fig. A-25 TENSION STRESS STRAIN DIAGRAM FOR PR-286/MODMOR II GRAPHITE/S GLASS COMPOSITE (2:1) TESTED AT ROOM TEMPERATURE

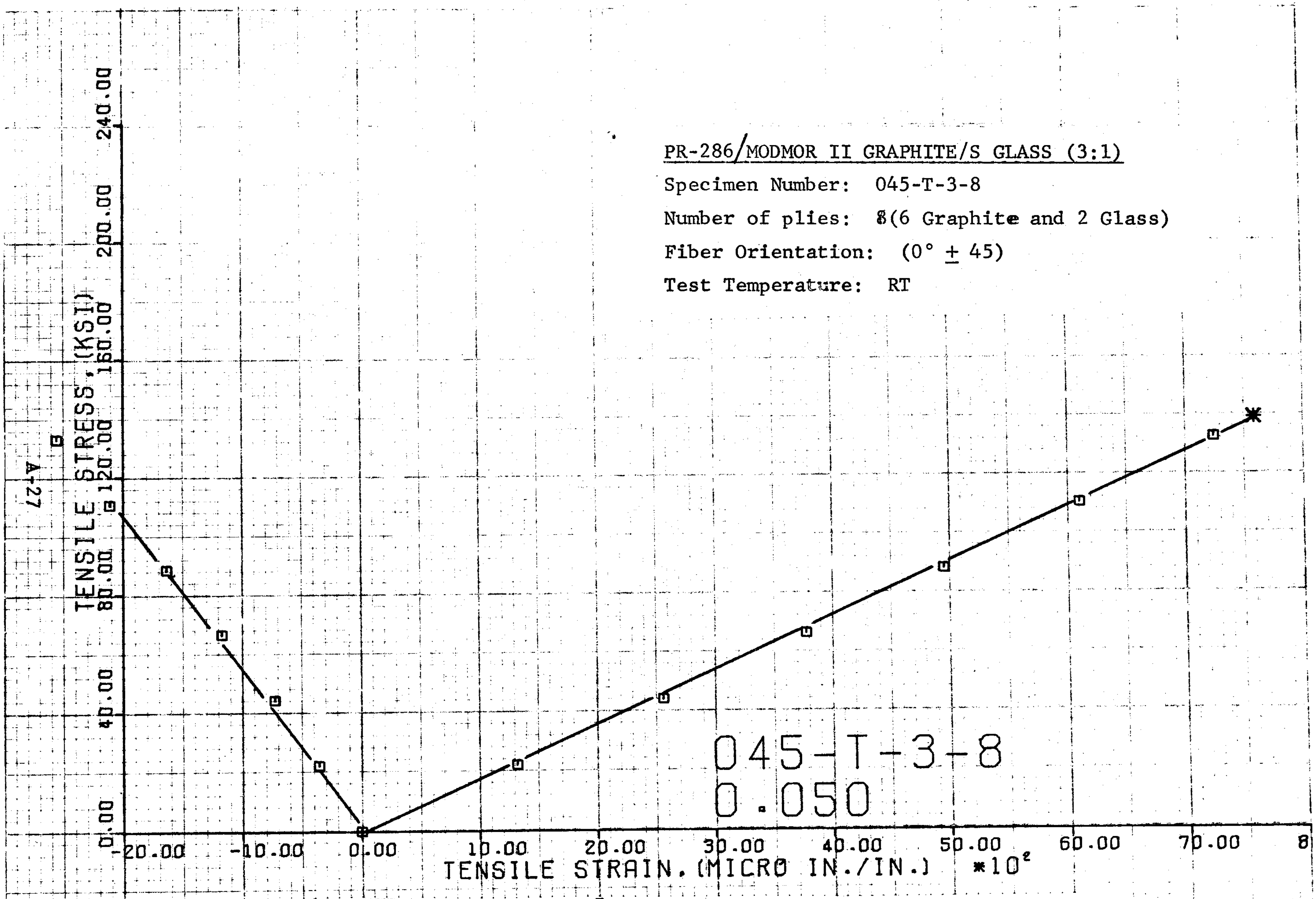

Fig. A-26 TENSION STRESS STRAIN DIAGRAM FOR PR-286/MODMOR II GRAPHITE/S GLASS COMPOSITE (3:1) TESTED AT ROOM TEMPERATURE

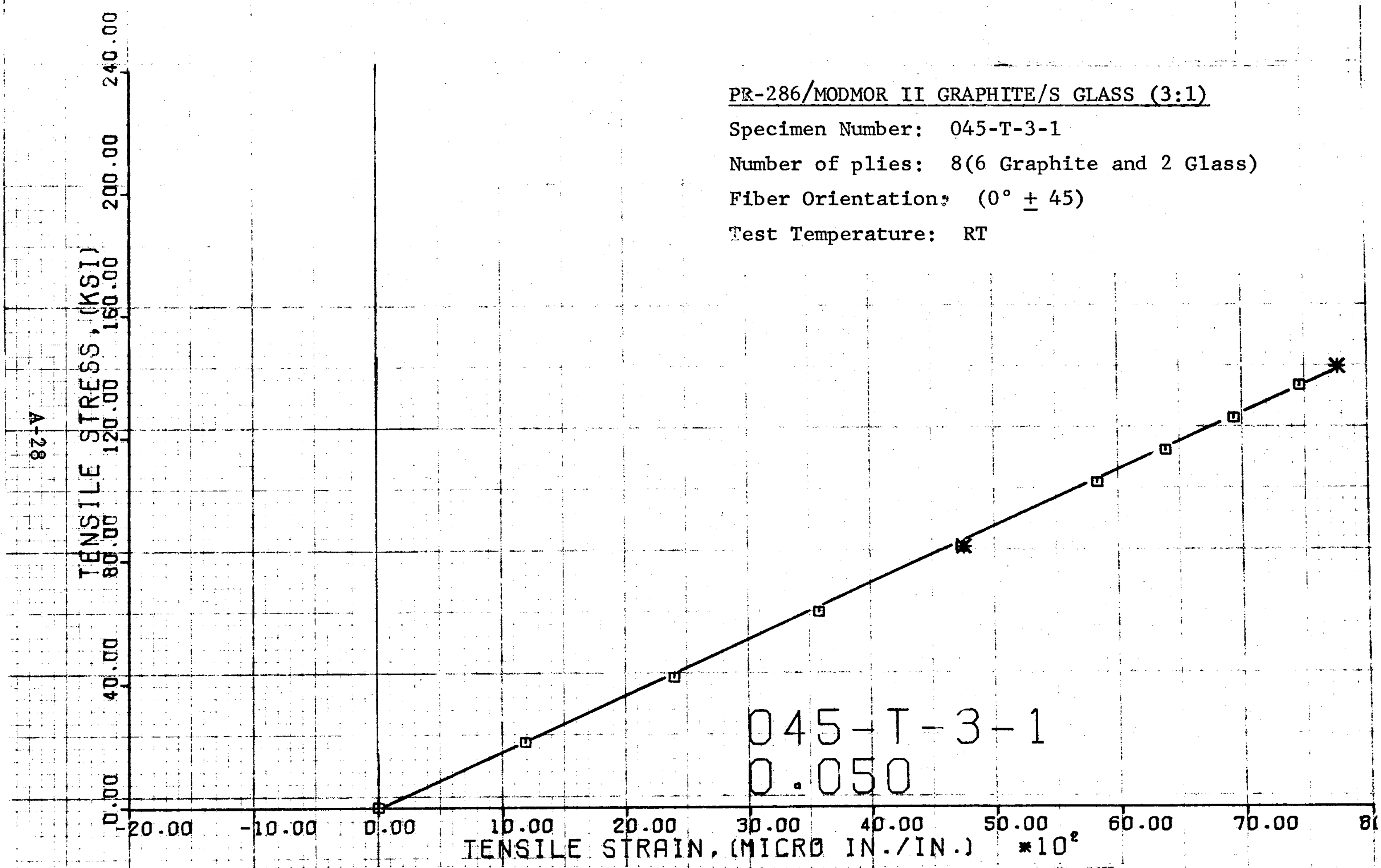

Fig. A-27 TENSION STRESS STRAIN DIAGRAM FOR PR-286/MODMOR II GRAPHITE/S GLASS COMPOSITE (3:1) TESTED AT ROOM TEMPERATURE

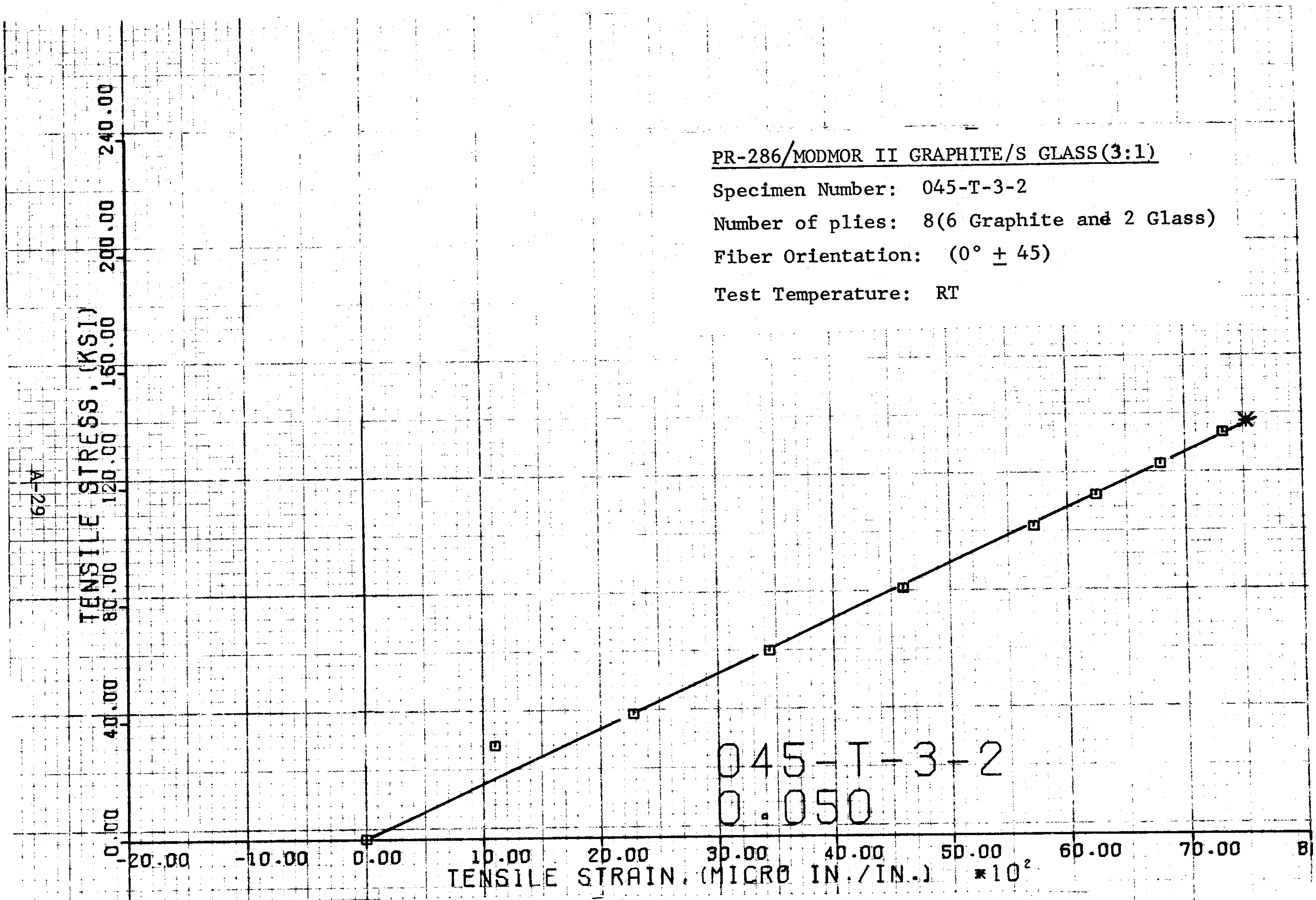

Fig. A-28 TENSION STRESS STRAIN DIAGRAM FOR PR-286/MODMOR II GRAPHITE/S GLASS COMPOSITE (3:1) TESTED AT ROOM TEMPERATURE

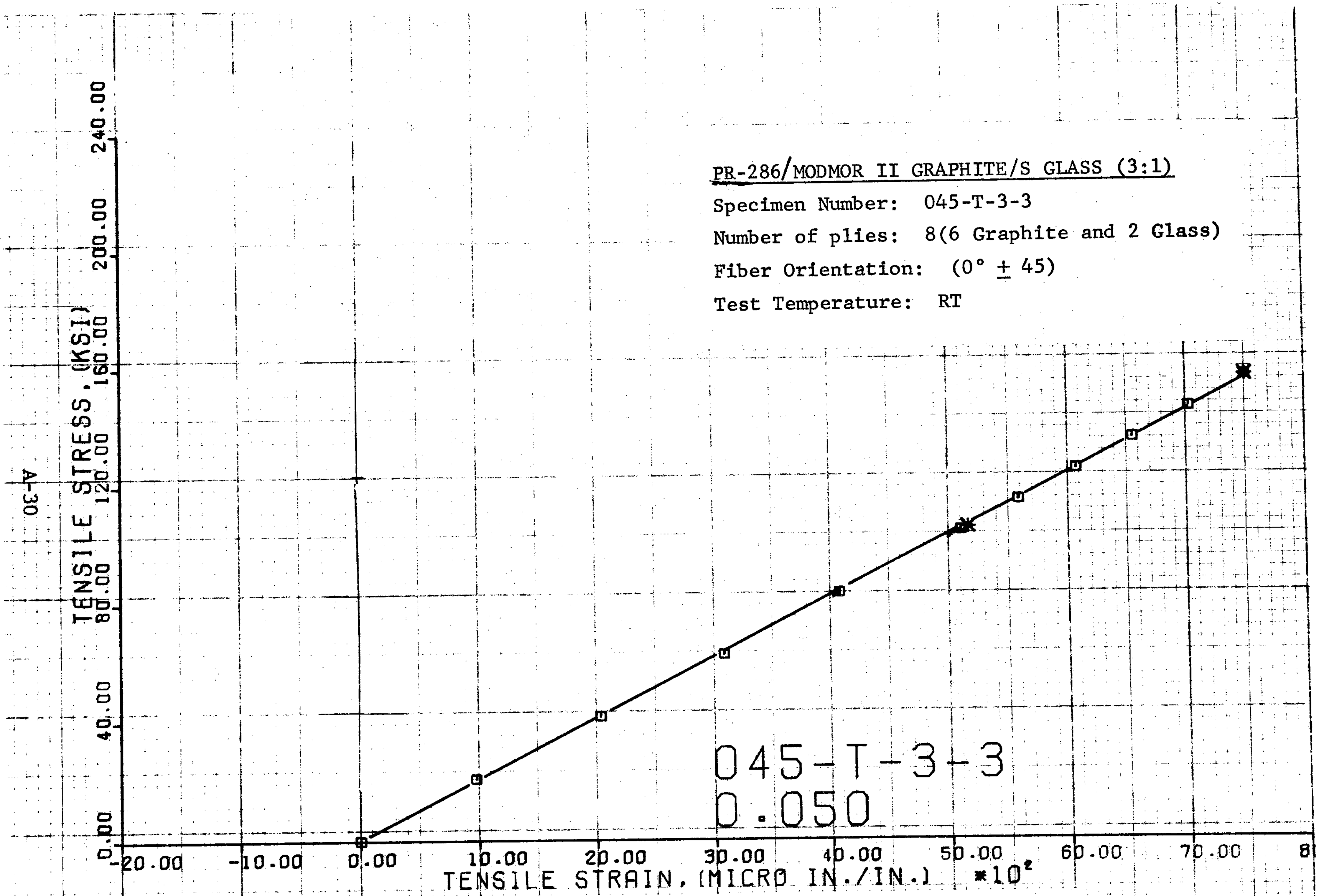

Fig. A-29 TENSION STRESS STRAIN DIAGRAM FOR PR-286/MODMOR II GRAPHITE/S GLASS COMPOSITE (3:1) TESTED AT ROOM TEMPERATURE

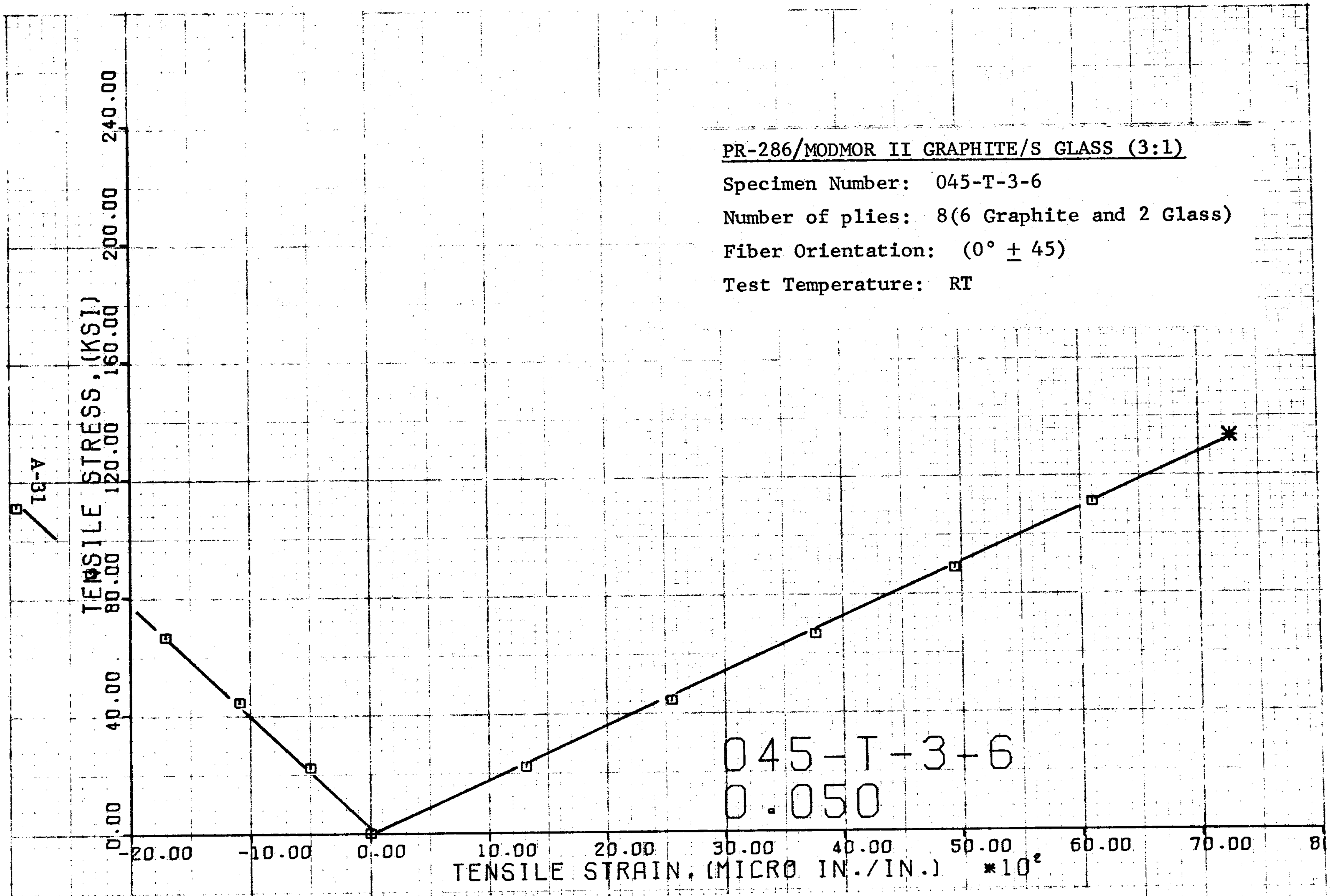

Fig. A-30 TENSION STRESS STRAIN DIAGRAM FOR PR-286/MODMOR II GRAPHITE/S GLASS COMPOSITE (3:1) TESTED AT ROOM TEMPERATURE

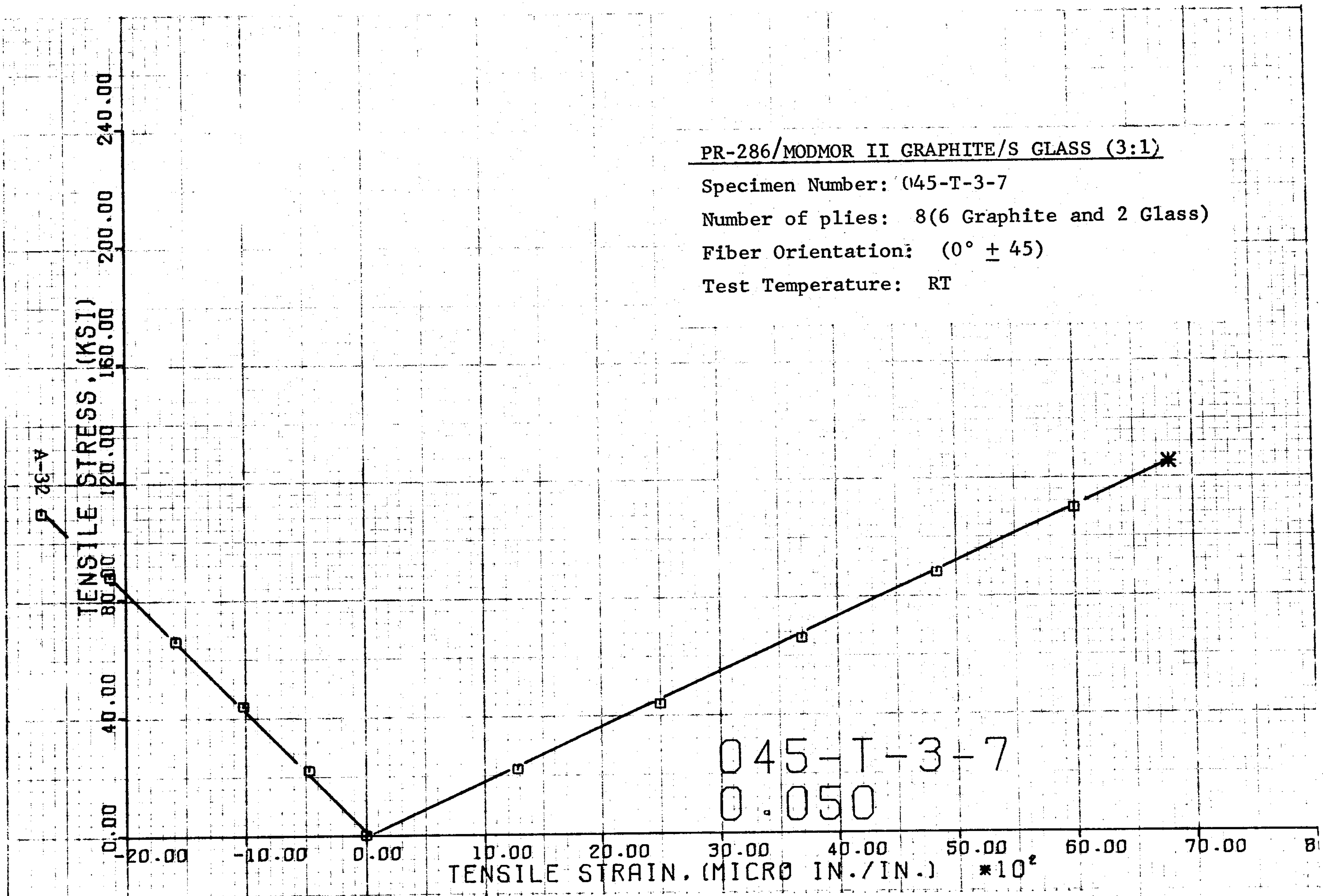

Fig. A-31 TENSION STRESS STRAIN DIAGRAM FOR PR-286/MODMOR II GRAPHITE/S GLASS COMPOSITE (3:1) TESTED AT ROOM TEMPERATURE

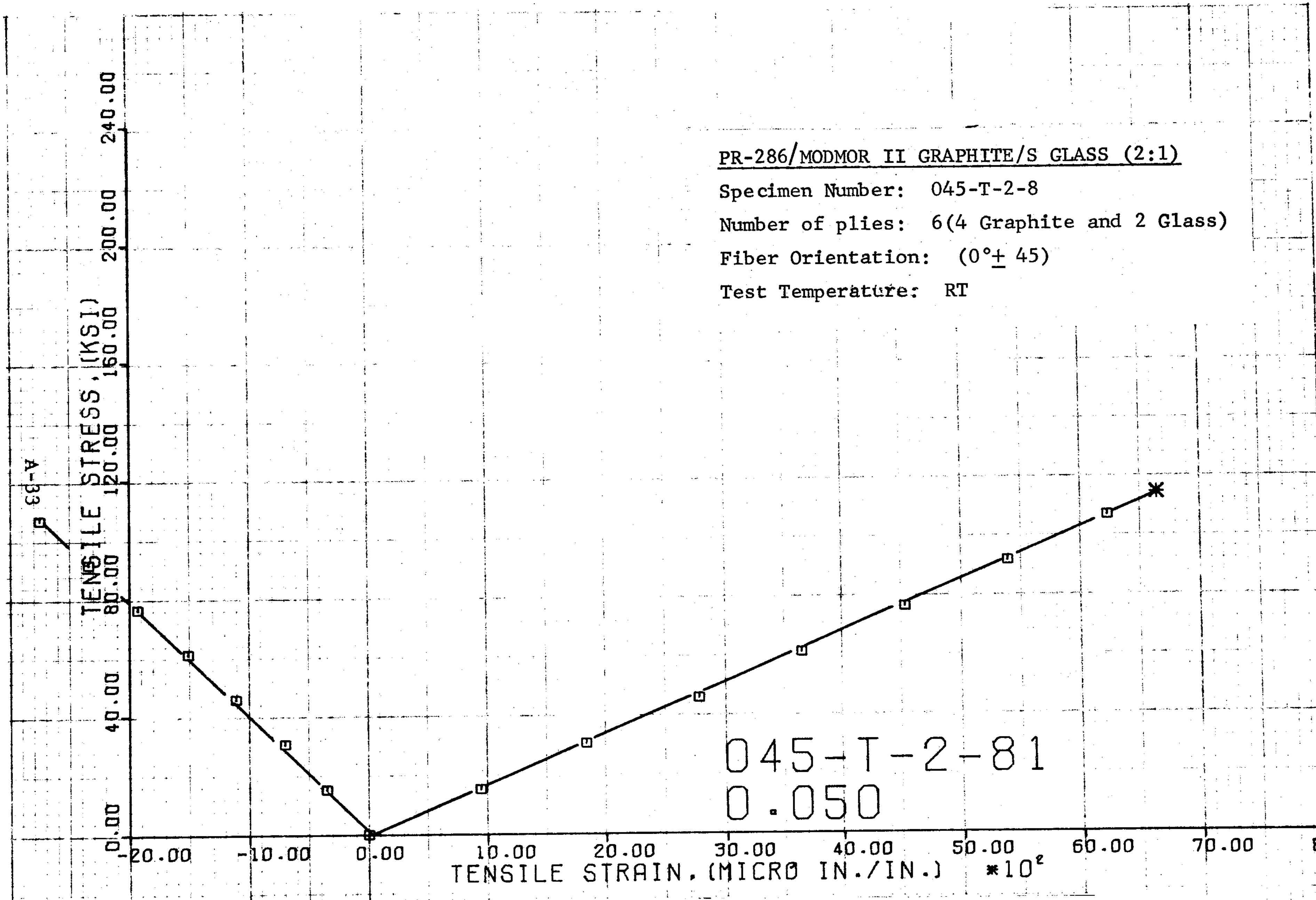

Fig. A-32 TENSION STRESS STRAIN DIAGRAM FOR PR-286/MODMOR II GRAPHITE/S GLASS COMPOSITE (2:1) TESTED AT ROOM TEMPERATURE

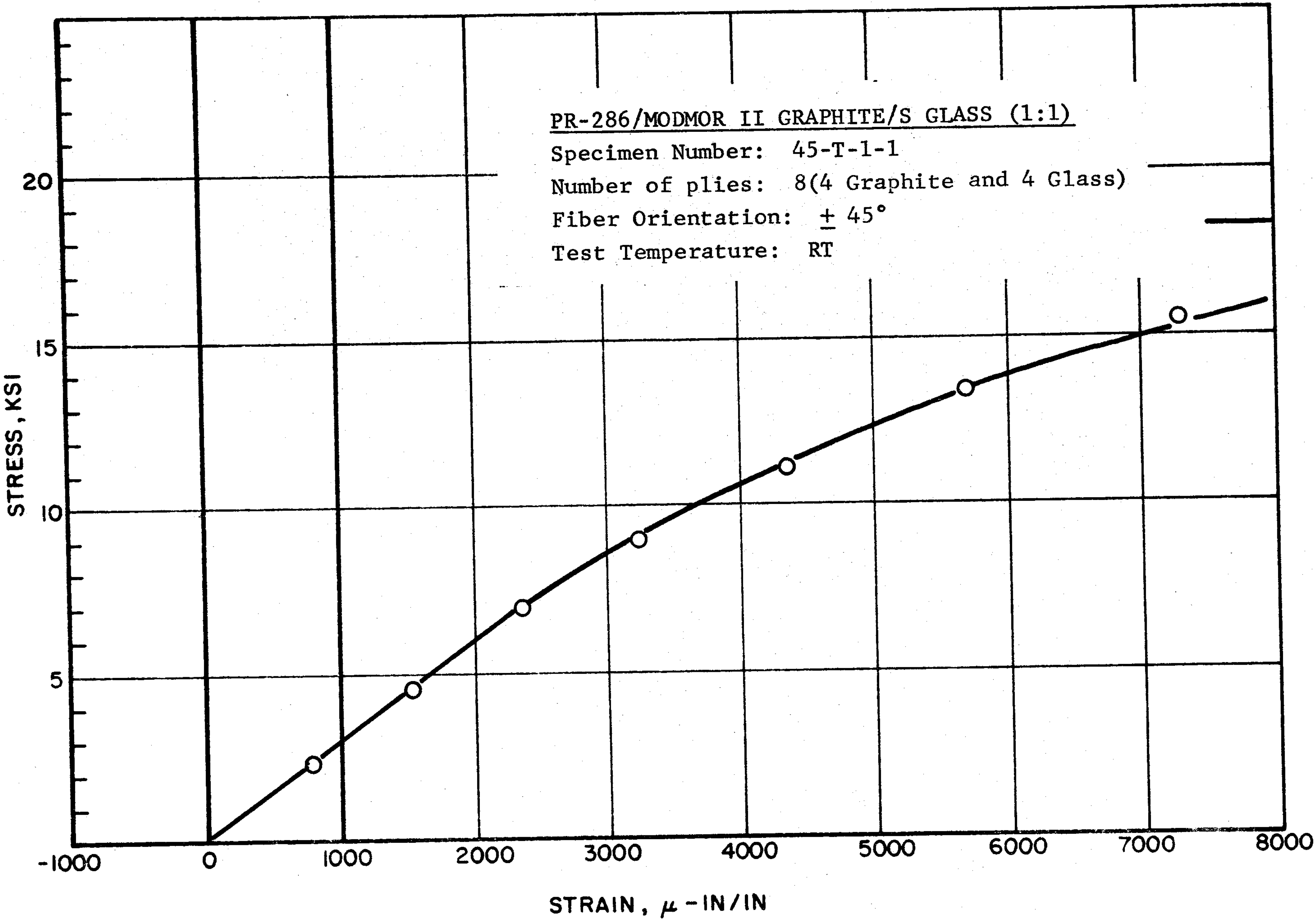

Fig. A-33 TENSION STRESS STRAIN DIAGRAM FOR PR-286/MODMOR II GRAPHITE/S GLASS COMPOSITE (1:1) TESTED AT ROOM TEMPERATURE

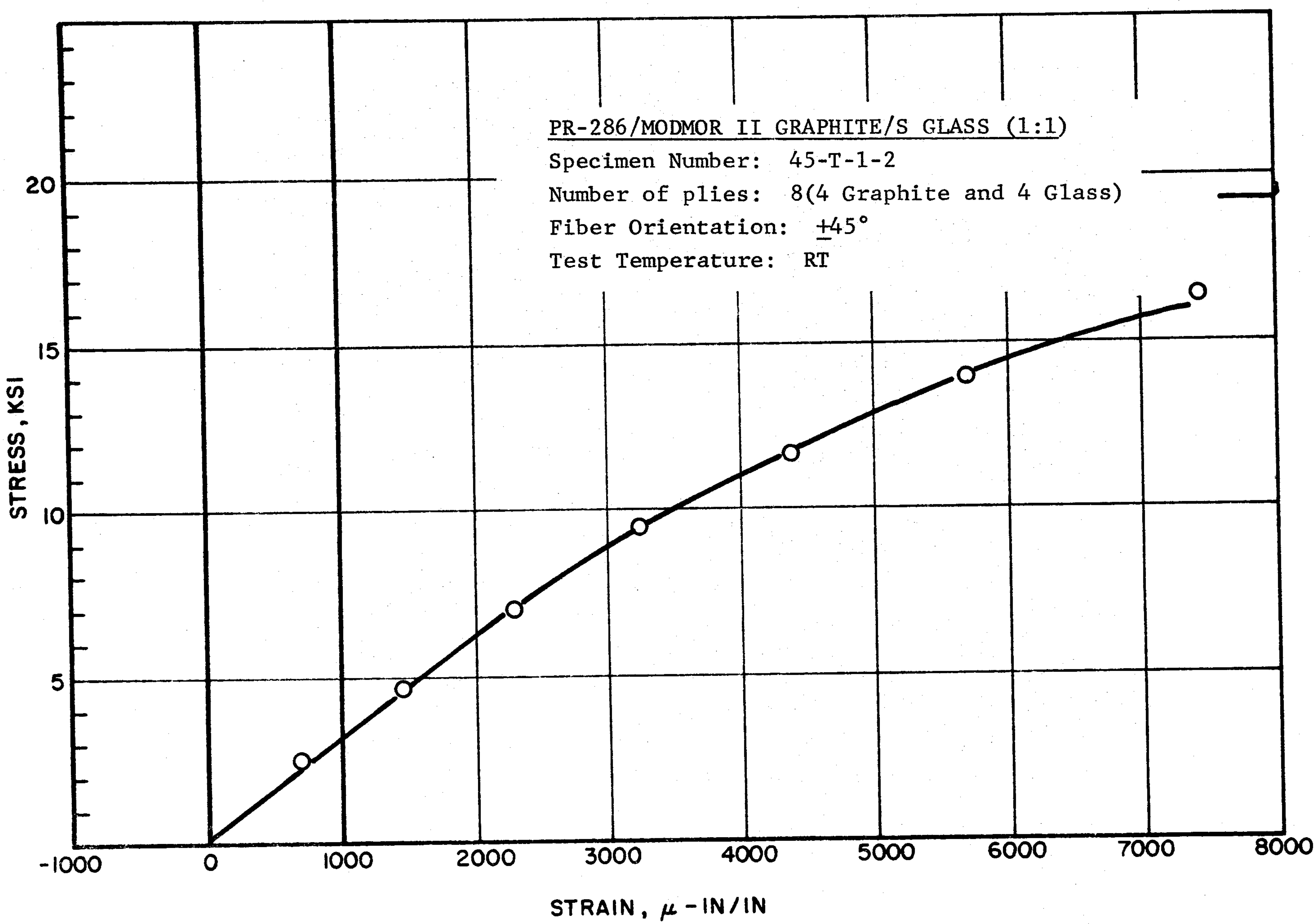

Fig. A-34 TENSION STRESS STRAIN DIAGRAM FOR PR-286/MODMOR II GRAPHITE/S GLASS COMPOSITE (1:1) TESTED AT ROOM TEMPERATURE

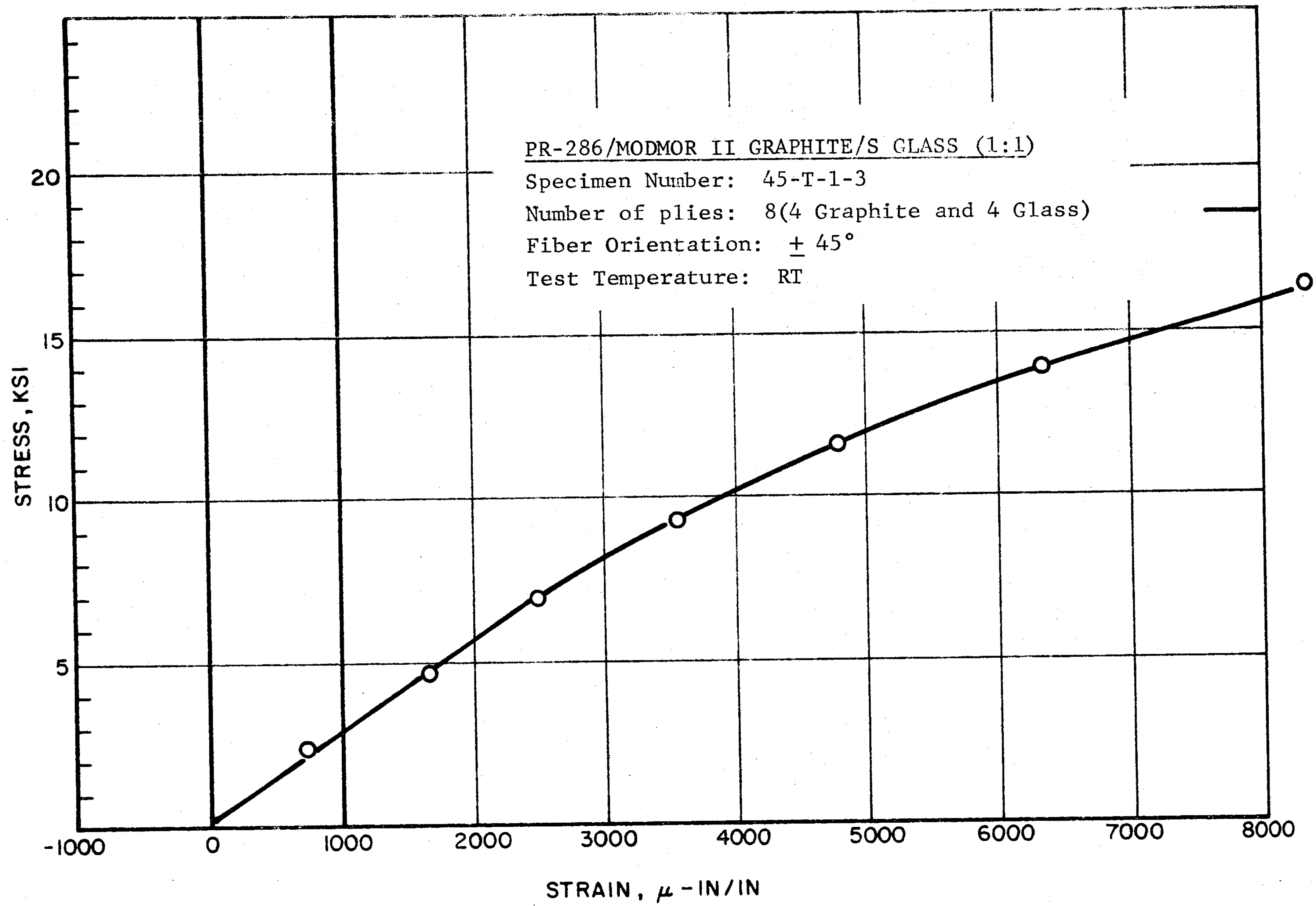

Fig. A-35 TENSION STRESS STRAIN DIAGRAM FOR PR-286/MODMOR II GRAPHITE/S GLASS COMPOSITE (1:1) TESTED AT ROOM TEMPERATURE

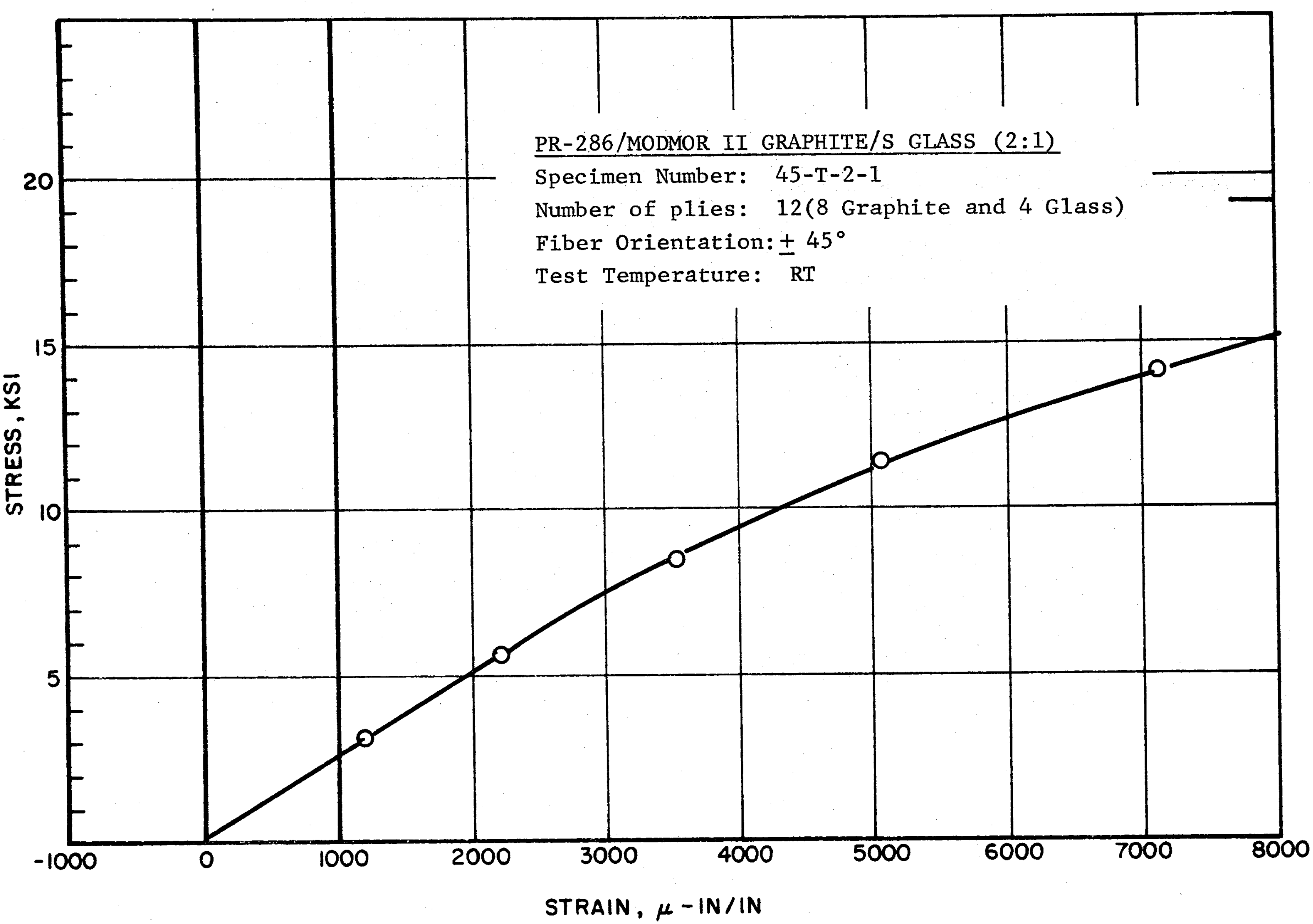

Fig. A-36 TENSION STRESS STRAIN DIAGRAM FOR PR-286/MODMOR II GRAPHITE/S GLASS COMPOSITE (2:1) TESTED AT ROOM TEMPERATURE

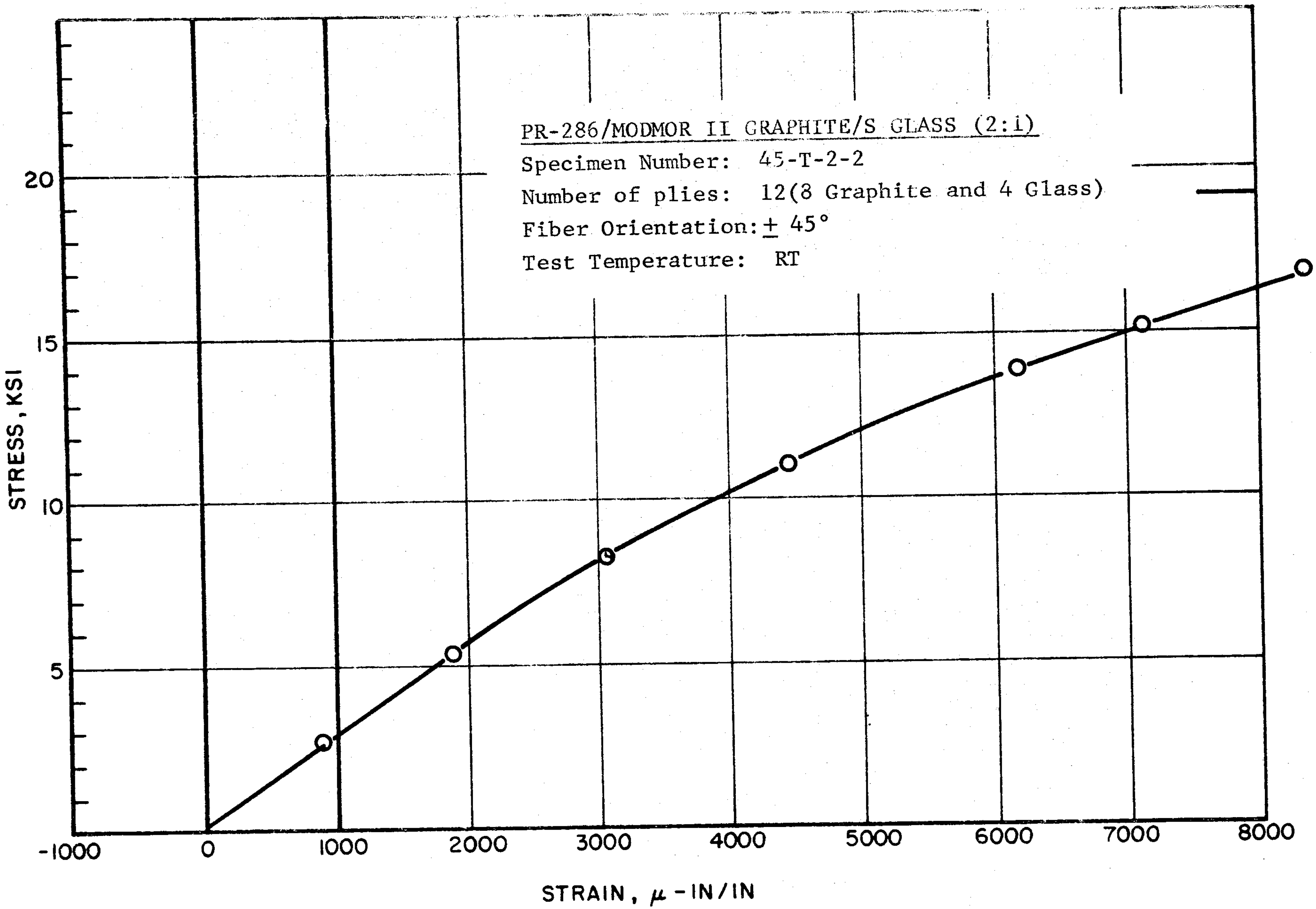

Fig. A-37 TENSION STRESS STRAIN DIAGRAM FOR PR-286/MODMOR II GRAPHITE/S GLASS COMPOSITE (2:1) TESTED AT ROOM TEMPERATURE

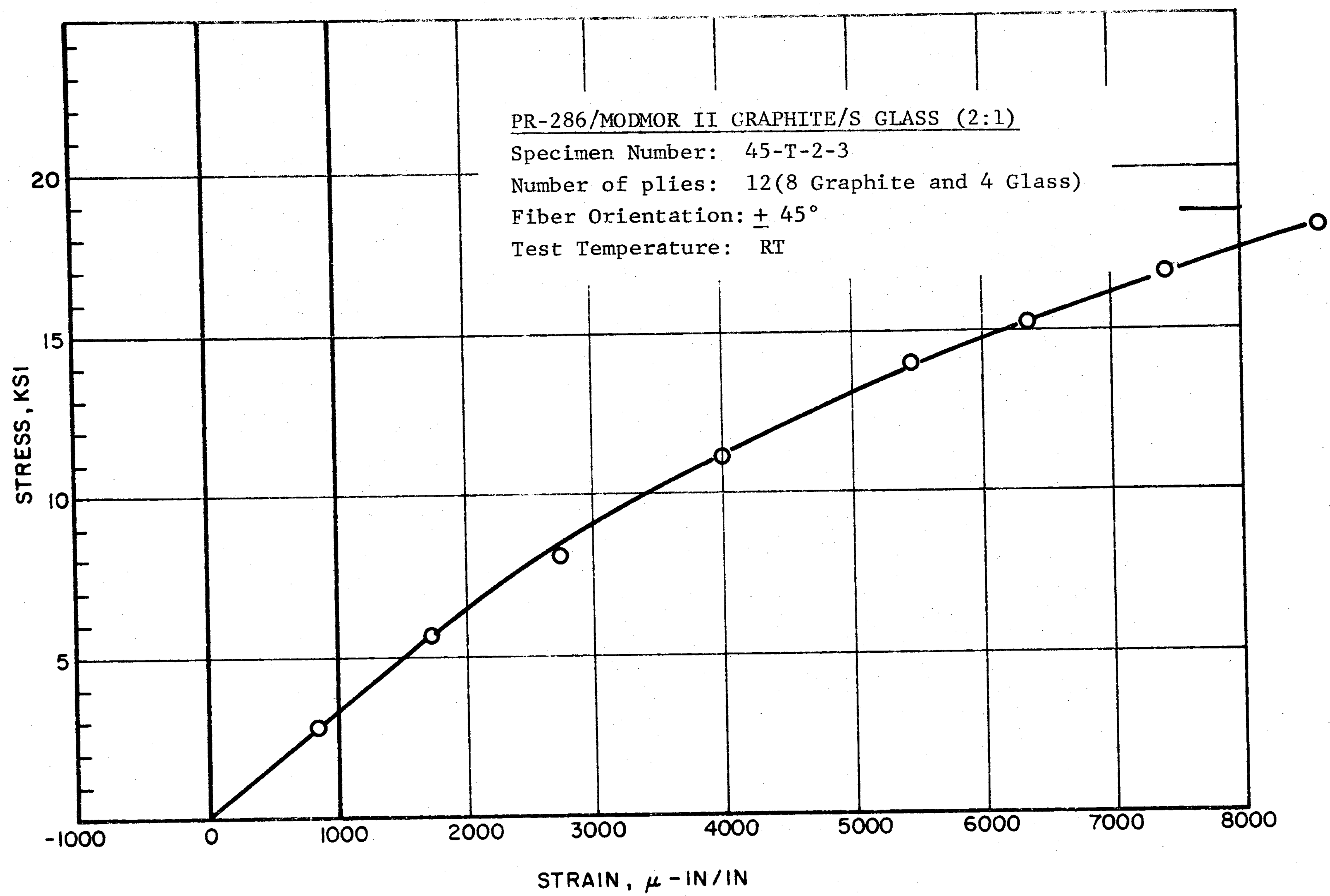

Fig. A-38 TENSION STRESS STRAIN DIAGRAM FOR PR-286/MODMOR II GRAPHITE/S GLASS COMPOSITE (2:1) TESTED AT ROOM TEMPERATURE

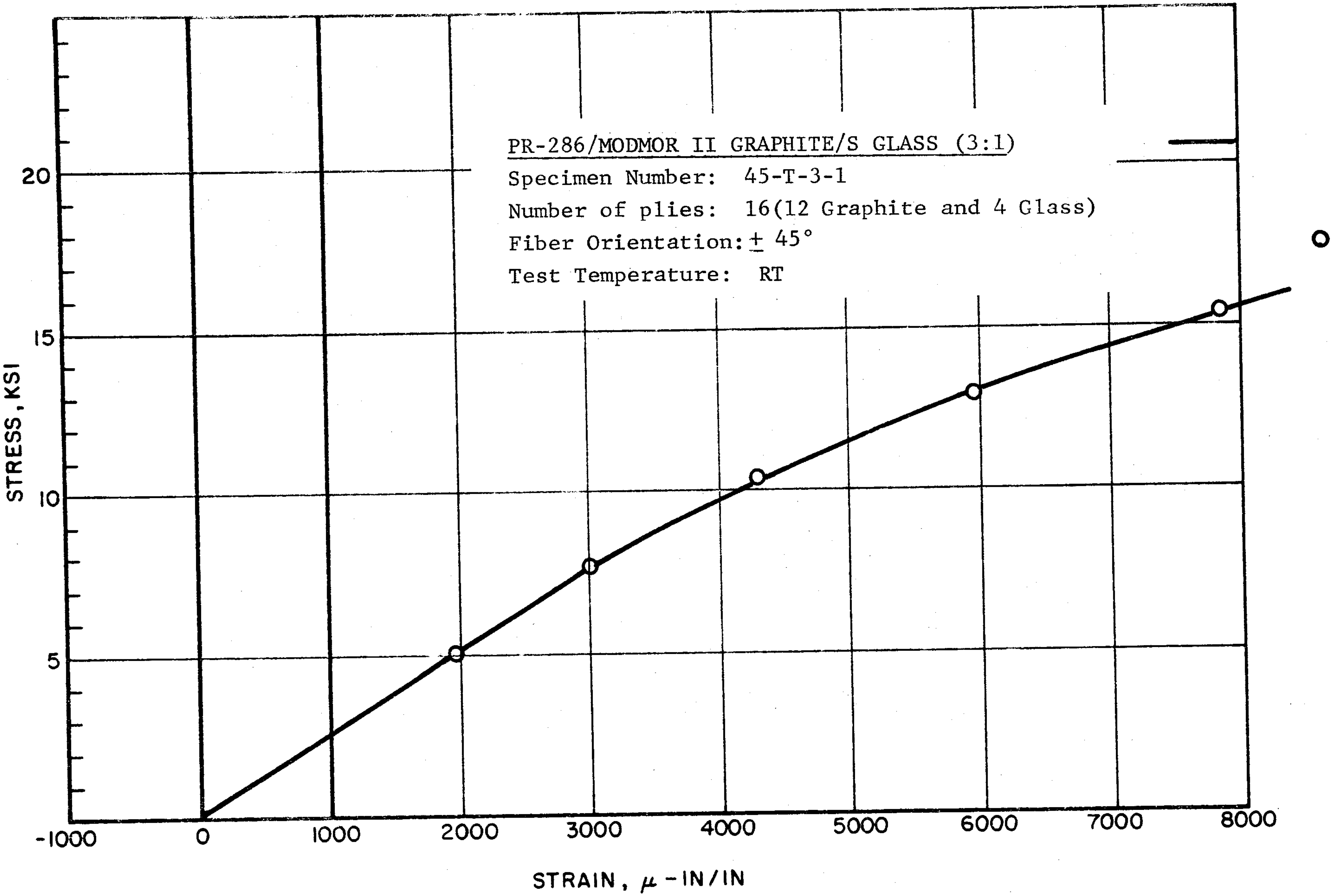

Fig. A-39 TENSION STRESS STRAIN DIAGRAM FOR PR-286/MODMOR II GRAPHITE/S GLASS COMPOSITE (3:1) TESTED AT ROOM TEMPERATURE

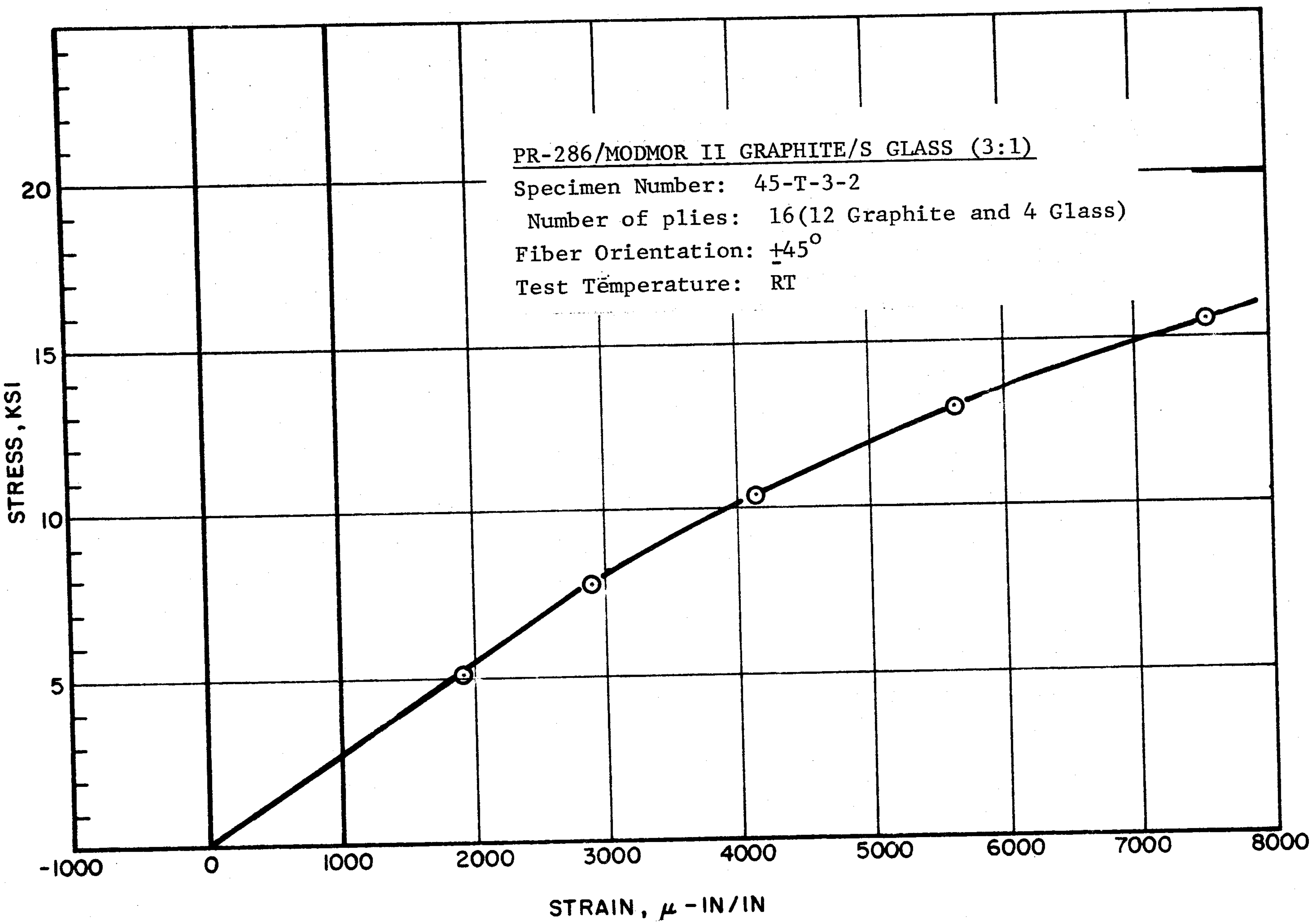

Fig. A-40 TENSION STRESS STRAIN DIAGRAM FOR PR-286/MODMOR II GRAPHITE/S GLASS COMPOSITE (3:1) TESTED AT ROOM TEMPERATURE

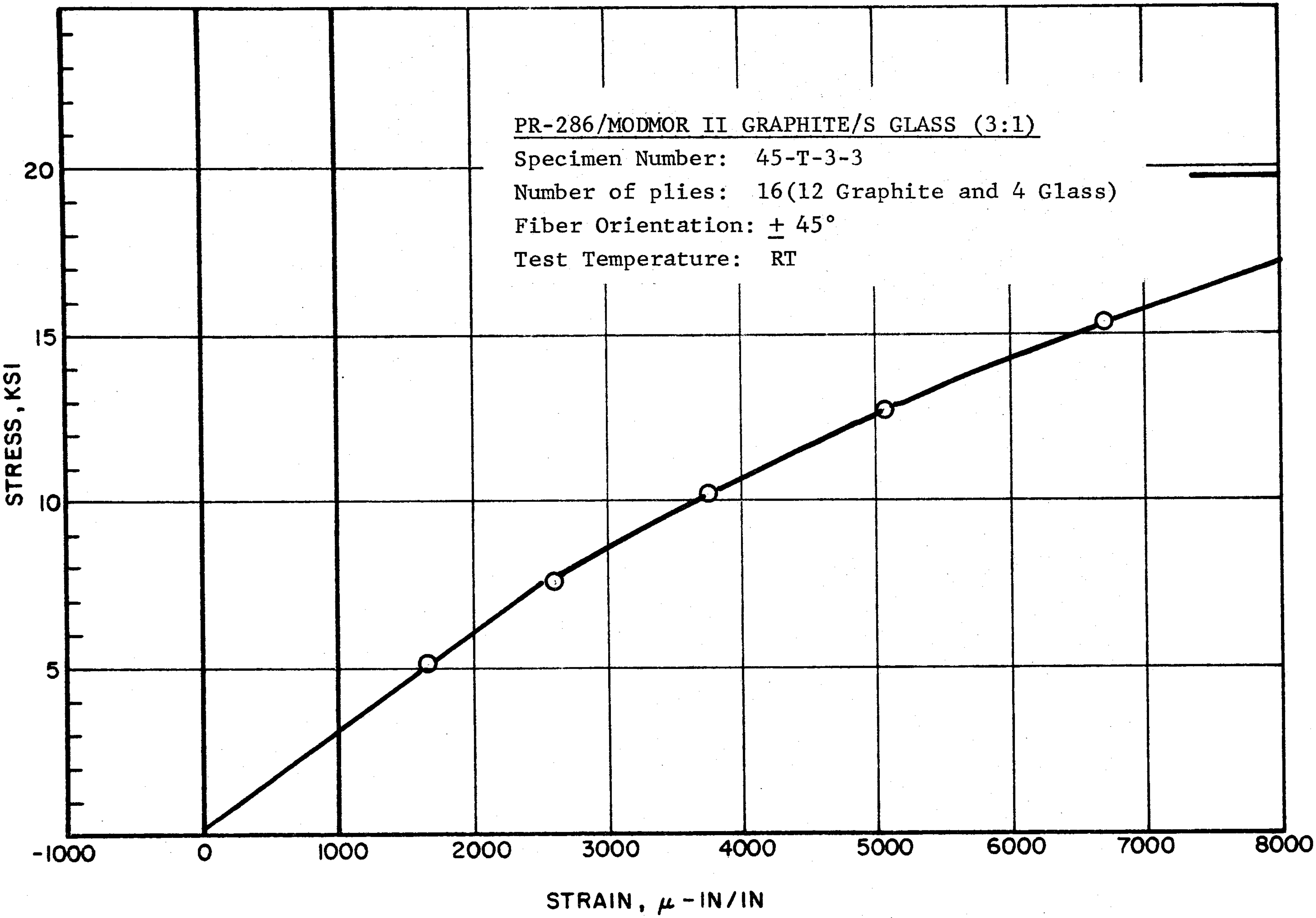

Fig. A-41 TENSION STRESS STRAIN DIAGRAM FOR PR-286/MODMOR II GRAPHITE/S GLASS COMPOSITE (3:1) TESTED AT ROOM TEMPERATURE

TABLE A-I

TENSION FATIGUE LIFE OF 0° PR-286/MODMOR II GRAPHITE/
S-GLASS 4 PLY COMPOSITE (GRAPHITE/GLASS = 1:1)
TESTED AT R = 0.1, ROOM TEMPERATURE DRY

Specimen Number	Specimen Thickness (in.)	Maximum Stress (ksi)	Cycles to Failure
0-T-1-4	0.022	85	840,000
0-T-1-5	0.023	90	472,000
0-T-1-6	0.023	100	54,000
0-T-1-7	0.021	105	1,000
0-T-1-8	0.021	102	Immediate failure

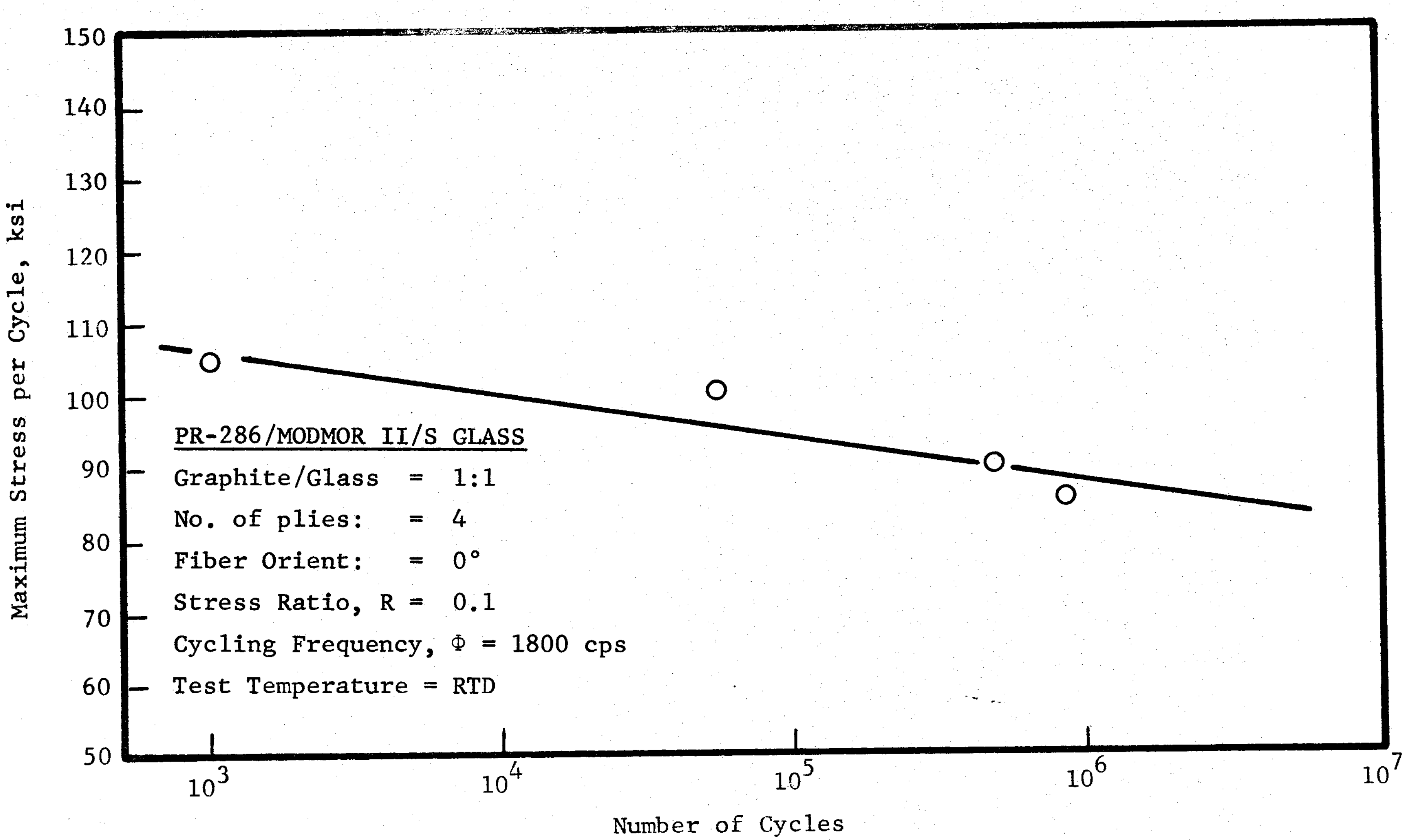

Fig. A-42 FATIGUE LIFE S-N DIAGRAM FOR 0° PR-286/MODMOR II GRAPHITE/S GLASS COMPOSITE (1:1)

TABLE A-II

TENSION FATIGUE LIFE OF 0° PR-286/MODMOR II GRAPHITE/
S-GLASS 6 PLY COMPOSITE (GRAPHITE/GLASS = 2:1)
TESTED AT R = 0.1, ROOM TEMPERATURE, DRY

Specimen Number	Specimen Thickness (in.)	Maximum Stress (ksi)	Cycles to Failure	Residual Strength (ksi)
0-T-2-4	0.035	110	1,168,000	-
0-T-2-5	0.035	120	2,000	-
0-T-2-6	0.034	118	1,116,000	-
0-T-2-7	0.035	125	5,000	-
0-T-2-8	0.034	120	2,000	-
0-T-2-9	0.032	115	5,261,000*	150
0-T-2-10	0.035	122	1,000	-

* No Failure, Run out

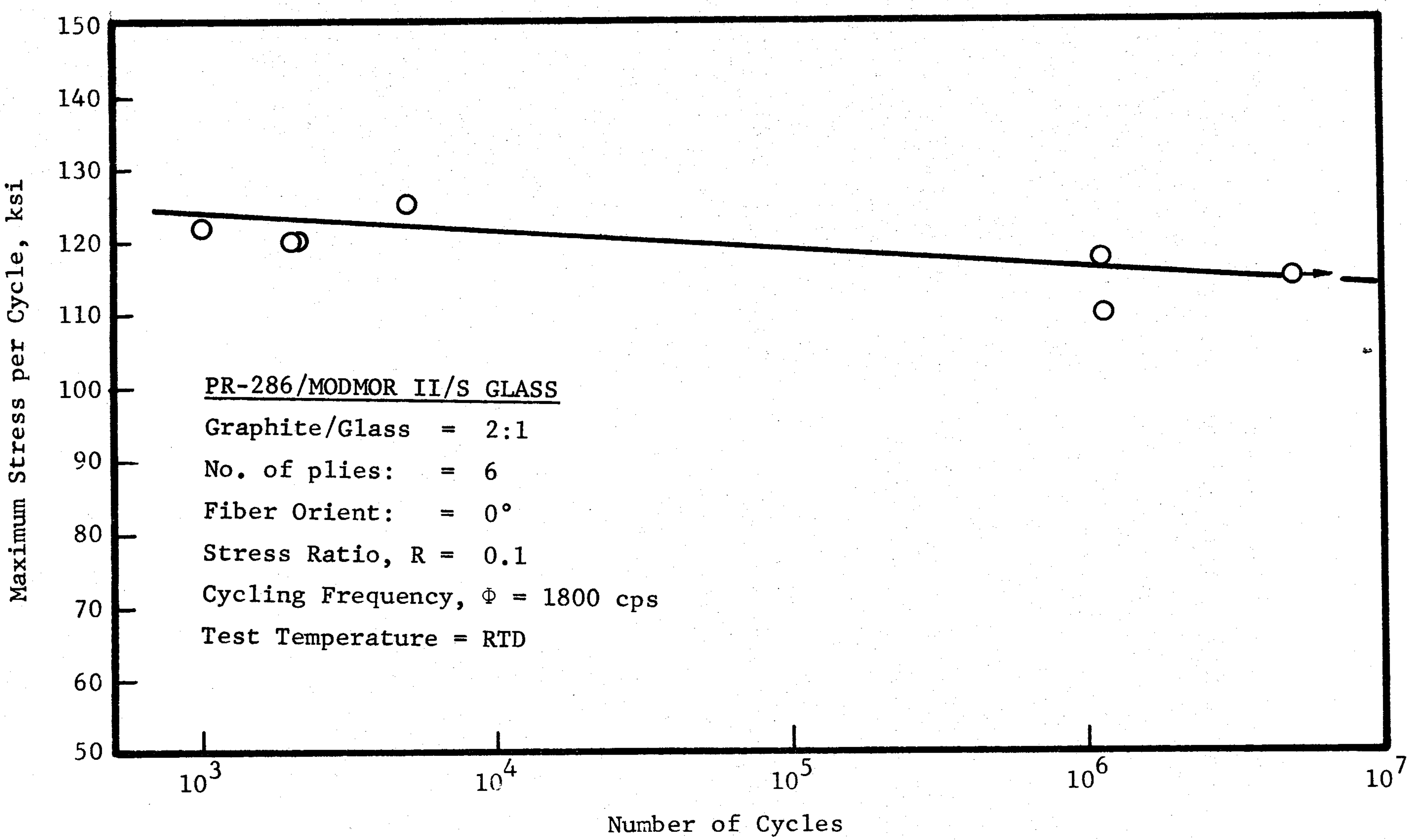

Fig. A-43 FATIGUE LIFE S-N DIAGRAM FOR 0° PR-286/MODMOR II GRAPHITE/S GLASS COMPOSITE (2:1)

TABLE A-III

TENSION FATIGUE LIFE OF 0° PR-286/MODMOR II GRAPHITE/
S-GLASS 8 PLY COMPOSITE (GRAPHITE/GLASS = 3:1)
TESTED AT R = 0.1, ROOM TEMPERATURE, DRY

Specimen Number	Specimen Thickness (in.)	Maximum Stress (ksi)	Cycles to Failure	Residual Strength (ksi)
0-T-3-4	0.046	115	1,000	
0-T-3-5	0.046	100	3,000	
0-T-3-6	0.049	90	2,472,000*	161.5
0-T-3-7	0.048	95	1,632,000	
0-T-3-8	0.049	105	2,417,000*	141.0
0-T-3-9	0.048	120	Immediate Failure	
0-T-3-10	0.047	110	2,000	

* No Failure, Run out

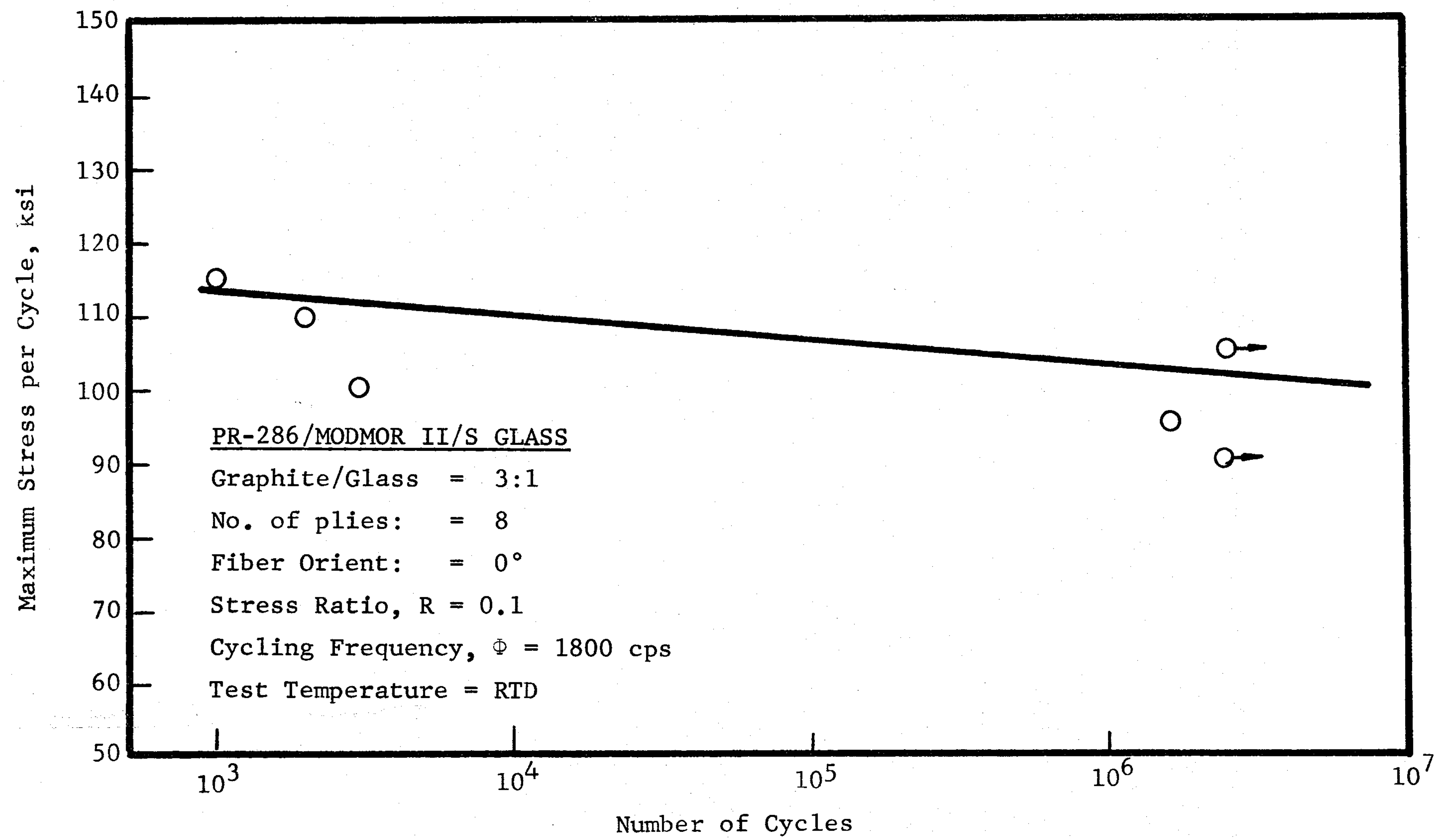

Fig. A-44 FATIGUE LIFE S-N DIAGRAM FOR 0° PR-286/MODMOR II GRAPHITE/S GLASS COMPOSITE (3:1)

TABLE A-IV

TENSION FATIGUE LIFE OF $0 \pm 45°$ PR-286/MODMOR II GRAPHITE/
S-GLASS 8 PLY COMPOSITE (GRAPHITE/GLASS = 1:1)
TESTED AT R = 0.1, ROOM TEMPERATURE DRY

Specimen Number	Specimen Thickness (in)	Maximum Stress (ksi)	Cycles to Failure	Residual Strength (ksi)
045-T-1-4	0.044	80	12,000	
045-T-1-5	0.044	70	2.054×10^6*	98.5
045-T-1-6	0.043	75	1.631×10^6	
045-T-1-7	0.046	78	14,000	
045-T-1-8	0.044	77	6,000	
045-T-1-9	0.044	76	1.889×10^6	

* Specimens run out; No failure

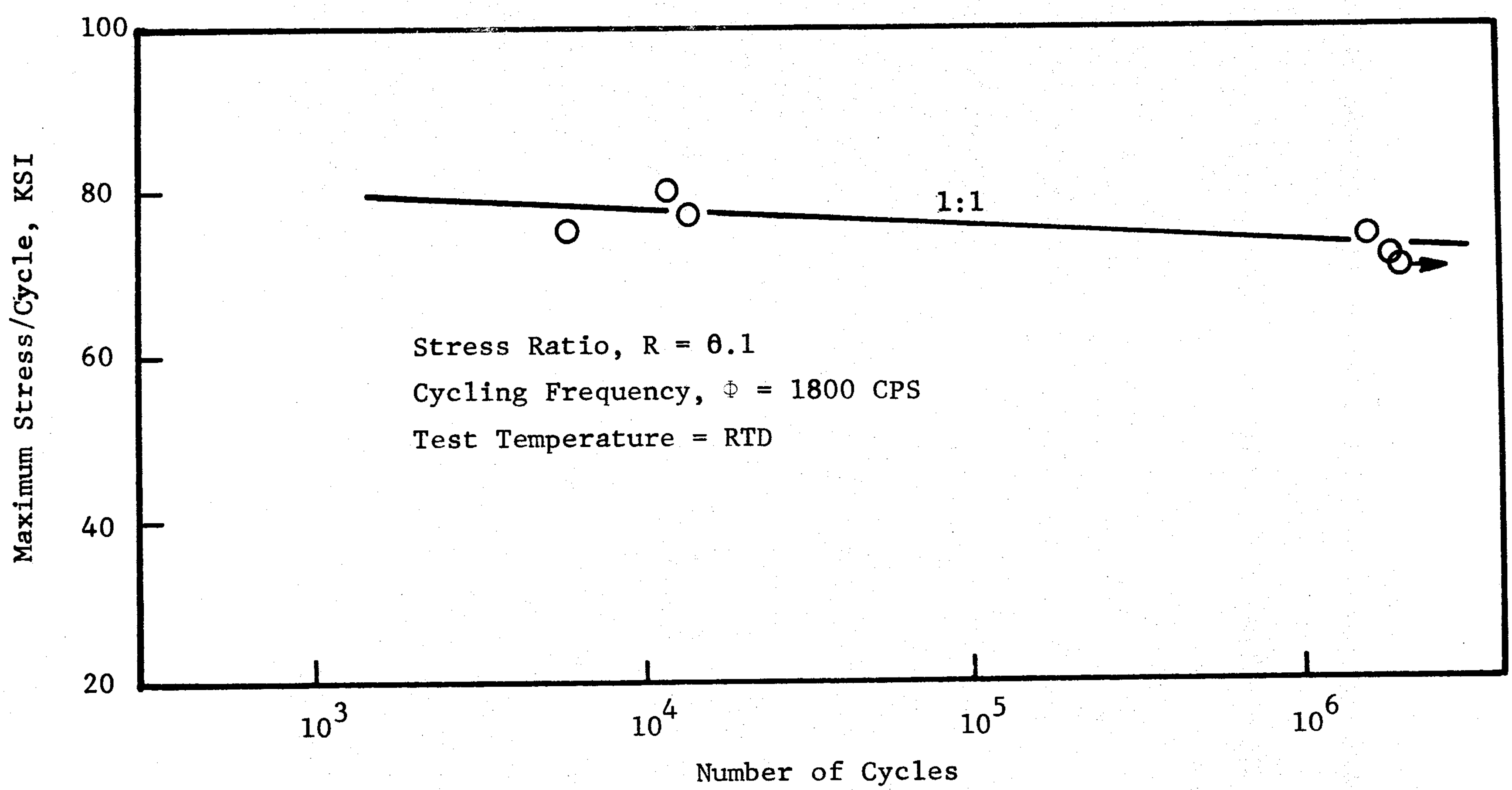

FIG. A-45 TENSION FATIGUE LIFE S-N DIAGRAM FOR 0° ± 45°PR-286/ MODMOR II GRAPHITE/S-GLASS COMPOSITE (1:1)

TABLE A-V

TENSION FATIGUE LIFE OF 0° $\pm$ 45° PR-286/MODMOR II GRAPHITE/
S-GLASS 12 PLY COMPOSITE (GRAPHITE/GLASS = 2:1)
TESTED AT R = 0.1, ROOM TEMPERATURE DRY

Specimen Number	Specimen Thickness (in)	Maximum Stress (ksi)	Cycles to Failure	Residual Strength (ksi)
045-T-2-4	0.069	90	2.501×10^6*	117
045-T-2-5	0.068	100	1,000	
045-T-2-6	0.070	93	2.186×10^6*	127
045-T-2-9	0.070	100	16,000	
045-T-2-10	0.070	98	2,000	
045-T-2-11	0.071	95	406,000	
045-T-2-12	0.067	97	422,000	

* Specimens run out; No failure

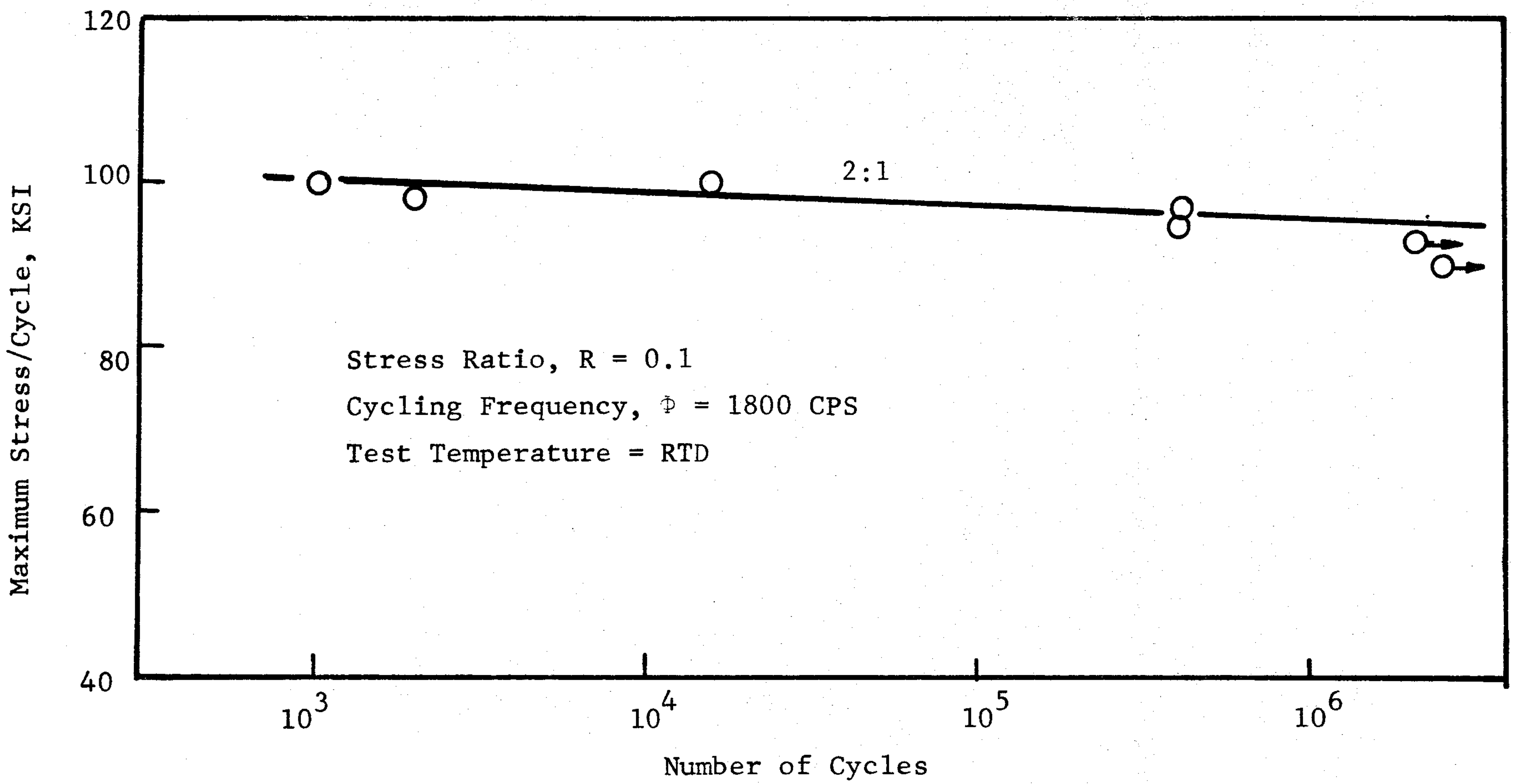

FIG. A-46 TENSION FATIGUE LIFE S-N DIAGRAM FOR 0° ± 45° PR-286/ MODMOR II GRAPHITE/S-GLASS COMPOSITE (2:1)

TABLE A-VI

TENSION FATIGUE LIFE OF 0° $\pm$ 45° PR-286/MODMOR II GRAPHITE/
S-GLASS 16 PLY COMPOSITE (GRAPHITE/GLASS = 3:1)
TESTED AT R = 0.1, ROOM TEMPERATURE DRY

Specimen Number	Specimen Thickness (in)	Maximum Stress (ksi)	Cycles to Failure	Residual Strength (ksi)
045-T-3-4	0.097	100	2.295×10^6*	142
045-T-3-5	0.095	105	48,000	
045-T-3-9	0.097	110	4,000	
045-T-3-10	0.098	103	5,000	
045-T-3-11	0.097	102	2,000	
045-T-3-12	0.094	101	2,000	
045-T-3-13	0.095	107	3,000	

* Specimens run out, No failure

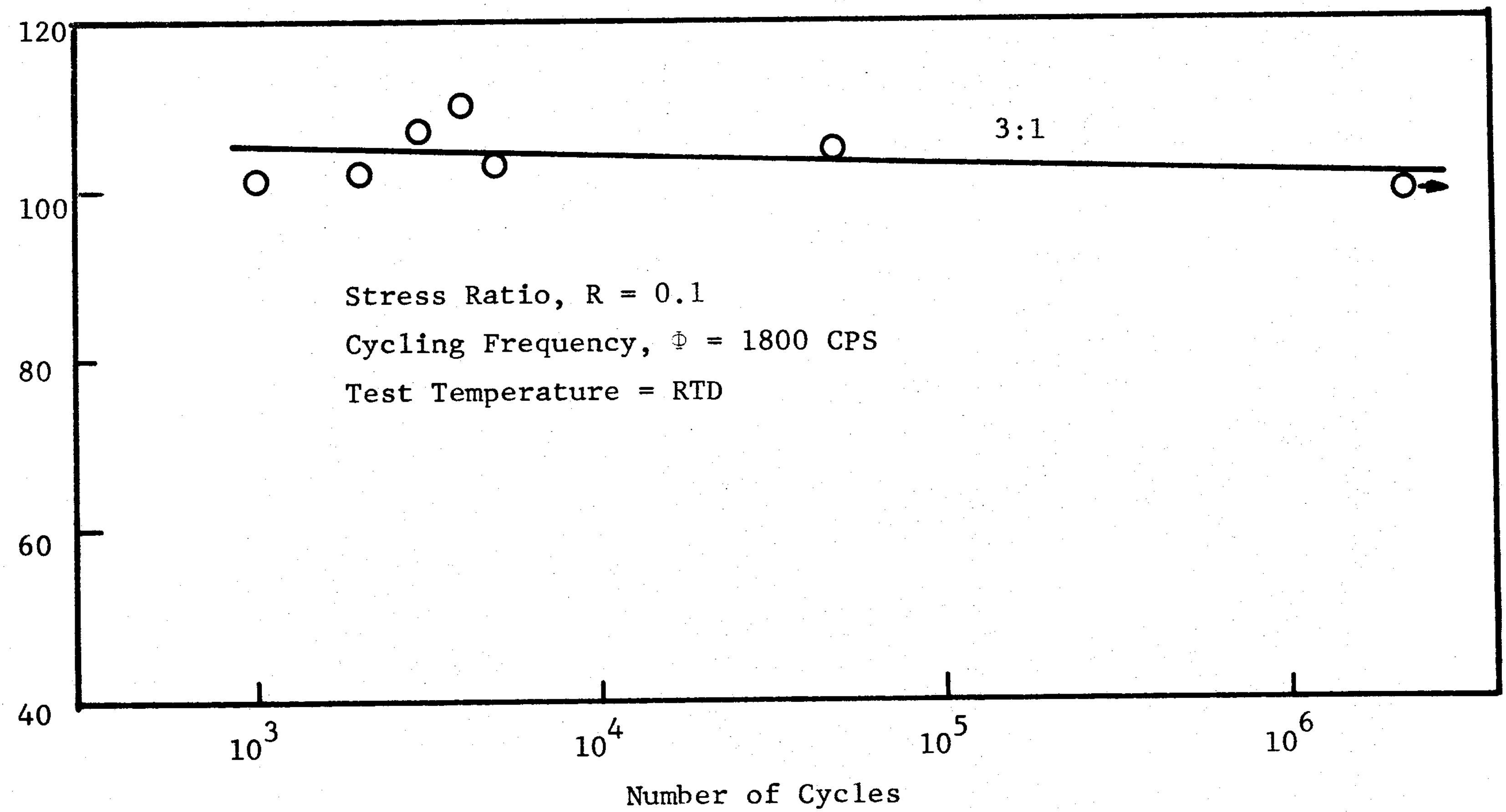

FIG. A-47 TENSION FATIGUE LIFE S-N DIAGRAM FOR 0° ± 45 PR-286/ MODMOR II GRAPHITE/S-GLASS COMPOSITE (3:1)

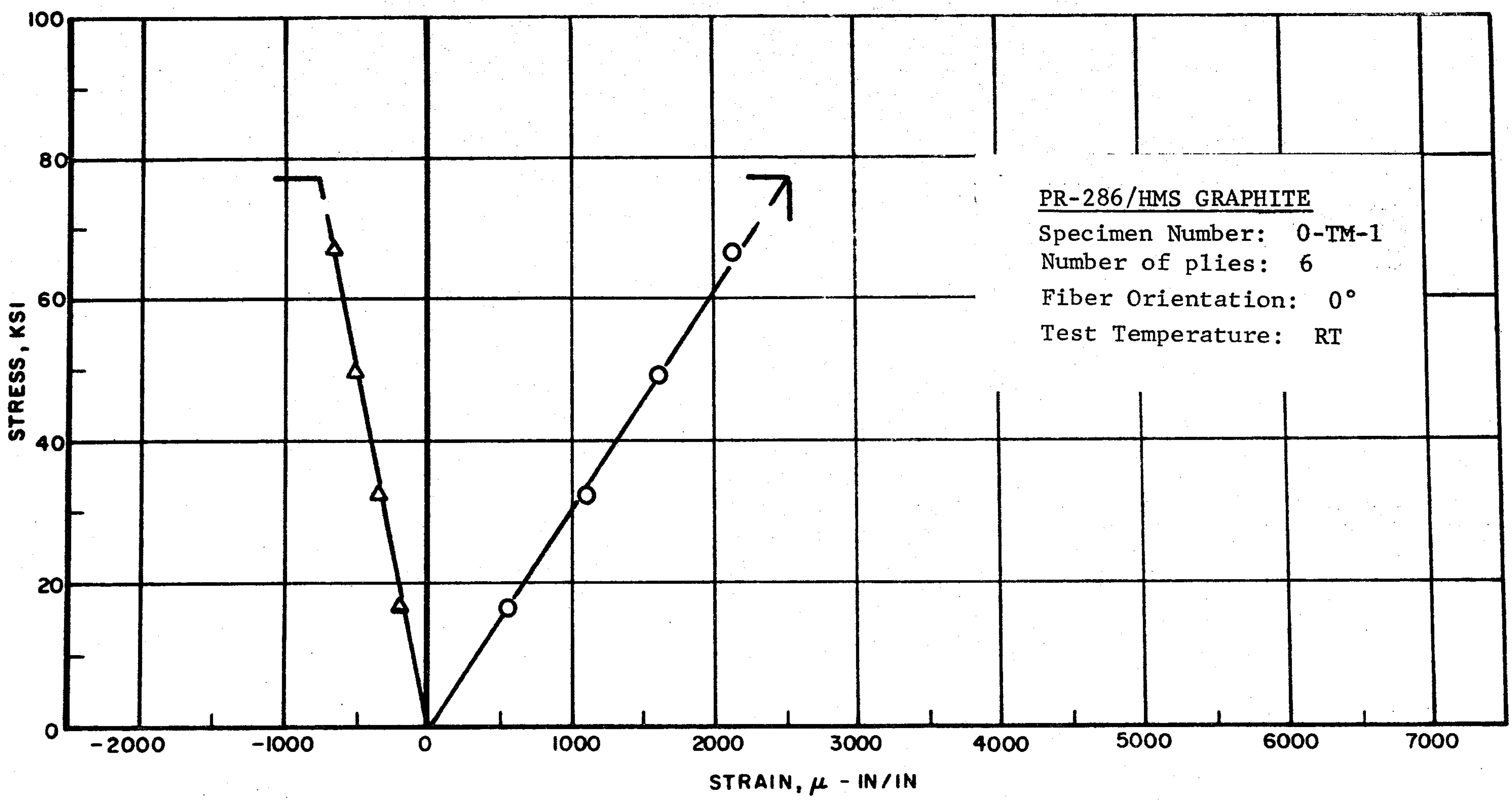

FIG. A-48 TENSION STRESS STRAIN DIAGRAM FOR PR-286/HMS GRAPHITE COMPOSITE TESTED AT ROOM TEMPERATURE

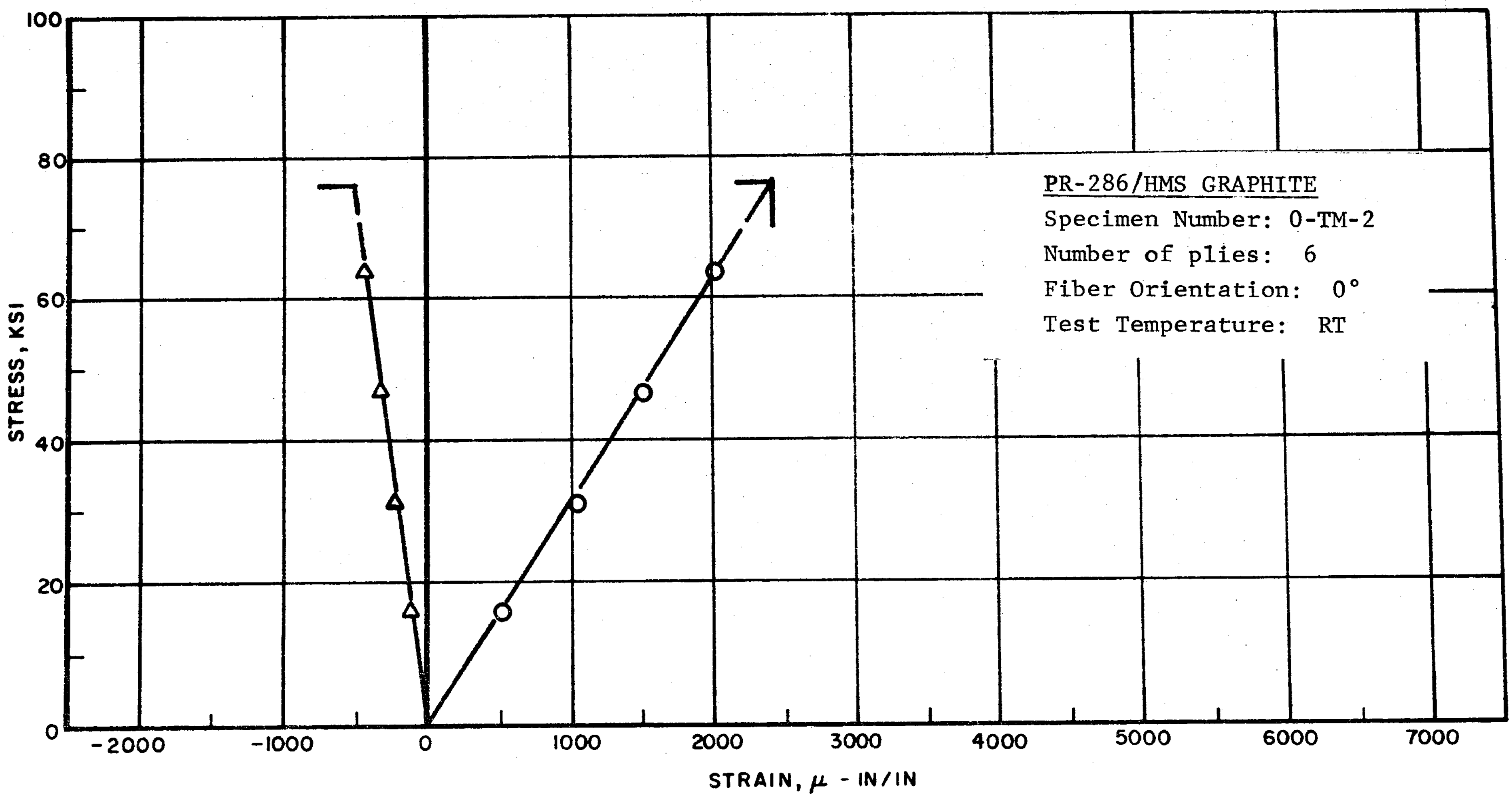

FIG. A-49 TENSION STRESS STRAIN DIAGRAM FOR PR-286/HMS GRAPHITE COMPOSITE TESTED AT ROOM TEMPERATURE

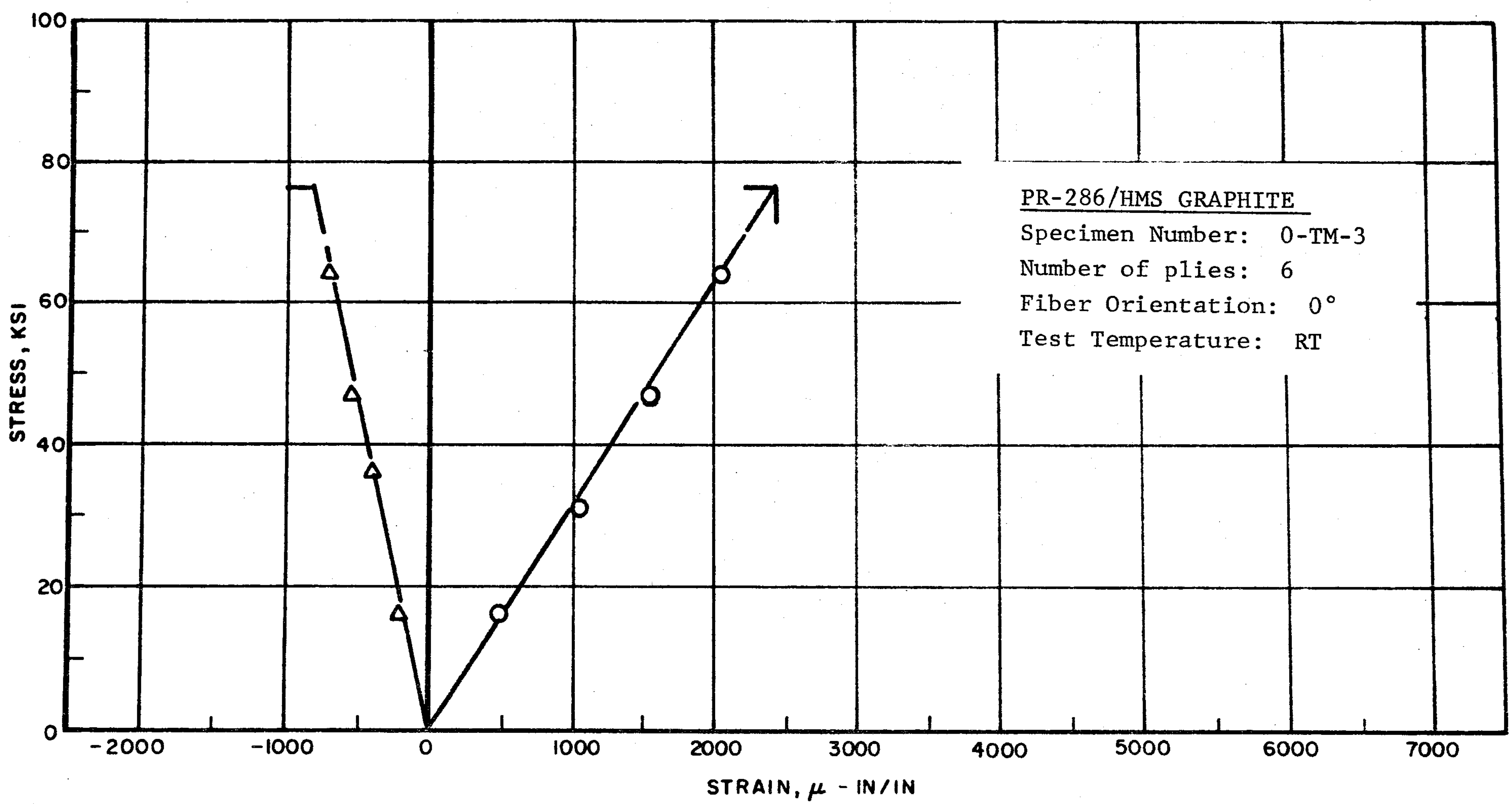

FIG. A-50 TENSION STRESS STRAIN DIAGRAM FOR PR-286/HMS GRAPHITE COMPOSITE TESTED AT ROOM TEMPERATURE

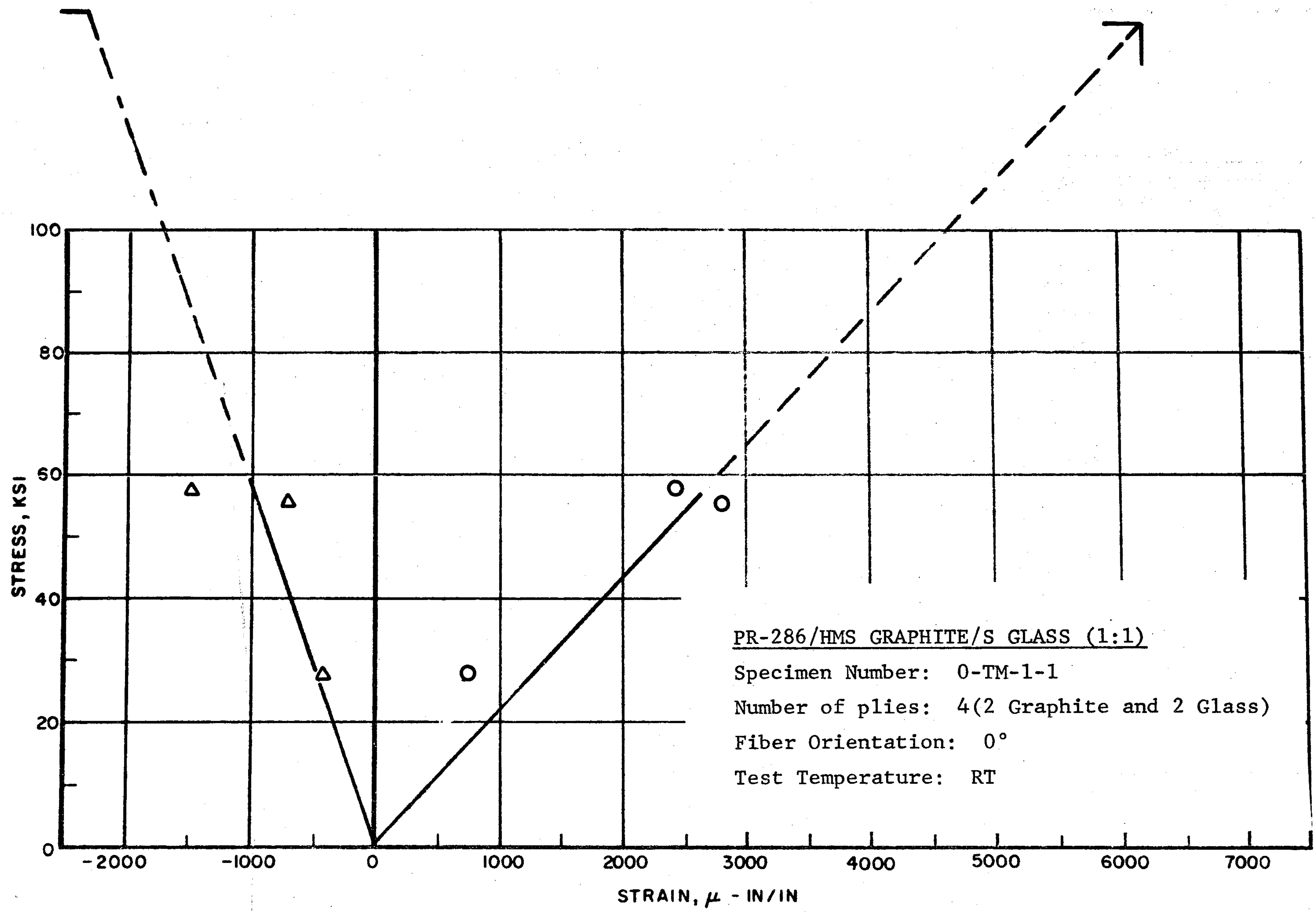

FIG. A-51 TENSION STRESS STRAIN-DIAGRAM FOR PR-286/HMS GRAPHITE/S GLASS COMPOSITE (1:1) TESTED AT ROOM TEMPERATURE

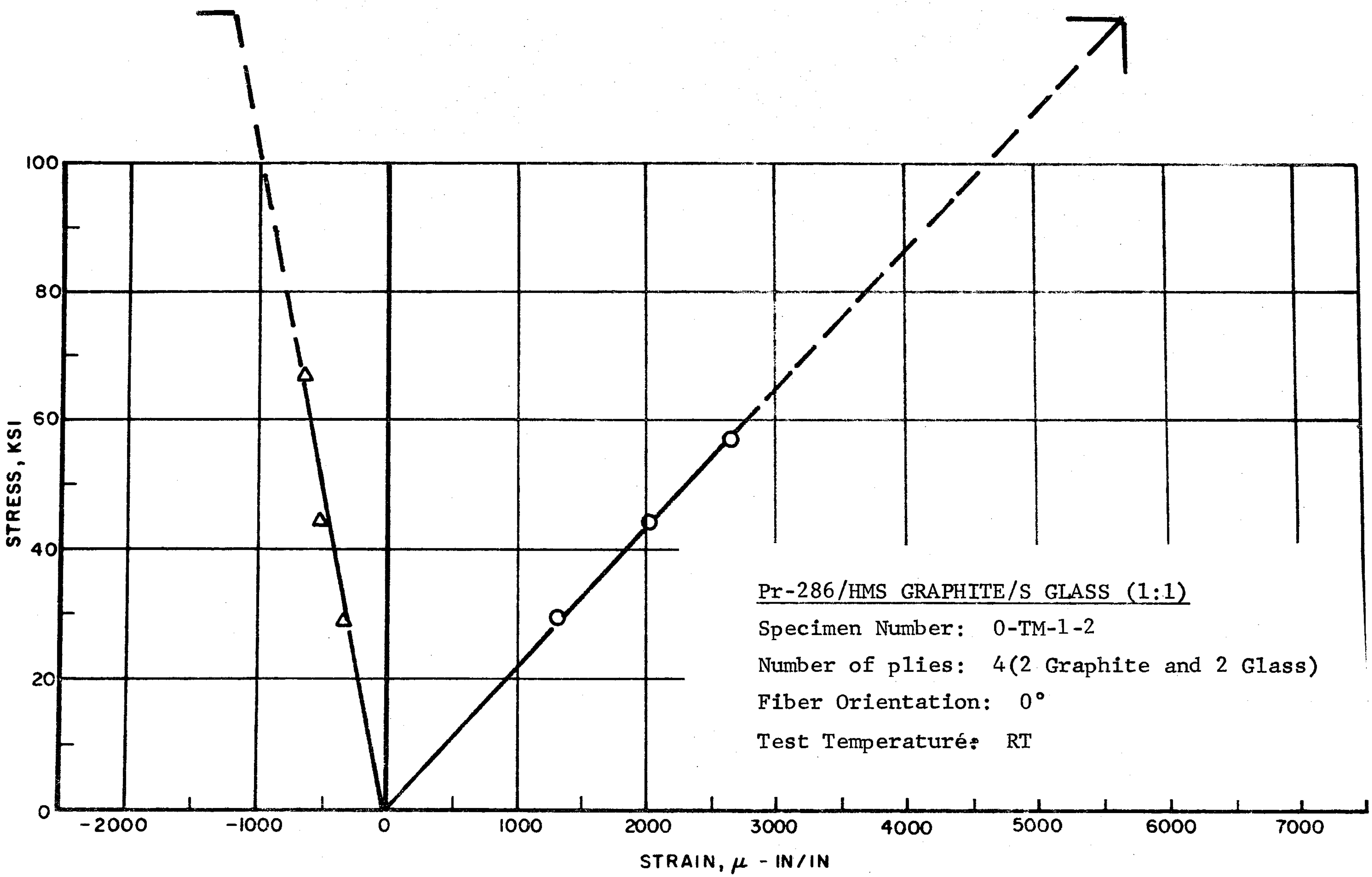

FIG. A-52 TENSION STRESS STRAIN-DIAGRAM FOR PR-286/HMS GRAPHITE/S GLASS COMPOSITE (1:1) TESTED AT ROOM TEMPERATURE

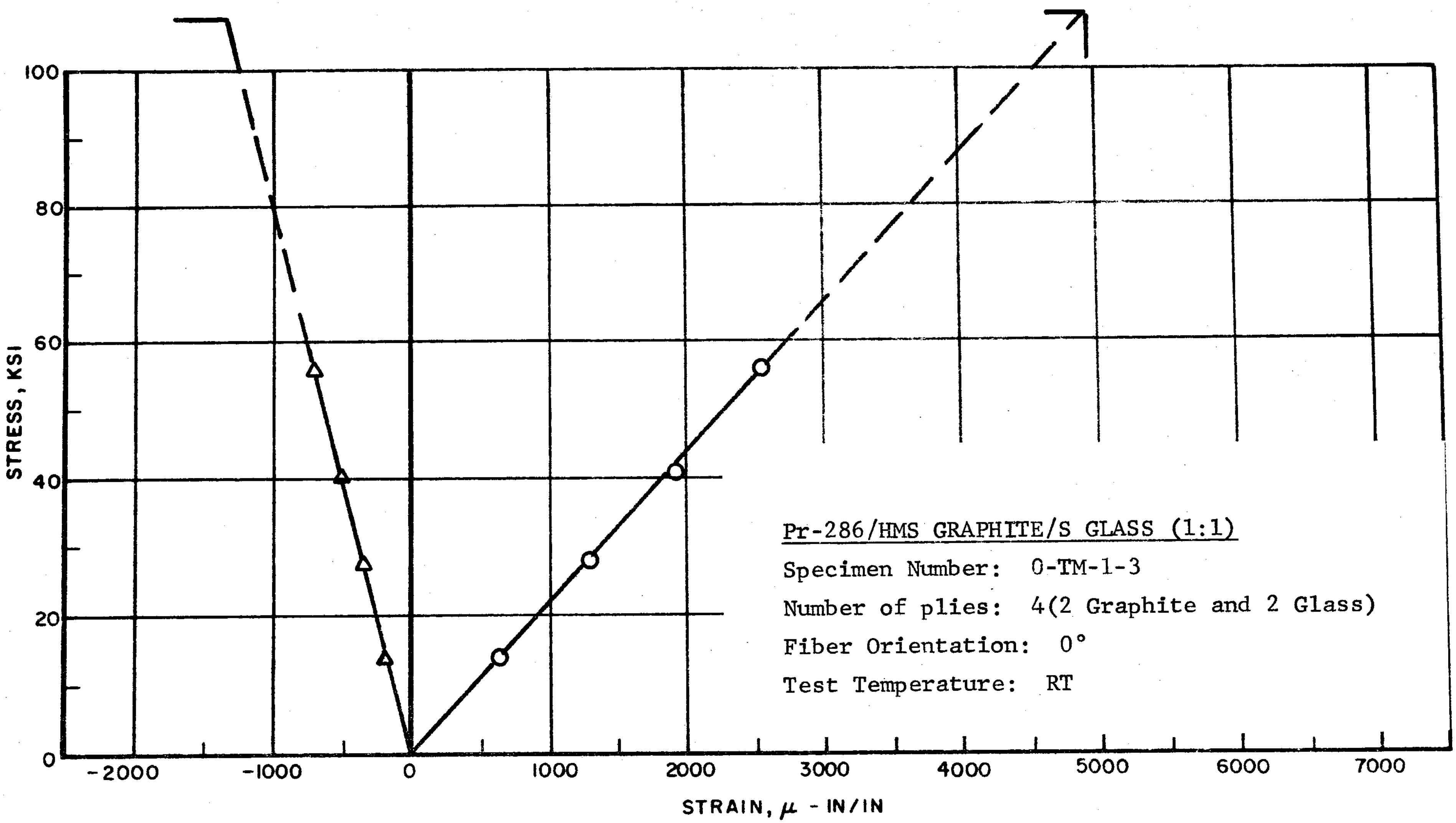

FIG. A-53 TENSION STRESS STRAIN-DIAGRAM FOR PR-286/HMS GRAPHITE/S GLASS COMPOSITE (1:1) TESTED AT ROOM TEMPERATURE

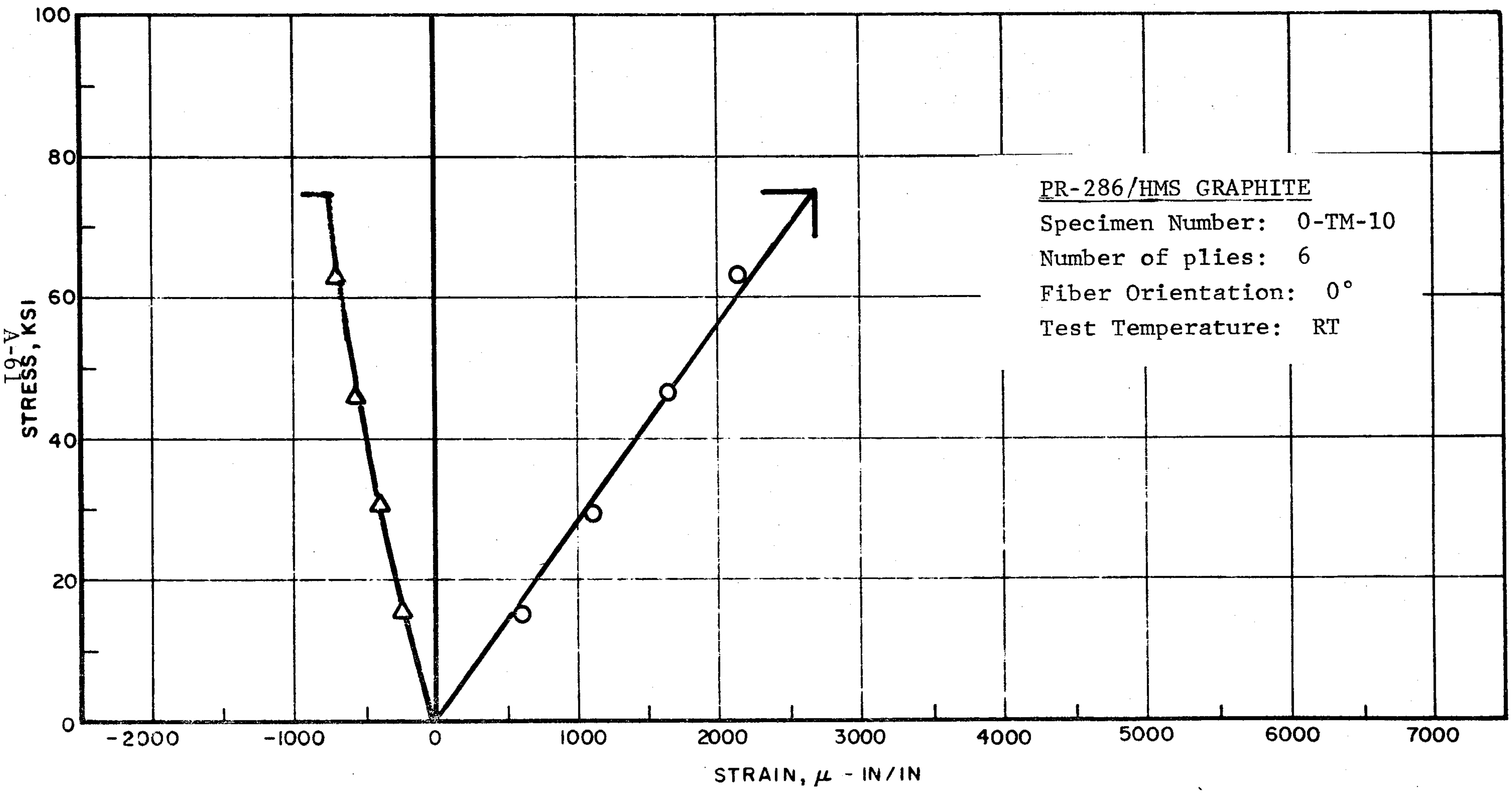

FIG. A-54 TENSION STRESS STRAIN DIAGRAM FOR PR-286/HMS GRAPHITE COMPOSITE TESTED AT ROOM TEMPERATURE AFTER 2 x 10^6 FATIGUE STRESS CYCLES (R=0.1)

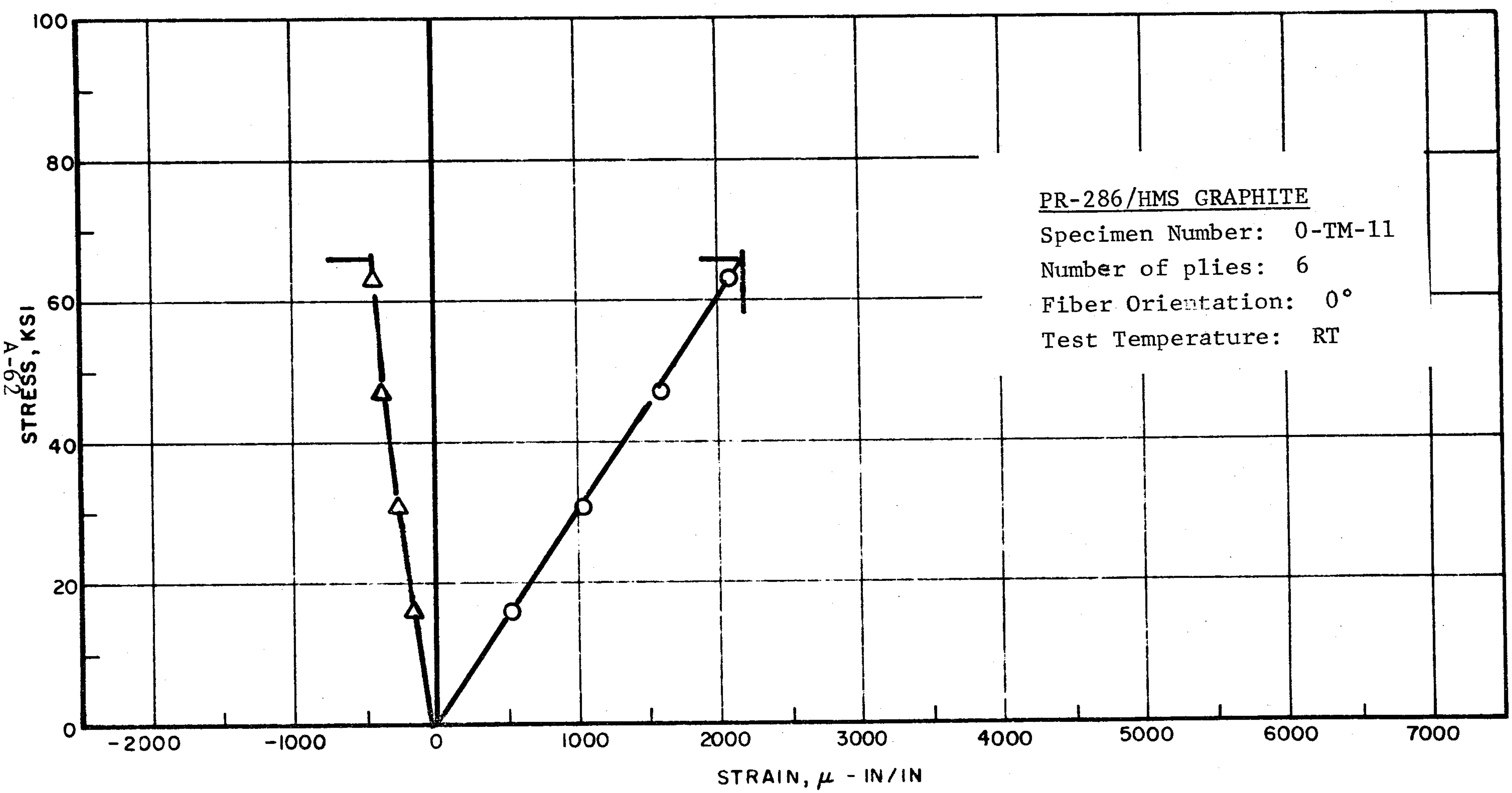

FIG. A-55 TENSION STRESS STRAIN DIAGRAM FOR PR-286/HMS GRAPHITE COMPOSITE TESTED AT ROOM TEMPERATURE AFTER 2×10^6 FATIGUE STRESS CYCLES (R = 0.1)

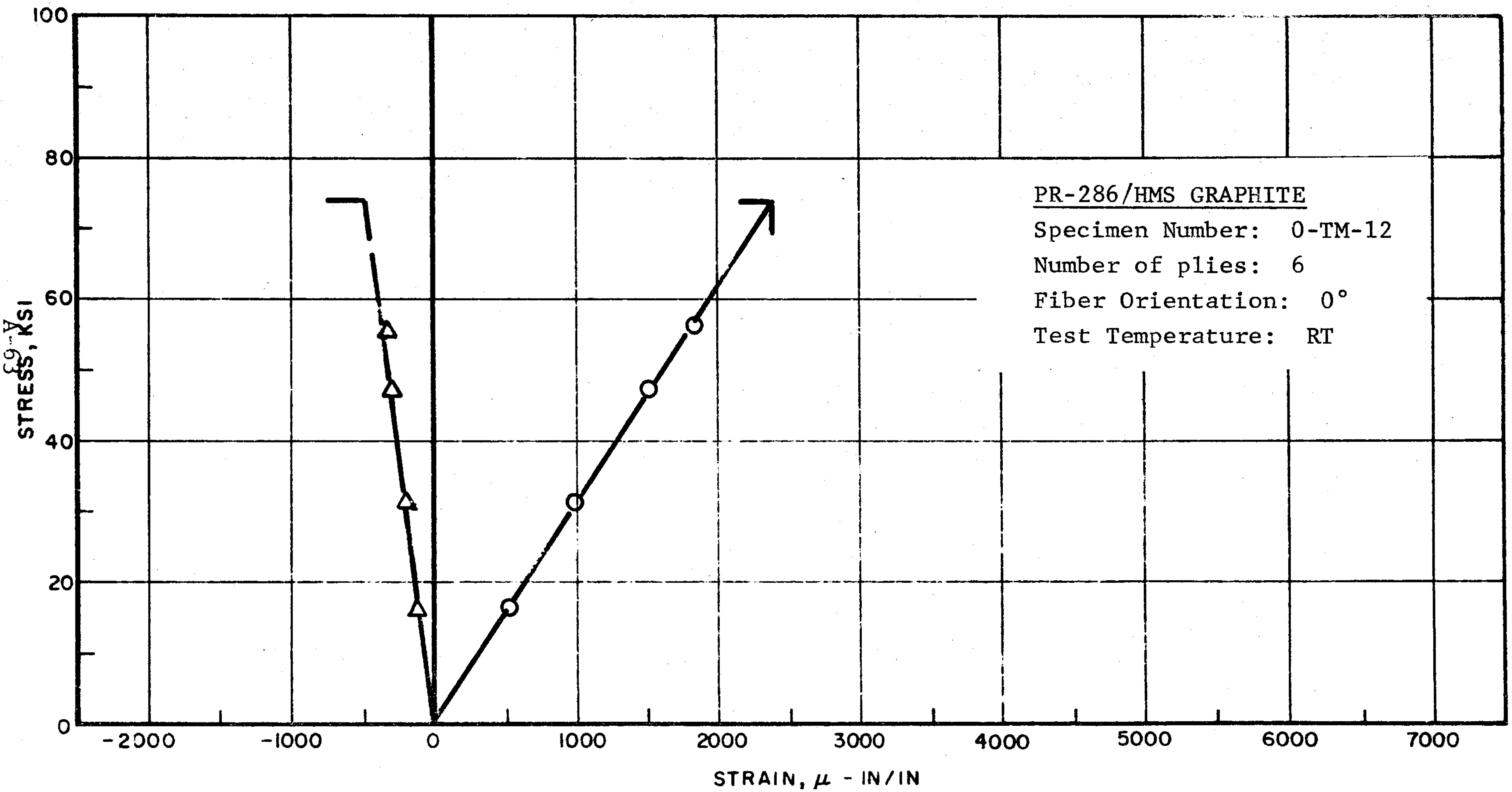

FIG. A-56 TENSION STRESS STRAIN DIAGRAM FOR PR-286/HMS GRAPHITE COMPOSITE TESTED AT ROOM TEMPERATURE AFTER 2 x 10^6 FATIGUE STRESS CYCLES (R= 0.1)

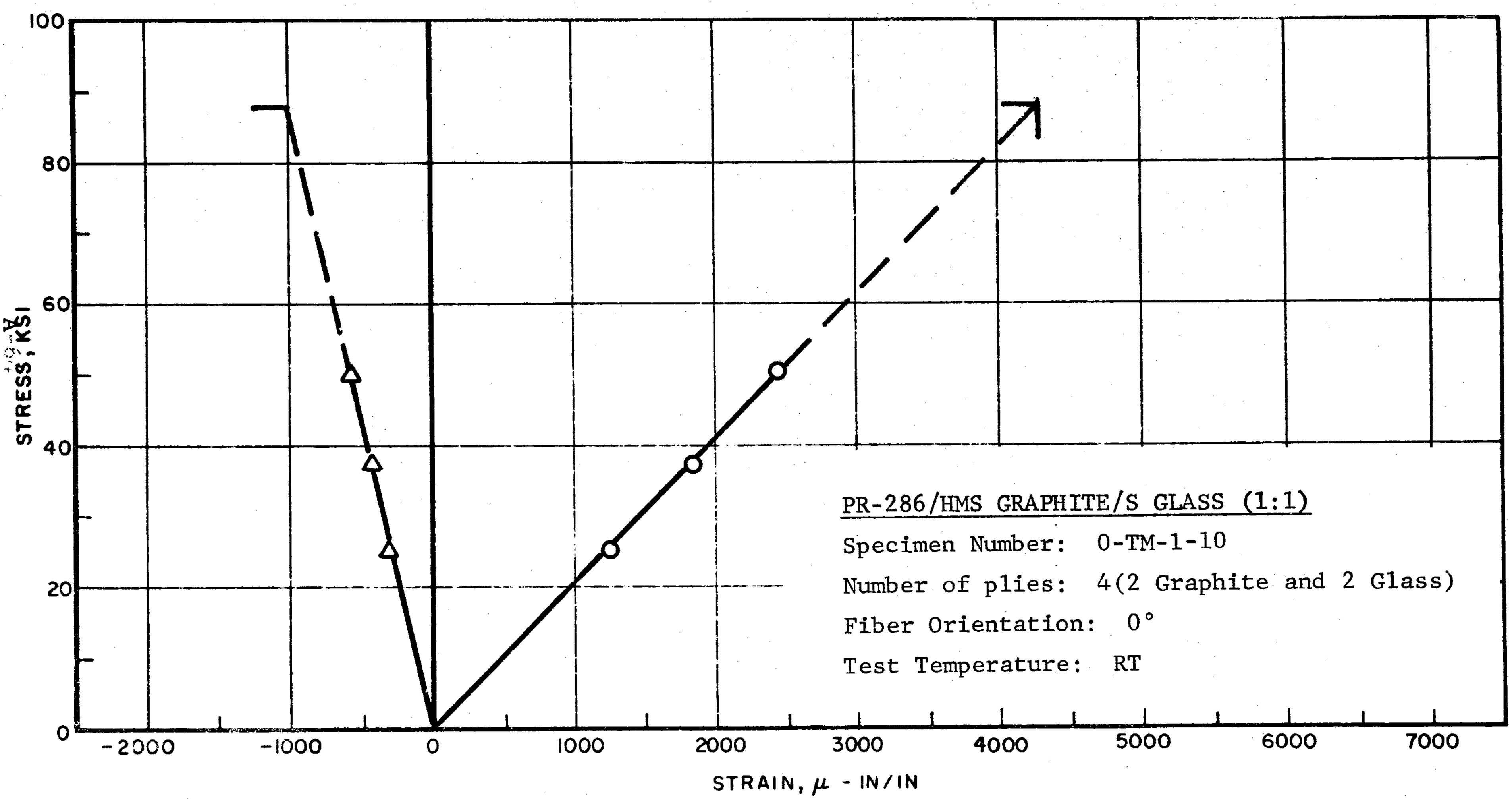

FIG. A-57 TENSION STRESS STRAIN-DIAGRAM FOR PR-286/HMS GRAPHITE/S GLASS COMPOSITE (1:1) TESTED AT ROOM TEMPERATURE AFTER 2 x 10^6 FATIGUE STRESS CYCLES (R = 0.1)

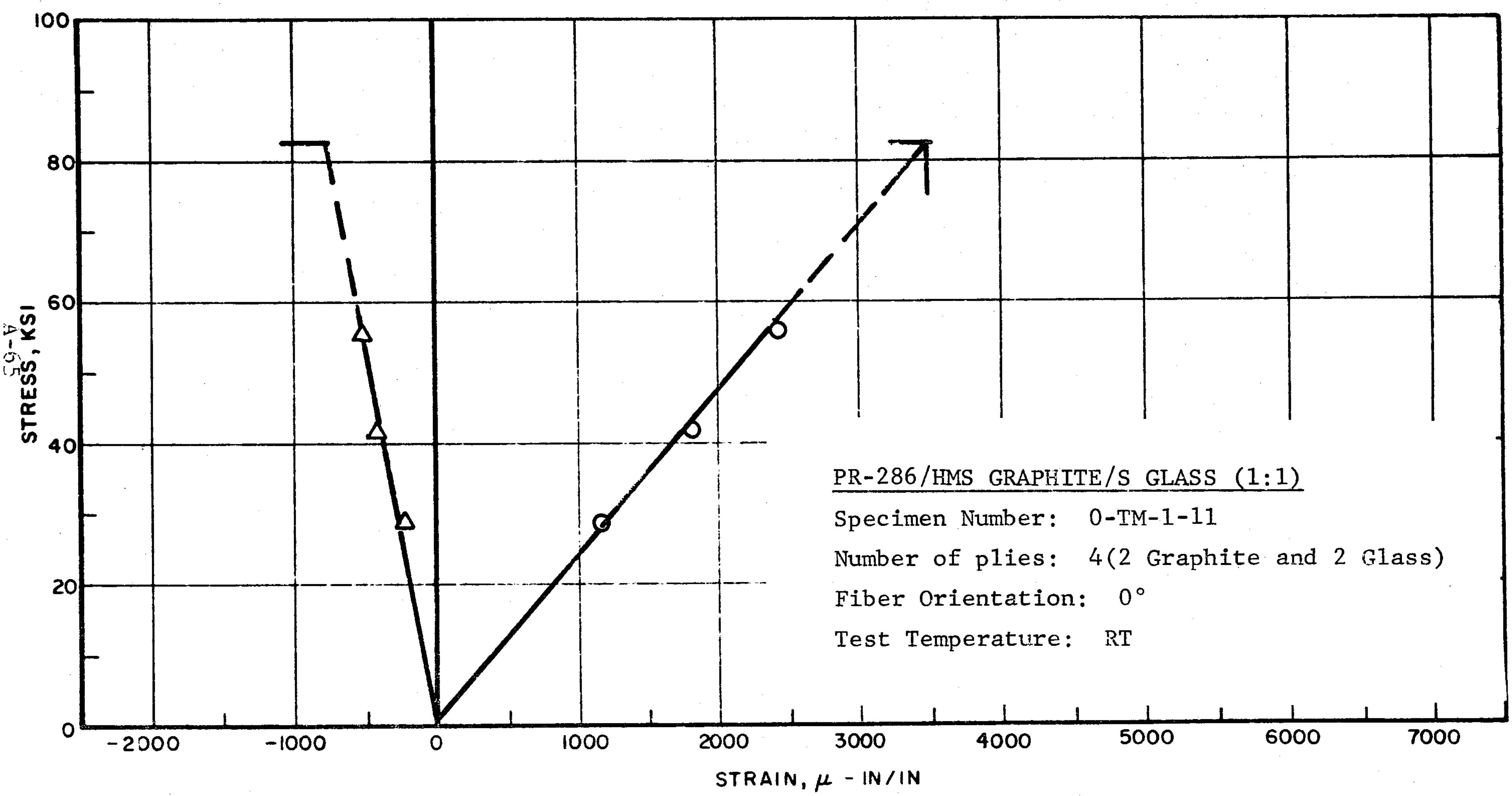

FIG. A-58 TENSION STRESS STRAIN-DIAGRAM FOR PR-286/HMS GRAPHITE/S GLASS COMPOSITE (1:1) TESTED AT ROOM TEMPERATURE AFTER 2×10^6 FATIGUE STRESS CYCLES (R = 0.1)

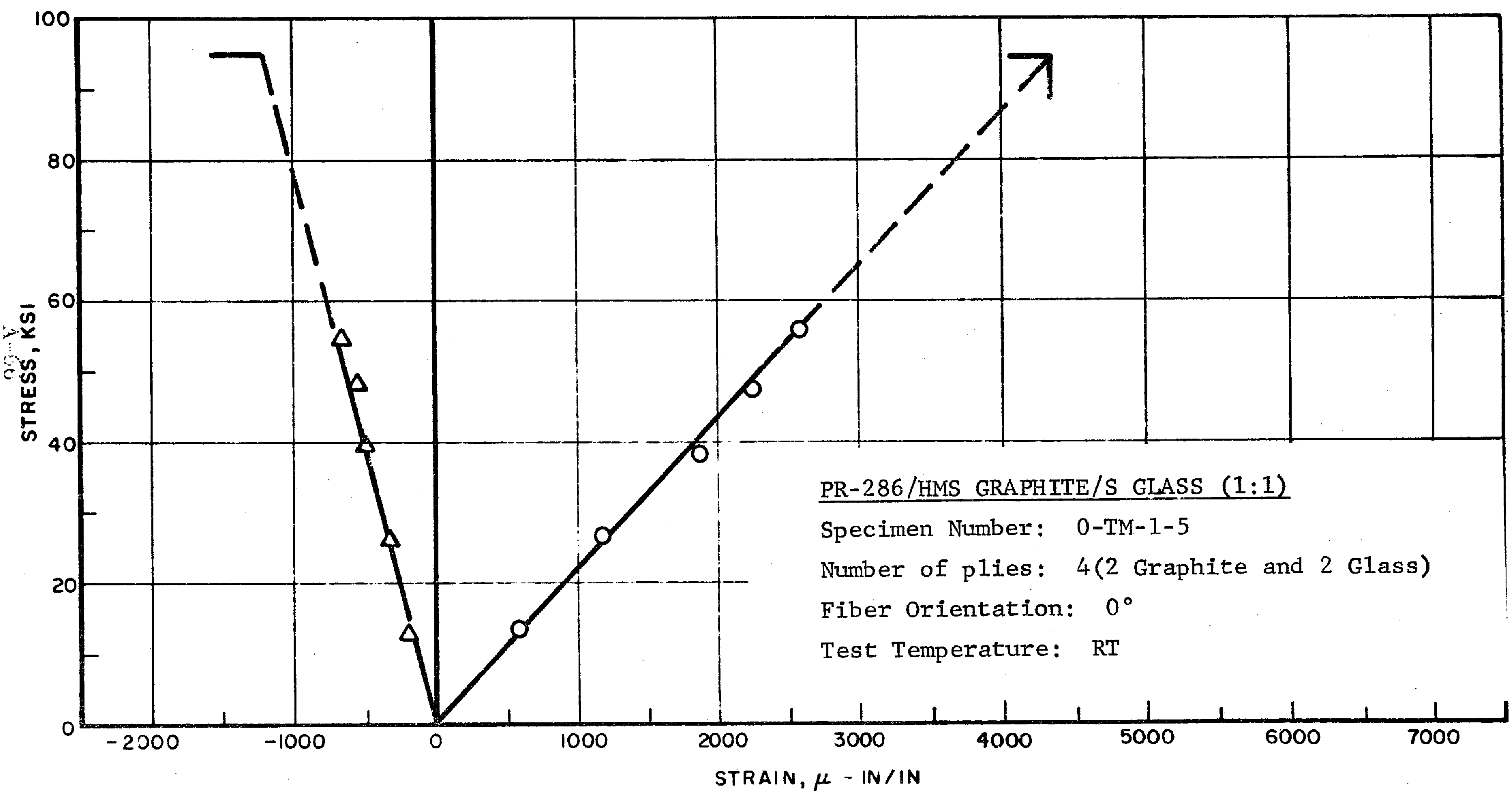

FIG. A-59 TENSION STRESS STRAIN-DIAGRAM FOR PR-286/HMS GRAPHITE/S GLASS COMPOSITE (1:1) TESTED AT ROOM TEMPERATURE AFTER 2×10^6 FATIGUE STRESS CYCLES (R = 0.1)

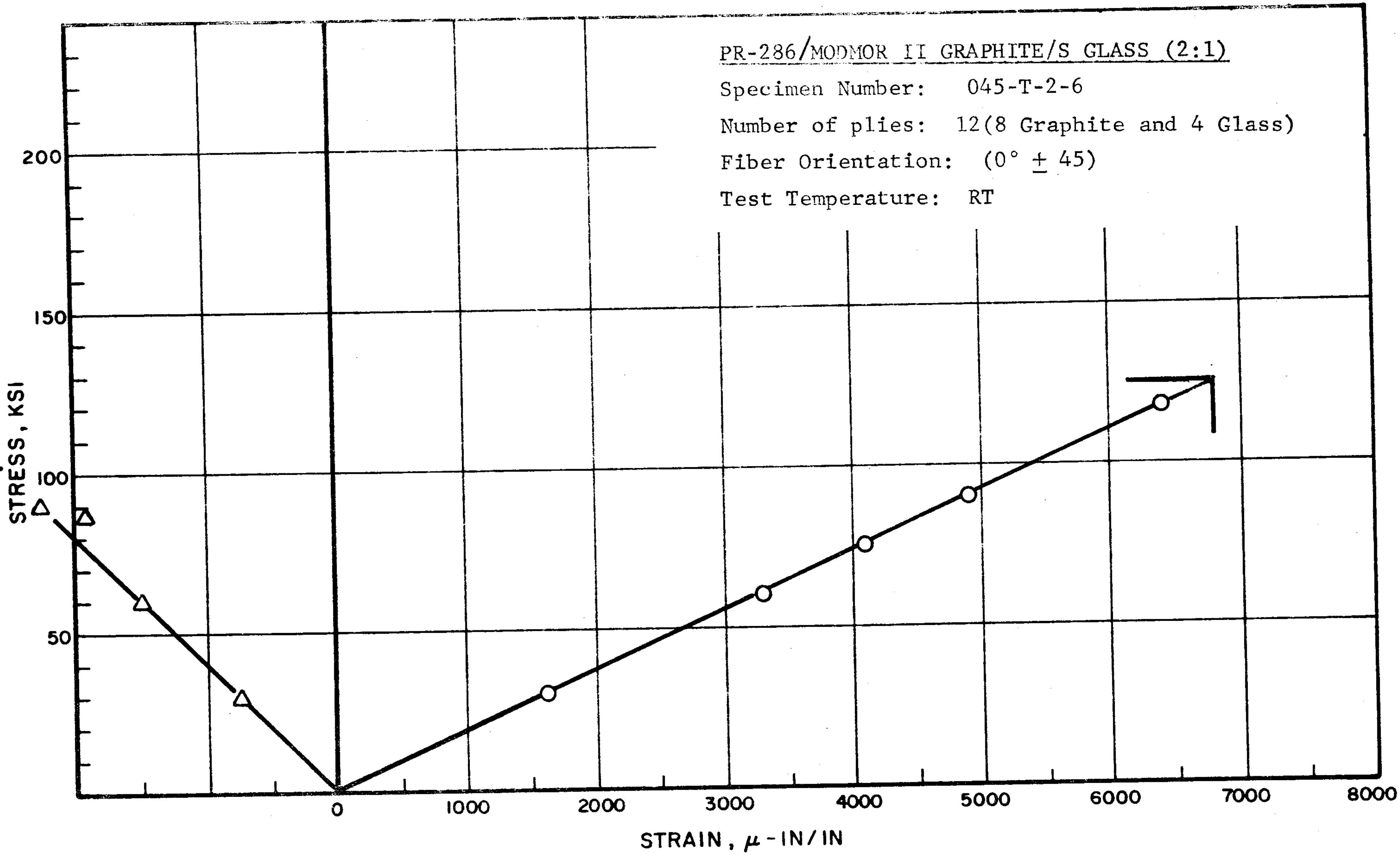

FIG. A-60 TENSION STRESS STRAIN DIAGRAM FOR PR-286/MODMOR II GRAPHITE/S GLASS COMPOSITE (2:1) TESTED AT ROOM TEMPERATURE AFTER 2.5×10^6 FATIGUE STRESS CYCLES (R = 0.1)

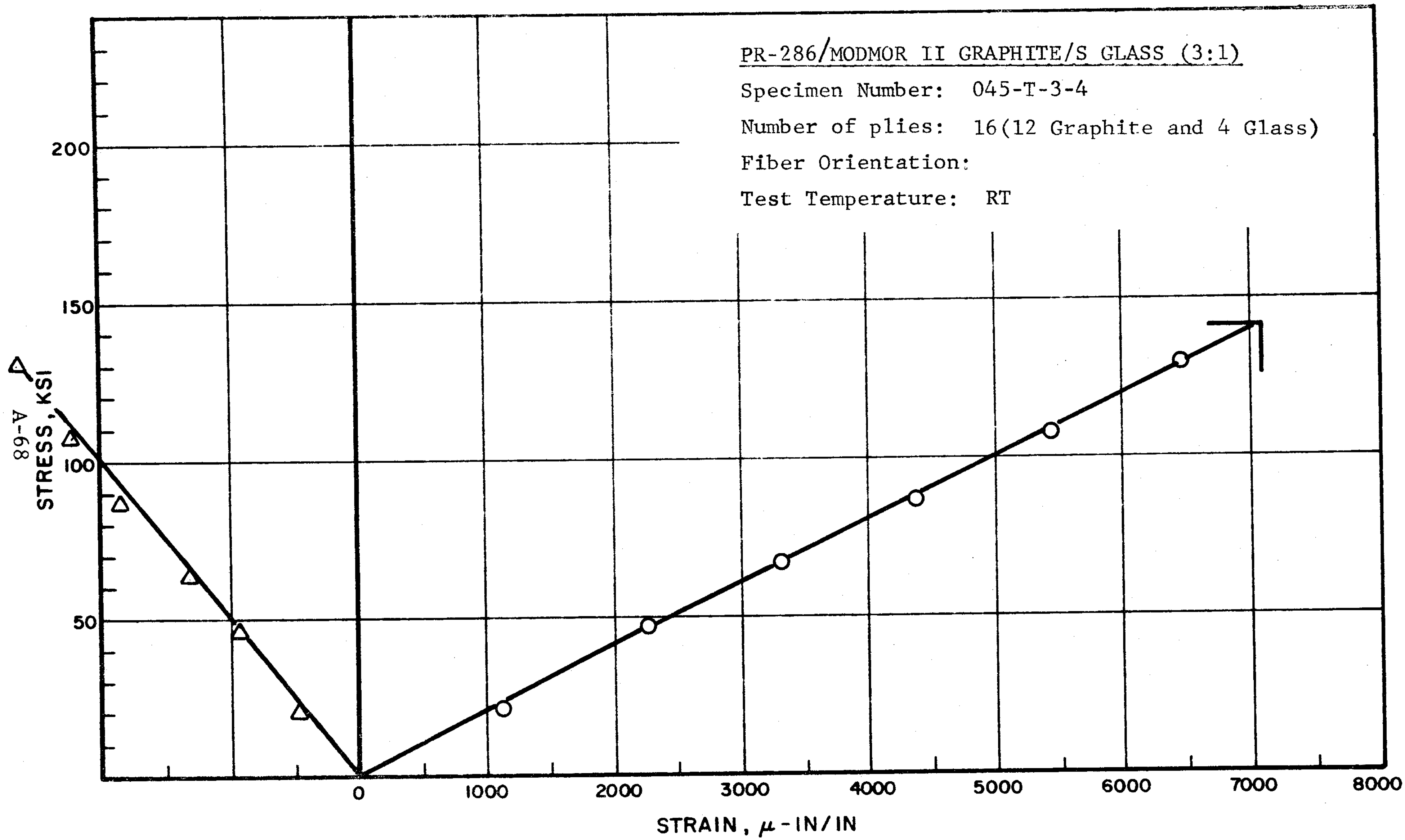

FIG. A- 61 TENSION STRESS STRAIN DIAGRAM FOR PR-286/MODMOR II GRAPHITE/S GLASS COMPOSITE (3:1) TESTED AT ROOM TEMPERATURE AFTER 2.3 x 10^6 FATIGUE STRESS CYCLES (R = 0.1)

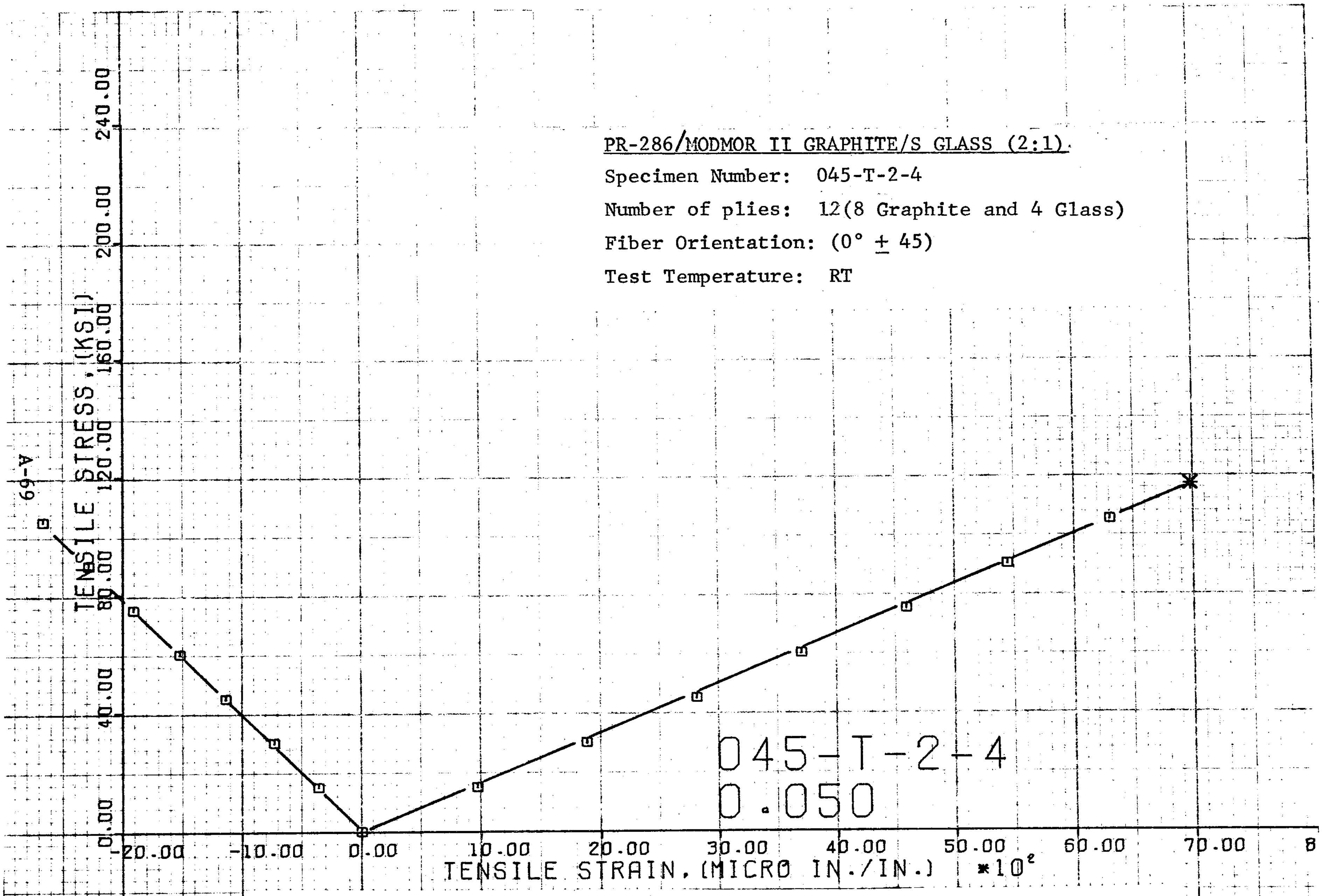

FIG. A-62 TENSION STRESS STRAIN DIAGRAM FOR PR-286/MODMOR II GRAPHITE/S GLASS COMPOSITE (2:1) TESTED AT ROOM TEMPERATURE AFTER 2.5 x 10^6 FATIGUE STRESS CYCLES (R = 0.1)

TABLE A-VII

TENSION FATIGUE LIFE OF 0° PR-286/HMS GRAPHITE/
4 PLY COMPOSITE TESTED AT R = 0.1, ROOM TEMPERATURE DRY

Specimen Number	Specimen Thickness (in)	Maximum Stress (ksi)	Cycles to Failure	Residual Strength (ksi)
0-TM-4	0.029	50	60,000	
0-TM-5	0.032	55	-	
0-TM-6	0.030	53	445,000	
0-TM-7	0.029	55	-	
0-TM-8	0.031	54	-	
0-TM-9	0.030	51	133,000	
0-TM-10	0.030	50	2.6×10^6*	
0-TM-11	0.031	45	2.004×10^6*	
0-TM-12	0.031	52	2.545×10^6*	
0-TM-13	0.031	49	920,000	

* Specimens run out; No failure

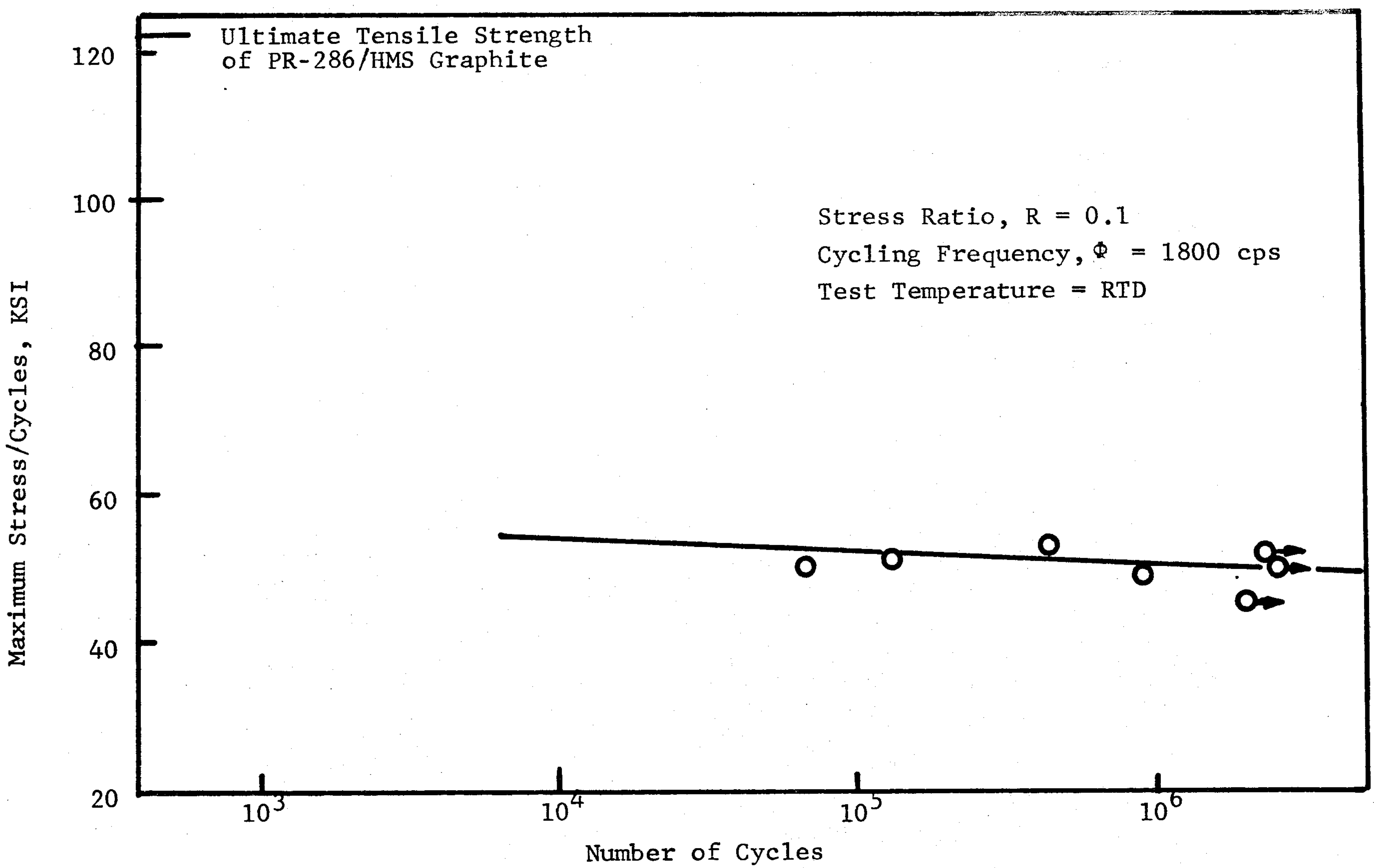

FIG. A-63 TENSION FATIGUE LIFE S-N DIAGRAM FOR 0° PR-286/HMS GRAPHITE COMPOSITE

TABLE A-VIII

TENSION FATIGUE LIFE OF 0° PR-286/HMS GRAPHITE/
S-GLASS 4 PLY COMPOSITE (GRAPHITE/GLASS = 1:1)
TESTED AT R = 0.1, ROOM TEMPERATURE DRY

Specimen Number	Specimen Thickness (in)	Maximum Stress (ksi)	Cycles to Failure	Residual Strength (ksi)
0-TM-1-4	0.036	90	-	
0-TM-1-5	0.036	40	2×10^6*	
0-TM-1-6	0.007	80	-	
0-TM-1-7	0.038	50	9,000	
0-TM-1-8	0.036	50	54,000	
0-TM-1-9	0.036	55	8,000	
0-TM-1-10	0.037	45	2.085×10^6*	
0-TM-1-11	0.037	48	2.482×10^6*	
0-TM-1-12	0.037	53	3,000	
0-TM-1-13	0.035	55	4,000	
0-TM-1-14	0.036	52	15,000	

* Specimens run out; No failure

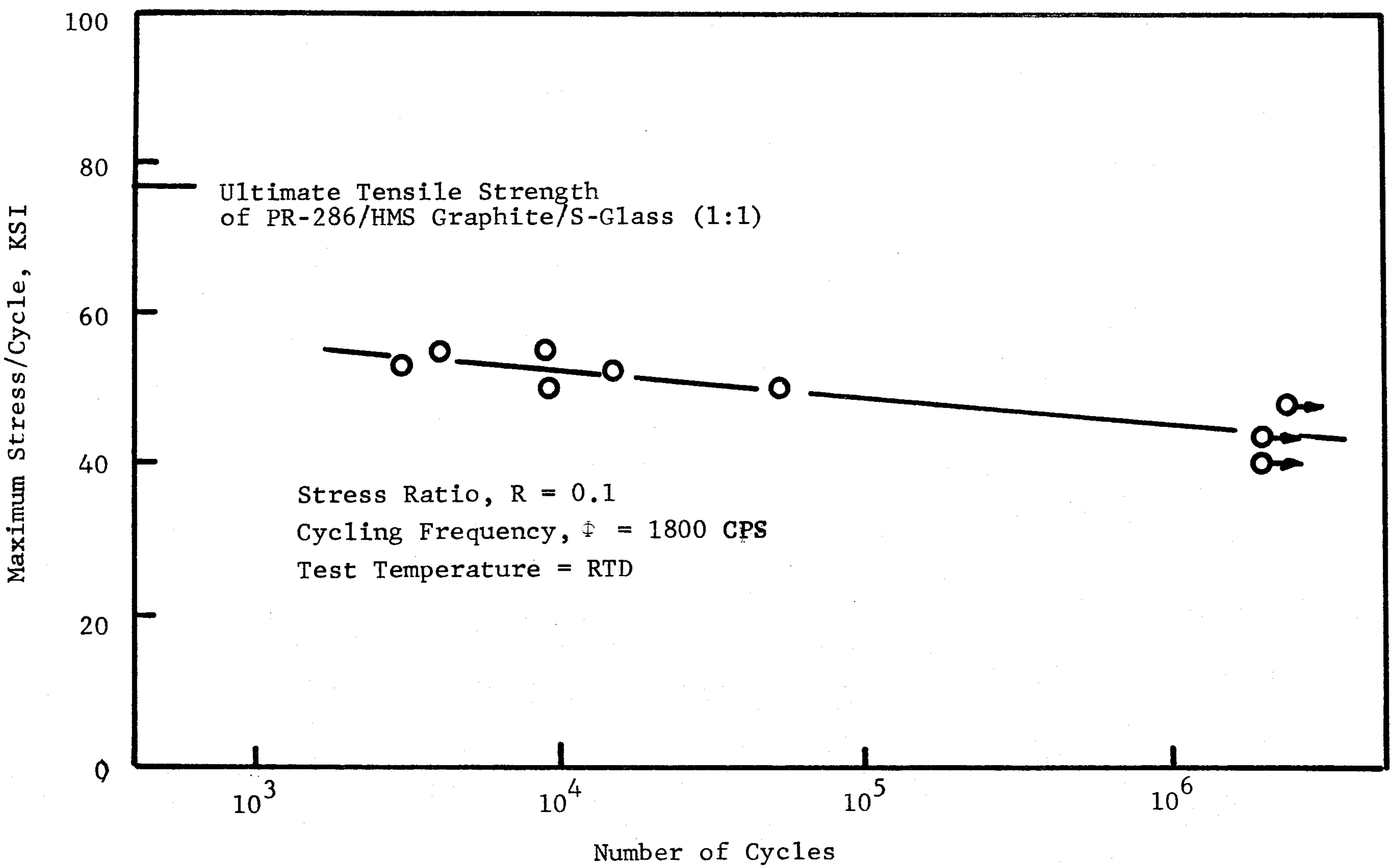

FIG. A-64 TENSION FATIGUE LIFE S-N DIAGRAM FOR PR-286/HMS GRAPHITE/S-GLASS GRAPHITE

APPENDIX B

REVIEW OF STATE OF ART OF MIXED FIBER COMPOSITES

APPENDIX B

B.0 REVIEW OF STATE OF ART OF MIXED FIBER COMPOSITES

Hybrid or mixed fiber composites will be used to improve the economics of advanced composite materials for application to Naval Aircraft structural components. This review is intended to present some of the past efforts to prepare and test hybrid composites.

B.1 Preparation of the Hybrid Composites

Previous studies (See Ref. 1) have concentrated on the hybridization of boron fiber and HTS Graphite tow. Evensen (Ref. 1) pointed out that three methods of mixing graphite and boron were available: 1) graphite tows drum-wound over boron/epoxy prepreg, 2) boron fibers drum-wound over graphite prepreg or 3) interply stacking of boron/epoxy and graphite/epoxy prepregs. For glass rovings/graphite tows/epoxy hybrids a fourth method is available: 4) mixing of the separate graphite and glass fibers and subsequent impregnation of the mixed system. Finally a fifth method is available for intraply mixing: 5) drum winding of alternate fibrous materials followed by impregnation of the fibers.

Pinckney (Ref. 2) prepared S-Glass/graphite hybrids by the interleaving of S-Glass/Epoxy and graphite epoxy prepreg (method 3 above). The particular interply process studied was: 3a) a core-shell concept wherein a symetric laminate is prepared with a core of one prepreg material and the top and bottom outer shells of another prepreg material. In the current IITRI program we looked at an alternative method: 3b) of uniformly distributed interply hybridization.

B.2 Testing of Hybrid Composites

Static testing of hybrid composites was accomplished by Evensen[1], Chamis[5] and Pinckney[2]. Creep testing of hybrid composites was performed by Pinckney[2] and impact testing by Chamis[5]. Some fatigue testing was also performed by Pinckney[2]. Other investigations are currently underway to establish the static and fatigue properties of hybrids, but most of this work is not now in the open literature.

Evensen[1] has presented analytical procedures for dealing with the mechanical properties of hybrids. These have largely been supplanted by more sophisticated means of analysis which have also not yet reached the open literature.

Unclassified
Security Classification

DOCUMENT CONTROL DATA - R&D

(Security classification of title, body of abstract and indexing annotation must be entered when the overall report is classified)

1 ORIGINATING ACTIVITY (Corporate author) IIT Research Institute 10 West 35th Street Chicago, Illinois 60616	2a REPORT SECURITY CLASSIFICATION Unclassified 2b GROUP N.A.

3 REPORT TITLE

Fatigue Properties of Graphite Composites

4 DESCRIPTIVE NOTES (Type of report and inclusive dates)

Final Report 9 February 1972 to 9 February 1973

5 AUTHOR(S) (Last name, first name, initial)

Nagaraja Rao and K.E.Hofer, Jr.

6 REPORT DATE April 1973	7a. TOTAL NO. OF PAGES 124	7b. NO OF REFS 5
8a CONTRACT OR GRANT NO N 00019-72-C-0294 NASC b. PROJECT NO c d.	9a. ORIGINATOR'S REPORT NUMBER(S) D 6070 9b. OTHER REPORT NO(S) (Any other numbers that may be assigned this report) N.A.	

10 AVAILABILITY/LIMITATION NOTICES

Approved for Public Release ; Distribution Unlimited

11 SUPPLEMENTARY NOTES N.A.	12. SPONSORING MILITARY ACTIVITY Naval Air Systems Command

13 ABSTRACT The specific objective of this program was to utilize a commercially available glass and commercially available high strength and high modulus graphite fibers with a common epoxy matrix to maximize the technical performance of the hybrid composite in fatigue applications.

Two ternary composite material systems, PR 286/Modmor II/Graphite/S-Glass and PR 286/HMS Graphite/S-Glass, involving two types of lamination fabrications namely Uniformly distributed interply hybrids and Core-shell hybrids were investigated.The test program included static tests, tensile fatigue tests, shear fatigue tests, modulus degradation studies and microscopic examination.

The study shows that (1) hybrid composites perform generally satisfactorily in fatigue and will survive rigorous stress cycling. (2) Distributed interply hybrids show a better mechanical performance than core-shell hybrids. (3) The mechanical behavior of hybrid composites generally follows the rule of mixtures and the Rule of mixtures can be used to predict elastic moduli of hybrids. (4) The performance (as a percentage of the fatigue strength at any given life) of 1:1 HMS Graphite/Glass/Epoxy relative to pure HMS Graphite is better than is that of 1:1 HTS Graphite/glass/epoxy relative to pure HTS graphite/epoxy.

DD FORM 1 JAN 64 1473

Unclassified
Security Classification

Unclassified
Security Classification

14. KEY WORDS	LINK A		LINK B		LINK C	
	ROLE	WT	ROLE	WT	ROLE	WT
Graphite/Glass/Epoxy composites, Fatigue, Modulus Degradation, Hybrid Composites.						

INSTRUCTIONS

1. ORIGINATING ACTIVITY: Enter the name and address of the contractor, subcontractor, grantee, Department of Defense activity or other organization *(corporate author)* issuing the report.

2a. REPORT SECURITY CLASSIFICATION: Enter the overall security classification of the report. Indicate whether "Restricted Data" is included. Marking is to be in accordance with appropriate security regulations.

2b. GROUP: Automatic downgrading is specified in DoD Directive 5200.10 and Armed Forces Industrial Manual. Enter the group number. Also, when applicable, show that optional markings have been used for Group 3 and Group 4 as authorized.

3. REPORT TITLE: Enter the complete report title in all capital letters. Titles in all cases should be unclassified. If a meaningful title cannot be selected without classification, show title classification in all capitals in parenthesis immediately following the title.

4. DESCRIPTIVE NOTES: If appropriate, enter the type of report, e.g., interim, progress, summary, annual, or final. Give the inclusive dates when a specific reporting period is covered.

5. AUTHOR(S): Enter the name(s) of author(s) as shown on or in the report. Enter last name, first name, middle initial. If military, show rank and branch of service. The name of the principal author is an absolute minimum requirement.

6. REPORT DATE: Enter the date of the report as day, month, year; or month, year. If more than one date appears on the report, use date of publication.

7a. TOTAL NUMBER OF PAGES: The total page count should follow normal pagination procedures, i.e., enter the number of pages containing information.

7b. NUMBER OF REFERENCES: Enter the total number of references cited in the report.

8a. CONTRACT OR GRANT NUMBER: If appropriate, enter the applicable number of the contract or grant under which the report was written.

8b, 8c, & 8d. PROJECT NUMBER: Enter the appropriate military department identification, such as project number, subproject number, system numbers, task number, etc.

9a. ORIGINATOR'S REPORT NUMBER(S): Enter the official report number by which the document will be identified and controlled by the originating activity. This number must be unique to this report.

9b. OTHER REPORT NUMBER(S): If the report has been assigned any other report numbers *(either by the originator or by the sponsor)*, also enter this number(s).

10. AVAILABILITY/LIMITATION NOTICES: Enter any limitations on further dissemination of the report, other than those imposed by security classification, using standard statements such as:

(1) "Qualified requesters may obtain copies of this report from DDC."

(2) "Foreign announcement and dissemination of this report by DDC is not authorized."

(3) "U. S. Government agencies may obtain copies of this report directly from DDC. Other qualified DDC users shall request through ________________."

(4) "U. S. military agencies may obtain copies of this report directly from DDC. Other qualified users shall request through ________________."

(5) "All distribution of this report is controlled. Qualified DDC users shall request through ________________."

If the report has been furnished to the Office of Technical Services, Department of Commerce, for sale to the public, indicate this fact and enter the price, if known.

11. SUPPLEMENTARY NOTES: Use for additional explanatory notes.

12. SPONSORING MILITARY ACTIVITY: Enter the name of the departmental project office or laboratory sponsoring *(paying for)* the research and development. Include address.

13. ABSTRACT: Enter an abstract giving a brief and factual summary of the document indicative of the report, even though it may also appear elsewhere in the body of the technical report. If additional space is required, a continuation sheet shall be attached.

It is highly desirable that the abstract of classified reports be unclassified. Each paragraph of the abstract shall end with an indication of the military security classification of the information in the paragraph, represented as *(TS)*, *(S)*, *(C)*, or *(U)*.

There is no limitation on the length of the abstract. However, the suggested length is from 150 to 225 words.

14. KEY WORDS: Key words are technically meaningful terms or short phrases that characterize a report and may be used as index entries for cataloging the report. Key words must be selected so that no security classification is required. Identifiers, such as equipment model designation, trade name, military project code name, geographic location, may be used as key words but will be followed by an indication of technical context. The assignment of links, rules, and weights is optional.

Unclassified
Security Classification

DISTRIBUTION LIST

ADDRESSEE	NO. OF COPIES
1. Naval Air Systems Command Department of The Navy Washington, D.C. 20361 Attention: AIR-50174 AIR-52032D	 6 3
2. Office of Naval Research Washington, D.C. 20360 Attention: (Code 472)	1
3. Naval Research Laboratory Washington, D.C. 20360 Attention: (Code 6306), (Code 6120)	2
4. Naval Ordnance Laboratory White Oak, Maryland 20910 Attention: (Code 234)	1
5. Air Force Materials Laboratory Wright-Patterson Air Force Base Ohio 45433 Attention: LC 1, LN 1, LTF 1, LAE 1	4
6. Air Force Flight Dynamics Laboratory Wright-Patterson Air Force Base Ohio 45433 Attention: FDTC	1
7. Defense Ceramic Information Center Battelle Memorial Institute 505 King Avenue Columbus, Ohio 43201	1
8. The Boeing Aerospace Company P. O. Box 3999 Seattle, Washington 98124 Attention: J. T. Hoggatt	1
9. Brunswick Corporation Technical Products Division 325 Brunswick Lane Marion, Virginia 24354	1

10. Plastics Technical Evaluation Center 2
Picatinny Arsenal
Dover, New Jersey 07801
Attention: Director

11. Hercules Incorporated 1
Magua, Utah 84041
Attention: Mr. E. G. Crossland

12. Commonwealth Scientific Corporation 1
500 Pendelton Street
Alexandria, Virginia 22314

13. Northrop Corporation 1
3901 W. Broadway
Hawthorne, California 90250

14. Naval Air Propulsion Test Center 1
Trenton, New Jersey 08628
Attention: Mr. J. Glatz

15. Chief of Naval Material 1
Deep Submergence Systems Project Office
Washington, D.C. 20360
Attention: Mr. H. Bernstein PM-11221

16. Commander 1
U. S. Naval Weapons Center
China Lake, California 92555

17. Celanese Research Company 1
P. O. Box 1000
Summit, New Jersey 07901
Attention: Mr. R. J. Leal

18. Naval Ship Engineering Center 1
Navy Department
Washington, D.C. 20360
Attention: (Code 6101E)

19. Naval Ordnance Systems Command 1
Navy Department
Washington, D.C. 20360
Attention: (Code ORD 033)

20. NASA Headquarters 1
600 Independence Avenue S. W.
Washington, D.C. 20546
Attention: Mr. N. Mayer (Code RV-2)

21. Philco-Ford Corporation 1
Aeronutronic Division
Ford Road
Newport Beach, California 92660

22. Commanding Officer 1
Naval Air Development Center
Warminster, Pennsylvania 18974
Attention: Air Vehicle Technology Dept.

23. Naval Ship Research & Development Center 1
Washington, D.C.
Attention: Mr. M. Krenzke (Code 727)

24. NASA 1
Lewis Research Center
21000 Brookpark Road
Cleveland, Ohio 44135

25. NASA 1
Langley Research Center
Hampton, Virginia

26. United Aircraft Corporation 1
United Aircraft Research Labs.
E. Hartford, Connecticut 06108

27. United Aircraft Corporation 1
Pratt & Whitney Aircraft Division
E. Hartford, Connecticut 06108
Attention: Mr. K. Boll

28. United Aircraft Corporation 1
Hamilton-Standard Division
Windsor Locks, Connecticut
Attention: Mr. T. Zajac

29. United Aircraft Corporation 1
Sikorsky Aircraft Division
Stratford, Connecticut 06602
Attention: Dr. M. Salkind

30. Union Carbide Corporation 1
Carbon Products Division
P. O. Box 6116
Cleveland, Ohio 44101

31. General Dynamics, Convair Division 1
P. O. Box 1128
San Diego, California 19210
Attention: Mr. W. G. Scheck
Dept. 572-10

32. The Rand Corporation 1
1700 Main Street
Santa Monica, California 90406

33. HITCO 1
1600 W. 135th Street
Gardena, California 90406

34. AVCO Corporation 1
Applied Technology Division
Lowell, Massachusetts 01851

35. Department of the Army 1
Army Materials & Mechanics Research Center
Watertown, Massachusetts 02172

36. North American Aviation 1
Columbus Division
4300 E. Fifth Avenue
Columbus, Ohio 43216

37. McDonnell-Douglas Corporation 1
Douglas Aircraft Company
3855 Lakewood Blvd.
Long Beach, California 90801
Attention: Mr. R. J. Palmer

38. General Electric Company 1
Valley Forge Space Center
Philadelphia, Pennsylvania 19101

39. Monsanto Research Corporation 1
1515 Nicholas Road
Dayton, Ohio 45407

40. Materials Sciences Corporation 1
1777 Walton Road
Blue Bell, Pennsylvania 19422

41. U.S. Army Air Mobility R & D Lab. 1
Fort Eustis, Virginia
Attention: SAVDL-EU-SS (Mr. J. Robinson)

42. B. F. Goodrich Aerospace and 1
Defense Products
500 South Main Street
Akron, Ohio 44318

43. Great Lakes Research Corporation 1
P. O. Box 1031
Elizabethton, Tennessee

44. Whittaker Corporation 1
Research and Development Division
3540 Aero Court
San Diego, California 92123

45. Washington University 1
St. Louis, Missouri 03130
Attention: Dr. J. Kardos

46. University of Maryland 1
College Park, Maryland 20742
Attention: Dr. W. J. Bailey